ENGINEERS/CONSULTANTS/CM

FINAL REPORT

CHARACTERIZATION OF THE LIBNA FEATURE

PROPOSED KRŠKO 2 NUCLEAR POWER PLANT

KRŠKO, SLOVENIA

REVISION 0

Engineering & Construction Management
Hydro • Nuclear • Fossil

Tunnel Engineering

Geotechnical Engineering

Seismic & Structural Engineering

Hydrological & Hydraulic Engineering

Environmental Engineering & Permitting

PAUL C. RIZZO ASSOCIATES, INC.
500 PENN CENTER BOULEVARD
PENN CENTER EAST
BUILDING 5, SUITE 100
PITTSBURGH, PENNSYLVANIA 15235 USA

PROJECT NO. 12-4835
27 DECEMBER 2013

FINAL REPORT

CHARACTERIZATION OF THE LIBNA FAULT AND TECTONIC FRAMEWORK OF THE KRŠKO BASIN, KRŠKO, SLOVENIA

GEN ENERGIJA, D.O.O.

PROJECT NO. 12-4835
REVISION 0
27 DECEMBER 2013

PAUL C. RIZZO ASSOCIATES, INC.
PENN CENTER EAST
500 PENN CENTER BOULEVARD, SUITE 100
PITTSBURGH, PENNSYLVANIA 15235
TELEPHONE: (412) 856-9700
TELEFAX: (412) 856-9749
WWW.RIZZOASSOC.COM

APPROVALS

Project No.: 12-4835

Report Name: Final Report
Characterization of the Libna Fault and Tectonic Framework of the Krško Basin, Krško Slovenia

Date: 27 December 2013

Revision No.: 0

Approval by the responsible manager signifies that the document is complete, all required reviews are complete, and the document is released for use.

Originators:

Michael Logan Cline, Ph.D.
Senior Project Geoscientist — Date: 12/27/2013

K. Michael Cline, PG
Principal - Geosciences — Date: 12/27/2013

Independent Technical Reviewer:

Richard Quittmeyer, Ph.D.
Vice President - Seismology — Date: 12/27/2013

Project Manager:

Michael J. Edwards, P.E.
Vice President
Power Generation Projects — Date: 12/27/2013

Principal-in-Charge:

Paul C. Rizzo, Ph.D., P.E.
President/CEO — Date: 12/27/13

CHANGE MANAGEMENT RECORD

Project No.: 12-4835

Report Name: Final Report
Characterization of the Libna Fault and
Tectonic Framework of the Krško Basin, Slovenia

REVISION NO.	DATE	DESCRIPTIONS OF CHANGES/AFFECTED PAGES
0	27 December 2013	Initial Submittal

TABLE OF CONTENTS

PAGE

TABLE OF CONTENTS
(CONTINUED)

PAGE

LIST OF TABLES

LIST OF FIGURES

LIST OF EXHIBITS

LIST OF APPENDICES

ACKNOWLEDGEMENTS

The investigations performed leading to and including the preparation of this Report were concluded in full cooperation and collaboration with Geoloski Zavod Slovenije (GeoZS). Specifically, Dr. Milos Bavec, Dr. Igor Riznar, and Dr. Marjian Poljak were of considerable assistance.

FINAL REPORT
CHARACTERIZATION OF THE LIBNA FAULT AND TECTONIC FRAMEWORK IN THE KRŠKO BASIN, KRŠKO, SLOVENIA

1.0 INTRODUCTION

GEN Energija, d.o.o. (GEN) has contracted (Contract 46/2012 and 46/2013) Paul C. Rizzo Associates, Inc. (RIZZO) to conduct scientific investigations to identify and characterize faults and other tectonic features within the vicinity of two sites being considered for the proposed Krško 2 Nuclear Power Plant (NPP) in Krško, Slovenia (***Figure 1-1***). The investigations commenced in October of 2012 and are a continuation of previous work performed by a consortium of organizations led by Bureau de Recherches Géologiques et Minières Consortium (BRGM) of France (BRGM, 2010). This work is also complimentary to the probabilistic fault displacement hazard analysis (PFDHA) prepared by RIZZO (2013b). This report presents the results of RIZZO's tectonic investigations of the Krško Basin and surrounding area.

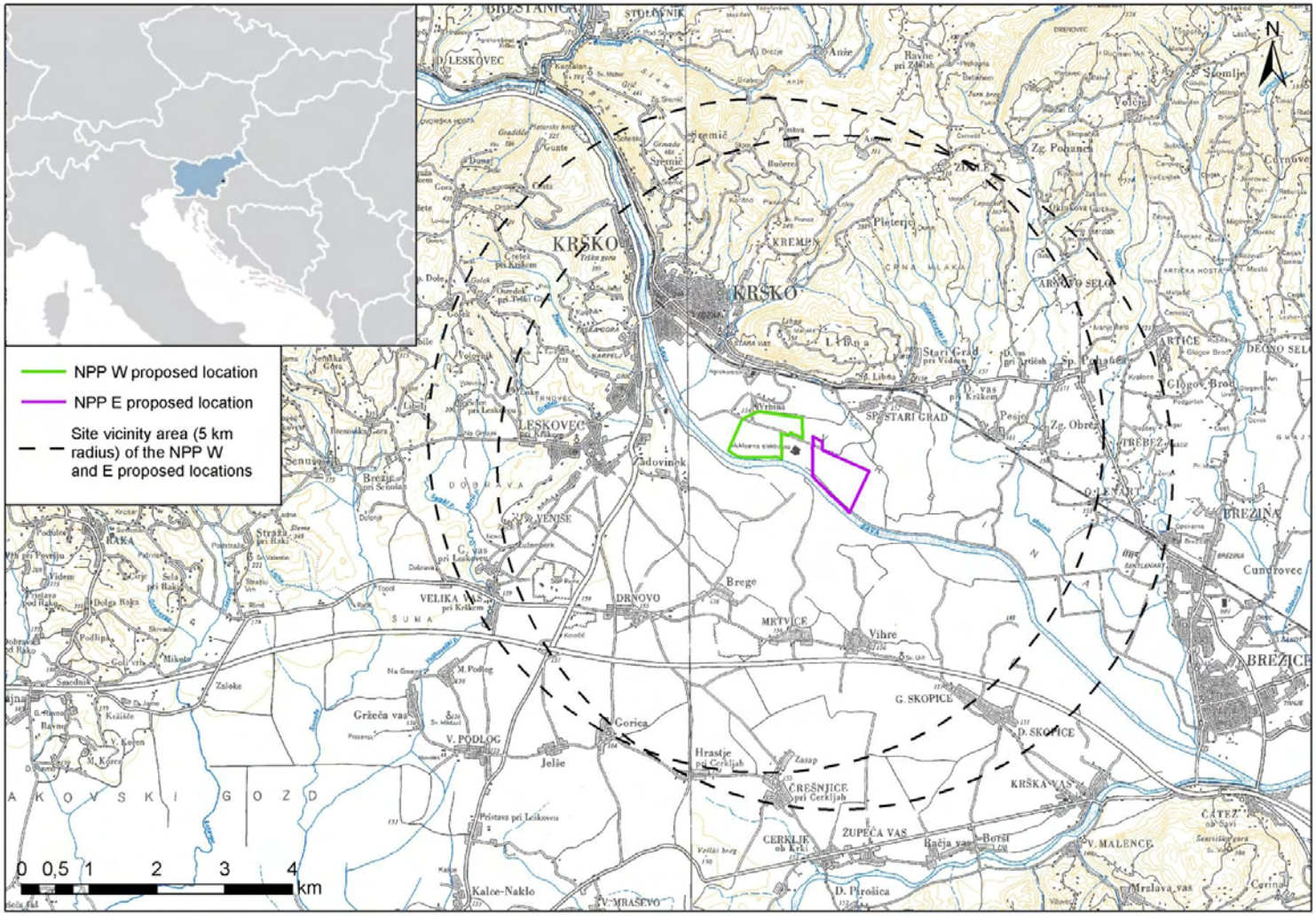

Source: Geozs

FIGURE 1-1
LOCATION OF PROPOSED NPP 2 SITES

Two sites being considered for the Krško 2 NPP are adjacent to the existing Krško 1 NPP, immediately east of the town of Krško. One potential site lies immediately to the east of the existing NPP and the other lies immediately to the west (***Figure 1-1***). In assessing these potential sites, the issue of active faulting at or near the proposed sites was investigated, as with all new nuclear plants around the world.

The scope of this study primarily focuses on the Libna Fault and the postulated Stara Vas features that are inferred to extend from Libna Hill to an undetermined location within the Sava River Basin to the south. In addition, other significant tectonic structures were investigated to understand the broader tectonic regime. RIZZO uses a multidiscipline approach, consisting of three separate investigations to assess the potential faults:

1. A High-Resolution Seismic (HRS) investigation along seven new profiles amounting to 17 kilometers (km), as well as the reanalysis of the 2008 HRS data (RIZZO, 2010). The objective of the HRS investigation is to determine if the faults displace the Plio-Quaternary sediments within the Krško Basin, and to constrain the length of the Libna Fault within the Krško Basin.

2. A geomorphic characterization of the region was performed by analyzing high-resolution topographic data derived from Light Direction and Ranging (LiDAR) followed by ground-truthing. Included in this study is the geomorphic characterization of a broader area in order to provide a Plio-Quaternary tectonic context. The overall objective of this study is to evaluate surface expressions that may be indicative of Plio-Quaternary deformation.

3. A geochronology (aka age-dating) investigation of the Krško Basin sediments with a particular emphasis on the Plio-Quaternary Globoko Formation. The Globoko formation has not been successfully dated analytically to this point, and only minimum ages have been attained based on previous geochronology attempts. The Globoko Formation is of particular interest because it may represent the youngest of the sedimentary deposits that would be considered for determining fault capability if it is tectonically deformed. The objective of this investigation is to determine the age of the Globoko Formation using ^{26}Al and ^{10}Be terrestrial cosmogenic radionuclide (CRN), and optically stimulated luminescence (OSL) dating of quartz and feldspar.

These investigations were performed between October 2012 and 2013. At the completion of each investigation an interim report (RIZZO, 2012 2013a, and 2013b) was prepared that summarizes the work performed and the results of the investigations. In addition, other reports were also prepared that addressed specific topics associated with the three investigations. This work was performed in collaboration with GeoZS and with the support of the following subcontractors:

- GeoExpert a.g., performed the HRS survey (GeoExpert, 2013).
- Geoid performed the topographic survey to support the layout of the seismic lines.
- Sterling Seismic Services (Sterling) processed the HRS data (*SGY file format).
- Geological Associates provided a geologic interpretation of the HRS data.
- ROVS, d.o.o performed the drilling.
- The University of Bern Laboratory in Switzerland performed the OSL age dating.
- The Purdue Rare Isotope Measurement Laboratory (PRIME Laboratory) at Purdue University performed the CRN age dating.
- Dr. Tammy Rittenour of the OSL Laboratory at the Utah State University (USU) performed the peer review of the work performed by the University of Bern.

This Report summarizes the results and findings of the three investigations and presents conclusions regarding:

- An interpretation of the postulated Stara Vas Feature, Libna Fault, Orlica Fault Zone (OFZ), and the inferred Artiče Fault.
- A new geochronology and corroborating stratigraphic facies study with implications for landscape evolution in the Krško Basin.
- Implications of the results on comments by the Probabilistic Fault Displacement Hazard Analysis Peer Review comments.
- The implications based on the results of this study to the seismotectonic model of the Krško Basin.

2.0 TECTONIC FRAMEWORK

2.1 REGIONAL GEOLOGIC AND TECTONIC SETTING

The proposed Krško NPP Sites are located 2 km east of the town of Krško on the northern bank of the Sava River, which flows through the Krško Basin. The Sava River is an important hydrological feature in southeastern Europe because it is the primary drainage for the Alps and Dinarides. It is the primary modern mechanism and the dominant historical mechanism for transporting sediment into and out of the Krško Basin. The regional geology is primarily understood through detailed investigations by GeoZS including geological mapping, geophysical surveying, structural drilling, a network for geodetic measurements, and a network of seismic stations. Understanding of the Krško Basin has been hindered by a lack of geochronology constraints on the sediments, and as a result, there are few constraints on the surface processes and rates of deformation.

The Krško Basin is a structural basin, defined by a large syncline (***Figure 2-1***) that stretches from the Novo Mesto District in the west to the Hrvatsko Zagorje in neighboring Croatia in the east (~40 km). The shape of the syncline is identified from gravimetric maps and from seismic reflection lines (Persoglia, 2000, Gosar, 1998; RIZZO, 2010; RIZZO, 2013c). The stratigraphic succession within the Basin consists of basement Mesozoic (~252-66 mega anum [Ma aka million years]) sedimentary rocks followed by mostly clastic, Miocene (~23-5.6 Ma) sediments. The Neogene succession consists of Ottnangian clay, sand and gravel, Badenian limestone and marl, Samartian calcarenite, Pannonian marl (or calcareous silt), and Pontian calcareous silt alternating with quartz sand. The Neogene syncline is further filled by Pliocene (~5.6-2.58 Ma) and Quaternary (2.6-0 Ma) terrestrial sediments that have been preserved in the form of several axial and tributary river terraces. Age constraints on these deposits are scarce. A broad designation has been adopted that refers to sediments ranging from the Quaternary to the Pliocene as the Plio-Quaternary.

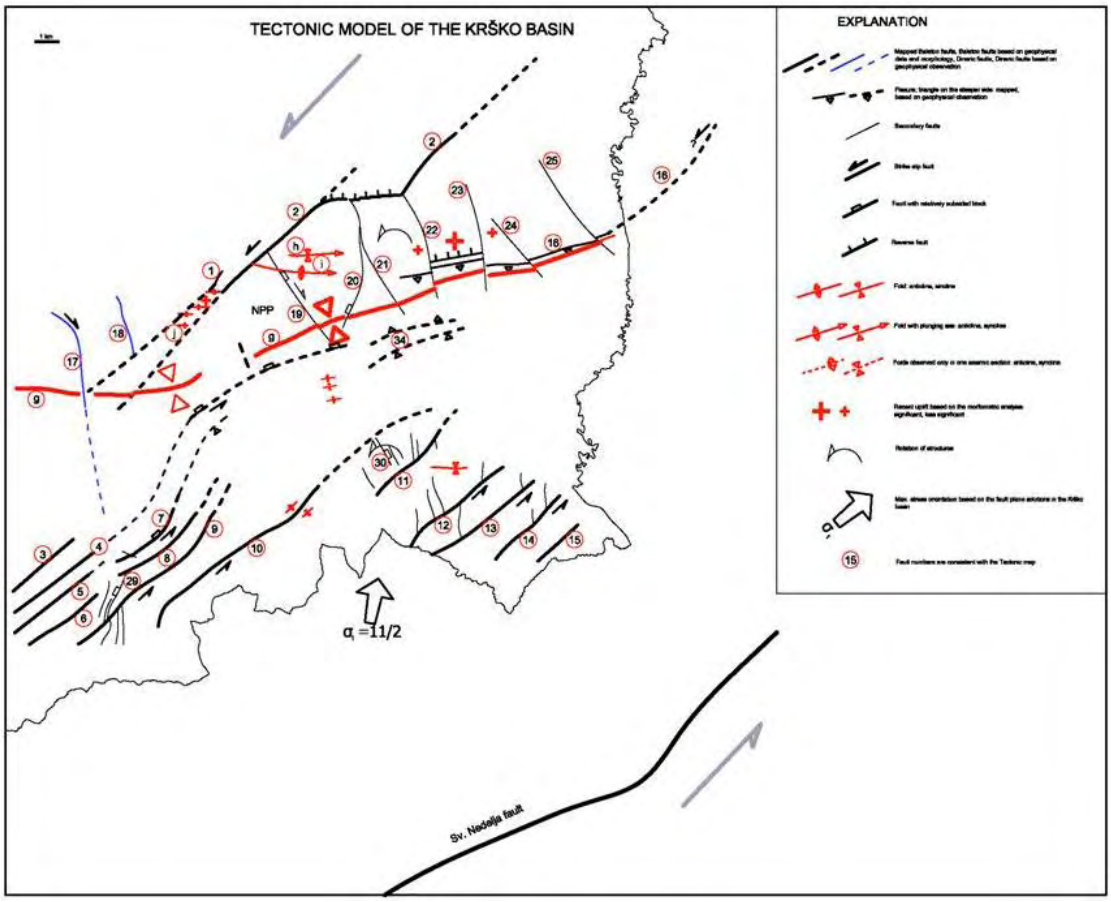

Note

The numbers associated with the faults represent their names. The names can be found in ***Exhibit 1***.

FIGURE 2-1
TECTONIC MODEL OF THE KRŠKO BASIN (BRGM, 2010)

The last and current phase of the syncline folding originated in mid Pontian (~7.2-5.3 Ma). This fact is exhibited in the relatively uniform thickness of the whole Neogene strata succession, from the Badenian (~16-13.3) to the Pontian, across the entire Krško syncline. The relative tilt of the so called Plio-Quaternary (Markič and Rokavec, 2002) and Mid-Pleistocene (Verbič, 2005) terrace remnants indicates that the syncline has continued to fold into Mid-Pleistocene, although these data are being debated due to the sparse geochronology. The tilt of fluvial deposits appears to diminish from the Plio-Quaternary to the Mid-Pleistocene (Verbič, 2005). The Late Pleistocene and Holocene surfaces do not exhibit post-depositional tilt. Geodetic observations do suggest that folding may be ongoing; however, these results are within the systematic error of the measurements.

The proposed Krško NPP Sites are located within the southwestern extension of the Mid Hungarian Tectonic Zone (MHZ), which is a tectonic element within the Adria microplate (***Figure 2-2***). The Adria microplate is moving northward, while rotating in a counter-clockwise direction (Poljak et al., 2010). The Krško Basin lies on the northern edge of the large sinistral strike-slip, northeast-trending, 40 km-wide, extension of the MHZ (Placer, 1999). The prominent deformation in the MHZ is accommodated by northeast-trending (Balaton) faults of general sinistral strike-slip character (Poljack et al., 2010), as exemplified by the OFZ which defines the northern extent of the southwestern extension of the MHZ. The OFZ is presently mapped several kilometers to the north of the Krško NPP Sites.

The OFZ, together with the Zagreb Line (located on the southern edge of the Gorjanci and Medvednica Mountains) also defines the southern border of the Sava Compressional Wedge (Placer, 1999). The Sava Compressional Wedge is characterized by the east-west trending folds and reverse faults between the extension of the MHZ, the north-west trending faults of the Idrija Tectonic Zone of the External Dinarides to the west, and the Sava fault as the southern margin of the Periadriatic Zone in the north (***Figure 2-2***).

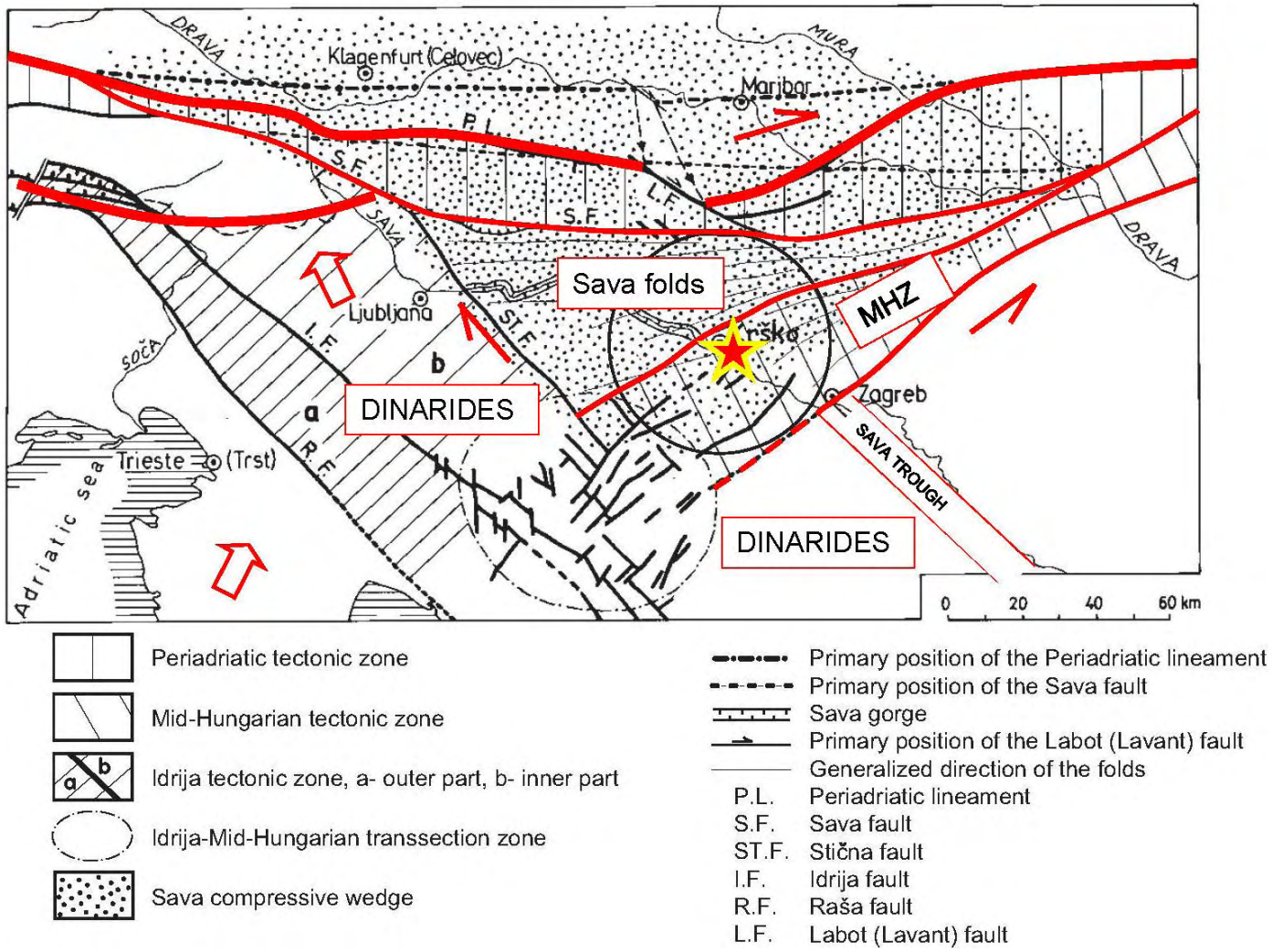

FIGURE 2-2
REGIONAL TECTONIC MODEL OF SLOVENIA (GEOMATRIX, 2004)

There are four sets of potentially active structures within the Krško region:

1. The Balaton faults, prominent left-lateral strike-slip faults.
2. Step-overs between the strike-slip Balaton faults that exhibit a component of reverse faulting.
3. North (northeast to northwest) trending faults between the Balaton faults that are considered as counter clockwise (CCW) rotating Riedel-type faults in the sinistral strike-slip zone.
4. In the western part of the Krško Basin, the northwest trending faults of the Idrija Zone of the Dinarides also affect the structural pattern.

2.2 HISTORICAL SEISMICITY OF THE KRŠKO REGION

The catalogue of the known events in the region (BRGM, 2010) extends back to the beginning of the 17th Century. The strongest earthquake listed in the earthquake catalog that has occurred in the Krško region was the 29 January 1917 earthquake with the estimated moment magnitude of 5.8 (GeoZS, 2010) and a highest intensity of VIII (Medvedev-Karnik-Sponheuer intensity scale) in Brežice. At that time, the closest seismic station was in Zagreb, some 45 km away.

With the installation of broad band seismographs in the Krško region monitoring of earthquakes has greatly improved both in sensitivity and in the accuracy of the location parameters determination. Consequently, the number of the earthquakes for which the determination of a Fault Plane Solution (FPS) is possible has increased. Most of the FPS analyzed indicate strike-slip faulting is dominant, but several FPS are reverse in character. The calculated maximum principal stress axis is based on the FPS and structural elements in the Krško Basin (Poljak et al., 2010). Since installation of the network in 2002, the strongest earthquake in the Basin has been a magnitude 3.1 event near Brežice (BRGM, 2010).

2.3 PHYSIOGRAPHIC AND GEOLOGIC SETTING OF THE KRŠKO BASIN

The modern landscape of the Krško region formed in response to folding and associated uplift that created the Dinarides and Southern Alps mountain systems, followed by the onset of the Pannonian Basin and its

tectonic evolution and the subsequent dissection of the landscape by fluvial incision. The greatest relief within the Krško region is located to the north of the Krško Basin at the intersection of the Southern Alps, with the Dinarides (***Figure 2-2***). The Sava River cuts a narrow canyon through these three regions until it breaks out into the broad Krško Basin which has acted as a significant zone of deposition throughout much of the Quaternary period and possibly longer.

The NE margin of the Gorjanci Mountains, south of the Krško Basin (Southeast corner on ***Figure 1-1***) display a smooth surface expression likely resulting from karst dissolution of carbonate rocks. This dissolution and mapped fault planes may have provided pathways to trigger a very large ~1.2 square kilometers (km^2), deep-seated (>10 meter [m]) landslide (***Figure 2-3***). This landslide is an example of other landslide features present in the southern hills as well as in other areas adjacent to the Krško Basin in the vicinity (5 km) around Krško. Karst features (sinkholes) can also be seen on ***Figure 2-3*** east and southeast of the landslide. The karst and landslide features are common in the Krško vicinity.

The Krško Basin is a broad fluvial plane. Historical data provided by GEN (2012) dating from the Roman period show the historical migration of the Sava River channel within the Krško Basin. These historical data demonstrate the river's natural and anthropogenic migration back and forth across the modern Krško Basin.

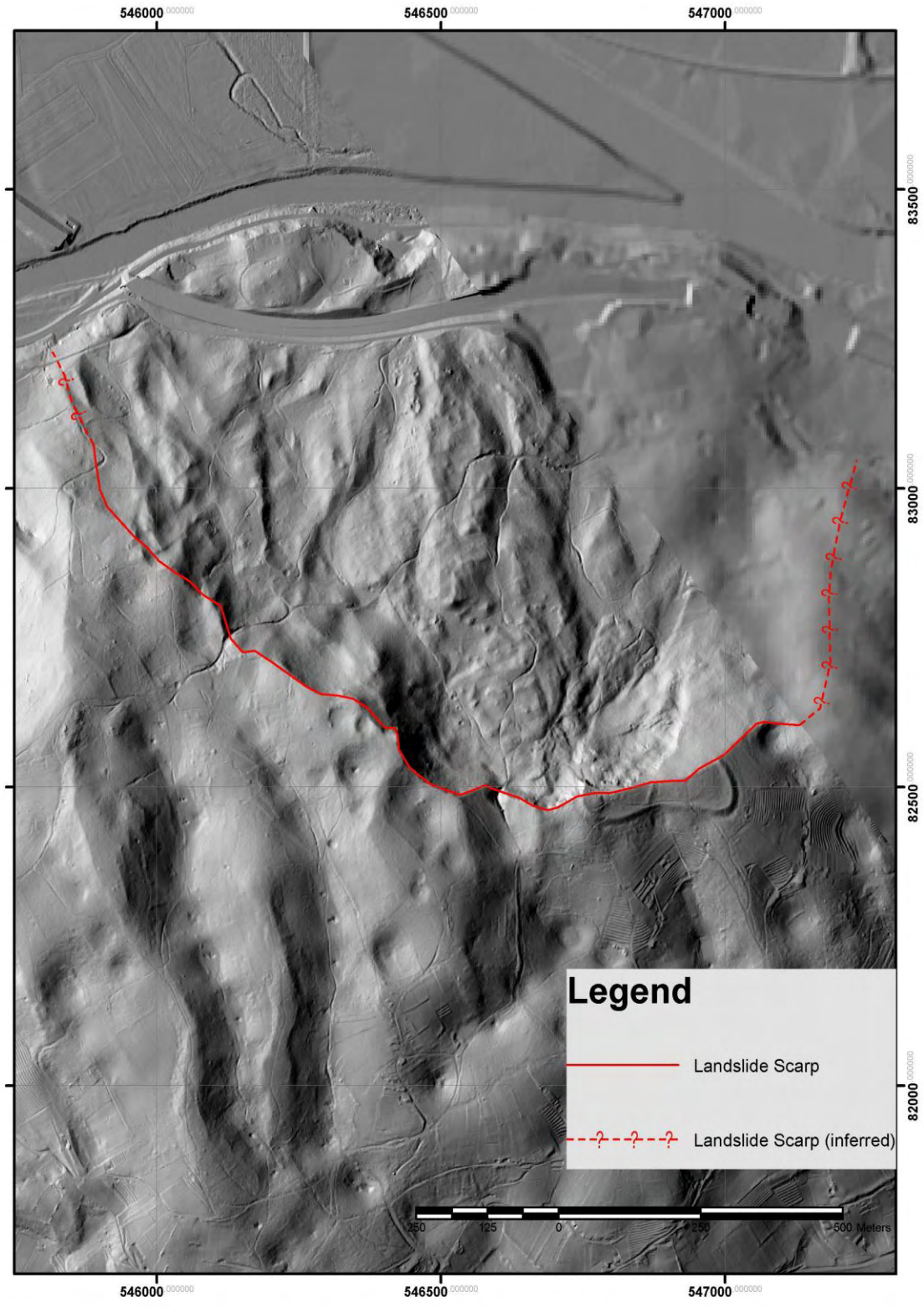

FIGURE 2-3
LARGE LANDSLIDE SOUTH OF SAVA RIVER AMONG KARST FEATURES

3.0 HIGH-RESOLUTION SEISMIC SURVEY INVESTIGATION

3.1 SUMMARY OF THE HRS INVESTIGATION

The HRS investigations consisted of two major activities. The first being the conduct of a new HRS survey and the second being the reinterpretation of existing 2008, 2009, and 2012 HRS data. A detailed discussion of the methodology, approach, and findings for both activities are presented in the reports "Interim Report: Interpretation of High Resolution Seismic Data," Revision 1 (RIZZO, 2013c) and "Reinterpretation of the 2008 and 2012 High-Resolution Seismic Data Compiled in the Krško Basin, Slovenia," Revision 1 (RIZZO, 2013e). The following Sections summarize the conclusions of the HRS survey investigation.

RIZZO (2013c) conducted an additional HRS survey to build on past HRS investigations (2008 and 2009) with the intent of:

- Constraining the length and width of the Libna Fault.
- Identifying the presence of other faults, if any, within the Krško 2 NPP site vicinity (approximately 5 km radius of the sites).
- Mapping of the topography of the bedrock surface and identifying of the Plio-Quaternary deposits and other tectonic features.

Based on the location of the 2008 and 2009 HRS survey lines and working with GeoZS representatives, approximately 17 km of new HRS lines were established and surveyed for conducting the HRS survey (***Figure 3-1***).

The survey was conducted in October 2012 using a variable asymmetric split spread alignment of 240 to 360 receivers (geophones), at 1.0 m to 2.0 m spacing. Available energy sources were of the impact type, consisting of different weights. An 8 kilogram (kg) sledge hammer was mostly used (75 percent of the records) because local land owners complained of surface disturbance when the wheel mounted weight drop

was used and in some cases the topography prohibited the use of the weight drop.

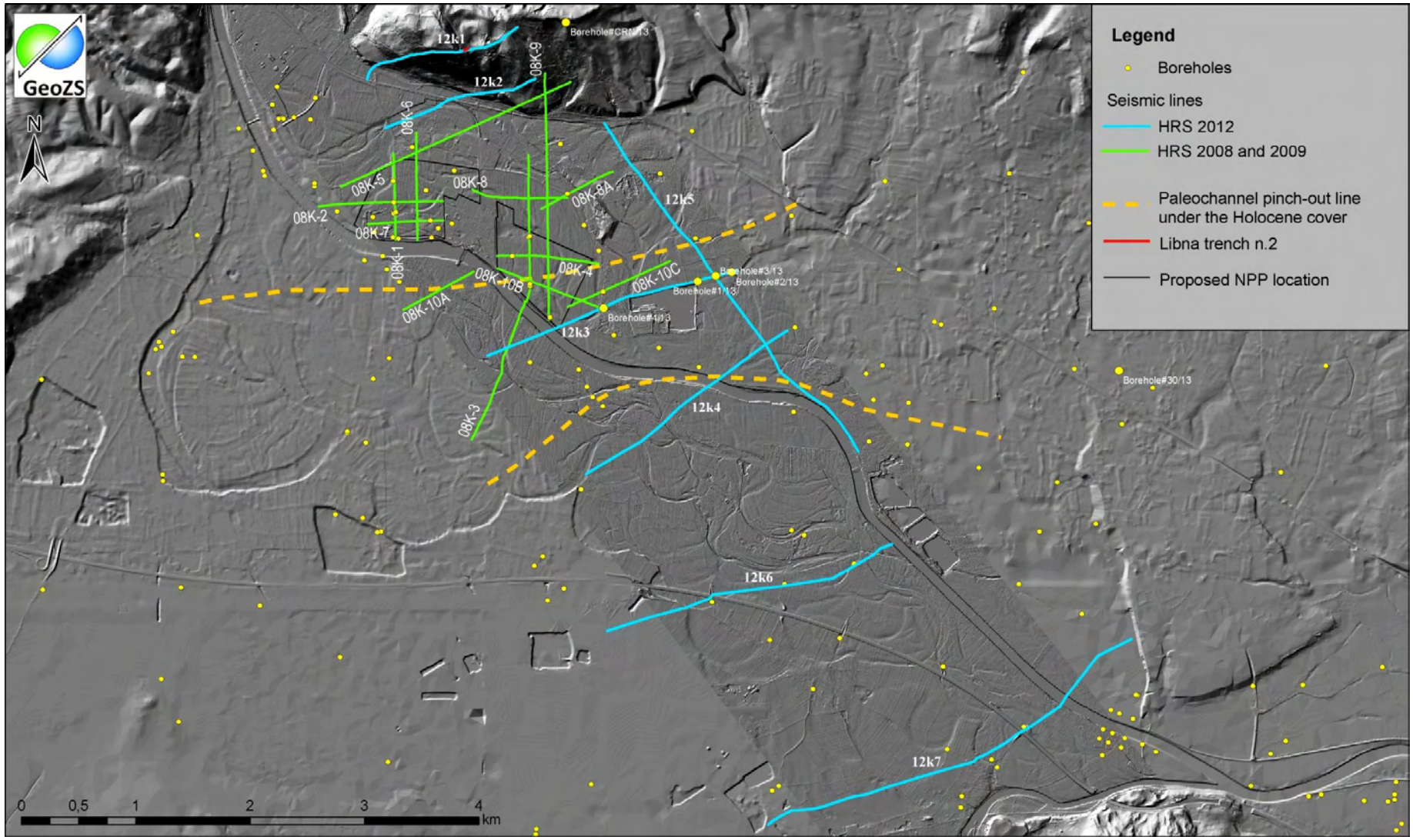

FIGURE 3-1
LAYOUT OF HRS SURVEY LINES AND HISTORICAL BORINGS

Sterling Seismic Services, Ltd., under subcontract to RIZZO, processed the data using PROMAX software, a standard processing code typically used by the deep geophysical industry (e.g., petroleum exploration). Because of the noise within the dataset, Sterling applied multiple filters to achieve an improved signal to noise ratio. However, the more the data are filtered, the more the reflectors are smoothed and subtle anomalies are lost, making interpretation of the data more challenging.

Geological Associates, under subcontract to RIZZO, performed an interpretation of the Sterling-processed data set (***Appendix 1***). The initial interpretation of the 2012 HRS data was reported in "Interim Report: Interpretation of High-Resolution Seismic Data Compiled in October 2012, Krško 2 Nuclear Power Plant, Krško, Slovenia," Revision 1 (RIZZO, 2013c).

In response to the noise issues, questionable representation of near surface conditions, and in light of new information on Holocene and Quaternary deposits in the Krško Basin (GeoZS, 2013 and ***Section 3.2***), the data were reinterpreted using GeoExpert's output from its refraction diving wave tomography that better represents near-surface conditions (RIZZO, 2013e). The technique that GeoExpert uses, known as HRS hybrid refraction/reflection tomography (HRS Hybrid), superimposes the refraction tomography velocity field on the reflection seismic depth data with depth estimates and variable velocities that represent the density of the stratigraphic units that the seismic wave is passing through (GeoExpert, 2013). This approach is designed to better highlight near-surface conditions.

RIZZO reinterpreted those 2008 and 2009 HRS profiles that crossed the inferred projection of the Libna Fault and the 2012 HRS profiles using the HRS Hybrid profiles. The interpreted HRS Hybrid profiles are presented in ***Appendix 2.*** For more information on the reinterpretation of the 2008, 2009, and 2012 HRS profiles, refer to the report entitled "Reinterpretation of 2008 and 2012 High-Resolution Seismic Data Compiled in the Krško Basin," (RIZZO, 2013e).

3.2 INTERPRETATIONS BASED ON THE 2008, 2009, AND 2012 HRS PROFILES

The GeoExpert Hybrid profiles are presented as depth sections, whereas the Sterling PROMAX software presents time sections. No attempt was made to compare the quality of the two approaches as they serve different purposes. Examples of the two different methods are presented in ***Exhibit 2***.

The GeoExpert raw HRS data contain both high-frequency noise (environmental) and abundant diffraction patterns (possibly from NPP operations). Of the processed profiles, the Hybrid profiles are more interpretable than the Sterling profiles. The HRS Hybrid profiles allow for the verification of the interpretations from the Sterling-processed datasets, specifically aiding in distinguishing geologic features from probable processing artifacts. However, neither the Hybrid profiles nor the Sterling-processed data profiles provide sufficient information to completely and unambiguously resolve the structural geometry and timing of deformation of the interpreted inferred faults.

The diffractions and high frequency noise could be caused by a combination of surface activity such as vehicles, the Krško NPP, and any operation that produces lateral heterogeneities or discontinuities in the subsurface. The presence of high frequency noise and diffraction patterns occurring in the areas where there should be limited environmental noise suggests that the rock units underlying the surficial deposits are complex and highly fractured (not necessarily faulted). In addition, the presence of shallow ground water and large gravel beds may impact the seismic signals and degrade the signal to noise ratio. Rock complexity can include heterogeneous deposition, mass wasting, deep weathering profiles, karst features, and highly fractured rocks. The exact cause(s) depend on the specific location.

The "A Horizon" identified in previous investigations conducted by GeoZS (GeoZS, 2010) was interpreted as a reflector within the Pontian Miocene. This same reflector was misinterpreted as the Miocene-Plio-Quaternary boundary in the RIZZO report (RIZZO, 2010) which reinterpreted the 2008 and 2009 HRS data. The RIZZO report shows faults either

displacing or warping the "A Horizon" in HRS Profile Lines 08K-8a, 08K-9, and 08K-10c (***Exhibit 3***). These profiles intersect the inferred projection of the Libna Fault. A rough estimate of depth, considering the two-way travel time and estimated velocities of subsurface rock units, suggests this reflector and associated displacements occur at approximately 100 m to 200 m depth, well within the Miocene succession.

GeoZS compiled subsurface information from historic borehole logs in the Basin. Interpretation of the boring logs suggests that sediment similar to that of the Plio-Quaternary is only preserved in a paleo-channel within the Basin (***Figure 3-1***). In general, the boring logs indicate that late Pleistocene-Holocene fluvial deposits directly overlie Miocene marls. The late Pleistocene–Holocene fluvial deposits range between 3 m and 6 m in thickness.

Borings within the paleo-channel often encounter young fluvial deposits overlying the Plio-Quaternary fluvial deposits before encountering the Miocene Marls. The absence of Plio-Quaternary deposits observed in boring logs, except those from the paleo-channel, and the presence of Miocene marls very near the surface provides robust support that the so-called "A-Horizon" from the RIZZO (2010) report does not correspond to a reflector within Plio-Quaternary deposits. It has been suggested by GeoZS that the "A Horizon" may be an artifact (possibly a replicate) which has also been exhibited in the original interpretation (GeoZS, 2010). The reinterpretation (RIZZO, 2013e) of the HRS Profile Lines 08K-8a, 08K-9, and 08K-10c using the Hybrid technology shows no evidence of an "A Horizon" and different expressions of possible faulting (***Exhibit 4***) in Miocene bedrock.

HRS Profile Lines 12K-1, 12K-2, and 08K-5 (***Appendices 1 and 2***) represent poor HRS data recovery due to either the close proximity of the bedrock to the surface, highly fractured bedrock, and/or karst dissolution of the bedrock. There is no evident concentration of shearing that represents a fault.

The other HRS profiles show areas of inferred (weak indicators) and possible (moderate to strong indicators) faulting within the Basin. In some cases interpreted faulting is observed to occur in close proximity

between multiple profiles as shown in HRS Profile Lines 08K-8a, 08K-10c, and 12K-3 (***Exhibit 5***). The interpreted offsets observed in HRS Profile Lines 08K-8a, 08K-10c, and 12K-3 show that these possible faults are not necessarily in the exact same location when observed in the different profiles of the same HRS profile line. In addition, some of these faults have different dip orientations. Plotting these faults from the different HRS Profiles gives the appearance that there are multiple faults in close proximity to one another. This is likely a product of the different processing techniques influenced by the noise. The Libna Fault may be a fault zone instead of a single fault trace; however, the apparent presence of multiple faults should not be interpreted as the width of the fault zone. To ensure that the all Fault configurations are captured in ***Exhibit 5***, the Fault is represented as a zone.

The Sterling and Hybrid profiles that either cross (08K-4, 08K-9, and 08K-10B) or pass adjacent to (08K-5, 08K-8, and 12K-3) the proposed NPP sites show possible faulting crossing through the two sites; however, the interpretations indicated that the faulting occurs well within the Miocene bedrock (deep faults). Photographs of the Krško NPP 1 foundation (Geomatrix, 2004) show unfaulted tilted Miocene bedrock, which supports the interpretation of HRS Survey Line 08K-8, indicating that the faulting occurs well within the Miocene stratigraphic units.

3.3 INTERPRETATION OF HRS PROFILES RELATED TO THE PROJECTION OF THE LIBNA FAULT

The interpretation of the Libna Fault in the HRS profiles is problematic as the faulting is not continuous across profiles. The absence of faulting in HRS Profile Lines 12K-1, 12K-2, and 08K-5 (***Appendices 1 and 2***) indicates there is no faulting at the base of Libna Hill or that the HRS data are too noisy (both anthropogenic and natural conditions) to record any reflectors that could be interpreted as offset. In addition, HRS Profile Lines 08K-5 and 08K-9 show no inferred or possible faults within the projection of the Libna Fault.

The results of the HRS investigation indicate that a concentration of interpreted offsets occurs in a relatively narrow zone in HRS Profile Lines 08K-8a, 08K-10c, and 12K-3. These concentrations of offsets are consistent with the inferred projection of the Libna Fault presented in the

Phase I Summary Report (BRGM, 2010). If the interpreted possible offsets represent the Libna Fault, the Fault extends within the Krško Basin between HRS Profile Lines 08K-8a and 12K-3, and possibly as far south as 12K-4.

The concentration of interpreted possible faults in HRS Profile Lines 08K-8a, 08K-10c, and 12K-3 occur within the projection of the Libna Fault. The close proximity of faults from the different interpretations only confirms the presence of the Libna Fault. The number of faults may indicate the presence of a Fault zone; however, different processing techniques can yield different interpretations of fault location and orientation; therefore the width of the concentration of faults should not be interpreted as the width of the fault zone.

The interpretations of faulting between the different processing techniques in HRS Profile Lines 12K-4, 12K-6, and 12K-7 brings into question the extension of the Libna Fault south of HRS Profile Line 12K-3. The expression of possible faulting is non-existent or is a manifestation of deep structures or fault mechanisms different (graben structures) from that of the Libna fault (strike-slip structure). Therefore, possible projection of the Libna Fault south of HRS Profile Line 12K-3 is speculative.

Based on the interpreted depth to faulting in the Sterling-processed profiles, the estimated depths of faulting in the Hybrid processed profiles, and the absence of Plio-Quaternary deposits where most of the seismic lines are located, there is no suggestion of Plio-Quaternary displacement.

There are four interpretations for the projection of the Libna Fault, south of Libna Hill summarized as follows:

1. The Libna Fault does not extend south of Libna Hill: The absence of possible faulting related to the projection of the Libna Fault in HRS Profile Lines 12K-1 and 12K-2 is supported by the interpretation of geomorphic features on Libna Hill as described in ***Sections 4.3 and 4.4***.

2. The Libna Fault extends south of Libna Hill to the vicinity of HRS Profile Line 12K-3 as a continuous fault: The concentration of

possible offsets in HRS Profile Lines 08K-8a, 08K-10c, and 12K-3 indicates the Libna Fault is present in the Krško Basin.

3. The Libna Fault extends south of Libna Hill to the vicinity of HRS Profile Line 12K-3, but is a discontinuous feature: The absence of interpreted possible faults in HRS Profile Lines 08K-5 and 08K-9 suggests that the Libna Fault is discontinuous within the Basin.

4. The Libna Fault extends to and includes HRS Profile Line 12K-4: The absence of interpreted faulting and inconsistencies in interpretations between the Sterling and Hybrid processing techniques does not support the continuation of the Libna Fault beyond 12K-4. In fact, interpretations greatly differ between the Sterling and Hybrid profiles for Line 12K-4.

With the exception of Plio-Quaternary terrace deposits on the perimeter of the Krško Basin, the occurrence of Plio-Quaternary deposits within the Krško Basin is limited to the paleo-channel. In most areas late Pleistocene-Holocene deposits ranging in thickness of 3 m to 5 m directly overlie Miocene formations. The interpreted faults from both the Sterling and Hybrid processed profiles fall within the Miocene Strata. There is no projection of faulting into Late Pleistocene-Holocene deposits. There is no evidence that the interpreted faults associated with the Libna Fault displace Plio-Quaternary deposits. The interpreted faulting associated with the Libna Fault occurs well within the Miocene bedrock.

4.0 SUMMARY OF GEOMORPHIC INVESTIGATION

This Section summarizes the tectonic geomorphic investigation of the Krško Basin and bounding mountains (RIZZO, 2012). As a result of this work, constraints on the neotectonics have been enhanced through the analysis of high-resolution topographic data.

RIZZO was provided with airborne LiDAR data, from which a 1.0 m bare earth Digital Elevation Model (DEM) was produced. The 1.0 m DEM is a narrow swath that follows the hypothetical projection of the Libna Fault (***Exhibit 6***) that includes an area from north of Libna Hill to the hills south of the Sava River near the junction with the Krka River. This DEM was combined with a 5 m DEM also provided by GEN.

Expressions of Quaternary faults are often preserved at the Earth's surface as aligned landscape features (i.e., lineaments). Large scale (>20 m) lineaments are usually recognizable from topographic maps, air photos, or satellite imagery; however, fine-scale features (<3 m) require extremely high-resolution data. LiDAR data has a major advantage over conventional air photos and other high-resolution imagery. Because the data are in x, y, and z coordinate space, filtering algorithms can be applied that strip the vegetation or other items that limit the interpretation of the tectonic landscape as compared to that of other remote sensing imagery. The level of detail and removal of vegetation allows for enhanced resolution of very small landscape features, which ultimately allowed for more accurate delineation of surface geomorphic features (e.g., tectonic, fluvial, and mass wasting).

4.1 APPROACH TO THE GEOMORPHIC INVESTIGATION

Tectonic geomorphology focuses on the surface expressions of tectonic processes. It analyzes landforms, including those resulting from the direct effects of tectonic processes such as ground ruptures, and to less obvious landforms such as over-steepened hillslopes related to blind thrusts (Roering et al., 1999). Additional direct effects of tectonic processes include offset channels, shutter ridges, laterally abandoned alluvial surfaces, and sag ponds. Many landscapes even take on self-organizing expressions of tectonic forcing (Hilley et al., 2010; DeLong, et

al., 2011; Perron et al., 2009). Indirect effects of tectonic forcing include the coupling of tectonics with fluvial processes (Whipple, 2009). These can often provide critical information about the tectonic youthfulness of a landscape. These may include drainage basin density (Tucker and Bras, 1998), longitudinal channel concavity/convexity (Snyder et al., 2000), and mountain front sinuosity (Bull and McFadden, 1977).

4.1.1 Application of LiDAR to Geomorphic Analyses

LiDAR data have revolutionized the field of tectonic geomorphology because of the level of detail at which the landscape can be resolved. For example, the surface-geologic expressions of active or recently active tectonics have been highlighted in the Idrija Fault region of western Slovenia (Cunningham et al., 2006). In many cases, these data can provide evidence for surface deformation features that are not readily observable in the field, provided the correct analytical tools are utilized (DeLong, et al., 2011).

For this study, RIZZO used a suite of analytical techniques to decompose the LiDAR DEM into its principal components. In addition, a regional 5 x 5 m DEM was made available for the broader region and many of the same methods were applied to it. Analyses of these data, combined with field-based ground truthing in October 2012, were used to characterize the tectonic geomorphology of the Basin, and to evaluate the surface expression of the Libna and postulated Stara Vas faults to assess their presence and activity.

4.1.2 Geomorphic Techniques for Lineament Analysis

The forms of landscapes are governed by tectonics and the laws of geomorphic erosion, transport, and deposition (Dietrich et al., 2003). Consequently morphologies are semi-predictable and in many cases, self-organizing (Perron et al., 2009). As a result of their predictability and organization, information about the formative processes can be deduced. Small perturbations to the semi-predictable evolution of landscapes (e.g., seismicity, meteor impacts, anomalous floods, and anthropogenesis) leave behind lasting features on the landscape that overprint the original form of the landscape. In some cases these features have easily identifiable characteristics such as fault scarps; however, in most cases

the features are more subtle, requiring careful observation, measurement, and analysis.

To ensure that the maximum number of relevant landscape features in the Krško Basin and surrounding hills were analyzed, high-resolution topographic data available from LiDAR point cloud data were used. Based on the 5.0 m and 1.0 m DEMs, careful lineament analysis was performed by decomposing the landscape into principal features using a suite of methods available within ArcGIS (DeLong et al., 2011). The following methods were utilized in this study in order to delineate lineaments:

- Topographic hillshading
- Topographic surface roughness mapping
- Slope aspect mapping
- Gradient mapping
- Profile curvature mapping

Details on each of these methods are described in RIZZO (2012).

In addition to the delineation of lineaments, the following morphometric techniques were applied to describe broader, spatial zones of potential uplift and/or stability:

- Regolith production and erosion analysis (i.e., landscape curvature approach)
- Basin morphology (i.e., density)
- Basin hypsometry

Details on each of these methods are described in RIZZO (2012).

4.2 RESULTS OF ANALYSIS

Lineaments identified on the 1.0 m and 5.0 m DEMs are based on the techniques listed above. For a full description of the derivative maps refer to RIZZO (2012). The lineaments define two dominant structural trends and one weak structural trend (***Exhibit 6***):

1. A dominant east-west structural trend north of Krško that is a part of the Sava Fold belt .

2. A second dominant north 30-45^{o} east trend that coincides with the OFZ.

3. A weak north 15-20^{o} west trend that includes the Libna Fault.

This determination of dominance is different from that reported in the "Interim Technical Report: Geomorphic Analysis of Tectonic Features in the Krško Basin, Slovenia" (RIZZO, 2012). The interim report identified the third structural trend as dominant, but a re-evaluation of lineaments indicates differently. This trend is defined by short and discontinuous lineaments that are typically represented by escarpments at the base of slopes along river channels. In comparison with the lineaments defining the other structural trends these lineaments fall into the moderate to weak category of lineaments. ***Exhibit 7*** shows a zoomed region that emphasizes Libna Hill and the Krško Hills.

4.3 LINEAMENT DESCRIPTIONS

The two dominant structural trends described in ***Section 4.2*** are addressed in some detail in the following sections. The third weak structural trend is not addressed any further as it is likely representative of older structures and/or erosional features. Lineaments are described as "weak," "moderate," and "strong" depending on the youthfulness, continuity, and prominence of the geomorphic expressions making up the lineament.

4.3.1 Lineaments Consistent with an East-West Structural Trend – The Sava Folds Region

The east-west structural trend is observed north of the Krško Hills (approximately 5 km north of Krško). The lineaments consist of multiple, sub-parallel to parallel, very pronounced, and continuous geomorphic features (***Exhibits 6 and 7***). These features are defined by straight stream valleys, dominant bedrock escarpments, right stepping second and third order drainages, and aligned first order drainages. The relief related to the bedrock escarpments is often very abrupt with steep slopes. No one lineament is more than approximately 7 km to 8 km long, but the geomorphic expression is generally strong.

These lineaments are interpreted to be related to the axis of folds or faults associated with the Sava Folds. They are the most dominant group of lineaments observed on the 5 m DEM and are observed from the western edge to nearly the eastern edge of the DEM coverage where the northeast trending lineament group appears to be more dominant.

4.3.2 Lineaments Associated with the Northeast Trending Structural Trend

The second dominant structural trend is interpreted to be related to the northeast trending Balaton Fault System (GeoZS, 2010). The lineaments making up this trend are most dominant on the southern flank of the Krško Hills and the Southern Flank of the Orlica Mountains (hereinafter referred to as the Artiče Hills) north of the Krško Basin (***Exhibit 6***). The trend is characterized by a broad zone of sub-parallel aligned geomorphic features consisting of narrow straight valleys, straight stream channels, and offset ridges. There is also some suggestion of shutter ridges and aligned offset stream channels in the northeastern segment on ***Exhibit 6***. This structural trend with associated lineaments appears to truncate the lineaments of the east-west structural trend. The OFZ falls within this structural trend (***Exhibit 7***).

4.4 Lineaments Associated with Significant Mapped and Postulated Faults

4.4.1 Postulated Stara Vas Fault

The only evidence for the postulated Stara Vas Fault is an outcrop with striations indicating movement (i.e., slickensides) in the Badenian limestone and a "disturbed" zone from the 2009 geophysical survey (GeoZS, 2010). The presence of slickensides alone cannot confirm the presence of a fault. They can form along jointed surfaces and along the surface of sliding blocks during mass-wasting events. There is no evidence for shearing or displacement of Plio-Quaternary sediments. There are no geomorphic features suggestive of faulting and no lineaments associated with the postulated Stara Vas Fault. The postulated Stara Vas Fault region was cropped and a 0.25 m DEM was produced in an attempt to identify very subtle changes in the surface. No

expression of faulting is identifiable with any of the qualitative or quantitative methods.

4.4.2 Libna Fault

Based on the hillshade map the geomorphic expression of the Libna Fault is limited to Libna Hill (***Exhibit 7 and Figure 4-1***). There is no geomorphic expression of the fault on the north side of Libna Hill and there is no expression of the fault in the Quaternary sediments of the Krško Basin. The Libna Fault is associated with a secondary northwest structural trend identified in the lineament analysis. It is interpreted to be truncated by the OFZ, a part of the northeast structural trend.

A broad shallow depression trending N15W on Libna Hill may define the width (approximately 100 m) and extent (approximately 1.25 km) of the fault zone; however, the depression can also be explained by the presence of karst and associated collapse features, deep-seated landsliding, or a combination of these processes (***Figure 4-1***). It is commonly the case that faulting may lead to increased localized dissolution, leaving pathways for localized karst development and subsequent landsliding. Combined, these may exaggerate the tectonic expression of a fault, and may also explain displacement that was observed in the Libna Hill trench log (GeoZS, 2013). One can postulate that the Libna Fault is isolated within the pre-Plio-Quaternary rock, but the development of karst and associated collapse features has continued to, and will continue to cause displacement of the Plio-Quaternary (and even younger sediments) in the future.

There are numerous examples documented in the academic and professional literature about the incorrect interpretations of active faults and landslides from trenches studies (Hart et al., 2013).

- In some cases, landslides have utilized older fault planes as the slide surface. This is expected, given that a fault plane is a structural plane of weakness. The chemical weathering often associated with a fault plane may further reduce the factor of safety, leading to additional, non-tectonic movements.
- Faults are often mapped solely based on linear scarp recognition; however, many scarps are often better

explained by landsliding processes. In fact, nearly every structural geometric configuration of a fault can also be caused by a landslide (Cotton, 1999; Hart et al., 2013)

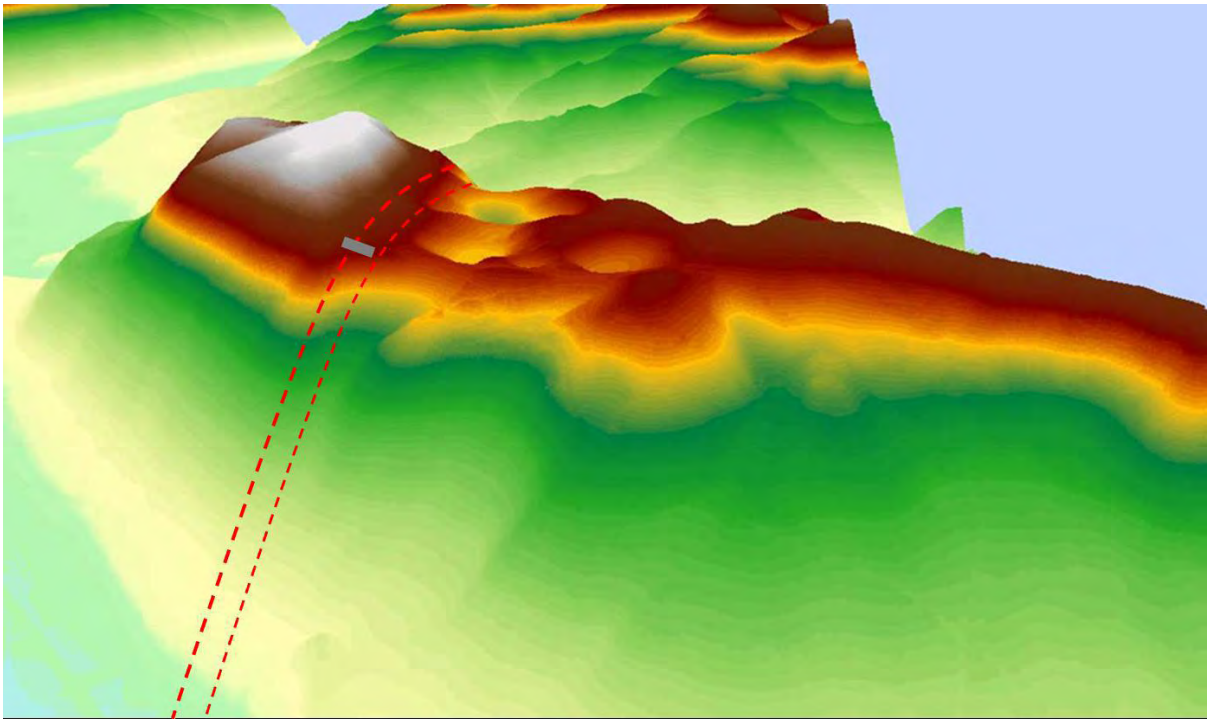

FIGURE 4-1
3D OBLIQUE IMAGE WITH RELEATIVE ELEVATIONS OF LIBNA HILL AND ITS KARST AND LANDSLIDE FEATURES

This is illustrated on ***Figure 4-2*** (Cotton, 1999), which presents an example of a landslide showing associated structures that appear as strike-slip faulting, thrust faulting, and normal faulting. Cotton (1999) demonstrated that, virtually any fault displacement observed in a trench can actually be a landslide feature, therefore a complete geomorphic understanding of the landform being observed is necessary to differentiate the processes observed in a trench.

The structural grain associated with lineaments is often difficult to identify on the hillshade map alone; however, the structural grain is well-defined by the aspect map, because it decomposes the landscape into principal forms that are easily identifiable as shown on the slope aspect map (compass direction the slope is facing as shown on ***Exhibit 8***). The 1.0 m DEM (darker area in northeast quadrant of the DEM) highlights the grain very well, whereas the 5.0 m DEM does not. The grain is somewhat

consistent with the Libna Fault, reflecting the past structural regime; although it is unlikely that the Libna Fault exists north of Libna Hill due to the lack of geomorphic expression based on the hillshade map and the structural control of the OFZ. The structural grain may simply suggest the presence of a weakened orientation in the rock that allows for differential erosion (Pelletier et al., 2009). Nevertheless, the orientation of the Libna Fault is consistent with a weak structural grain, suggesting the Libna Fault may be part of a broader stress alignment in the region, and not solely related to differential folding on the Libna Anticline, as is currently hypothesized.

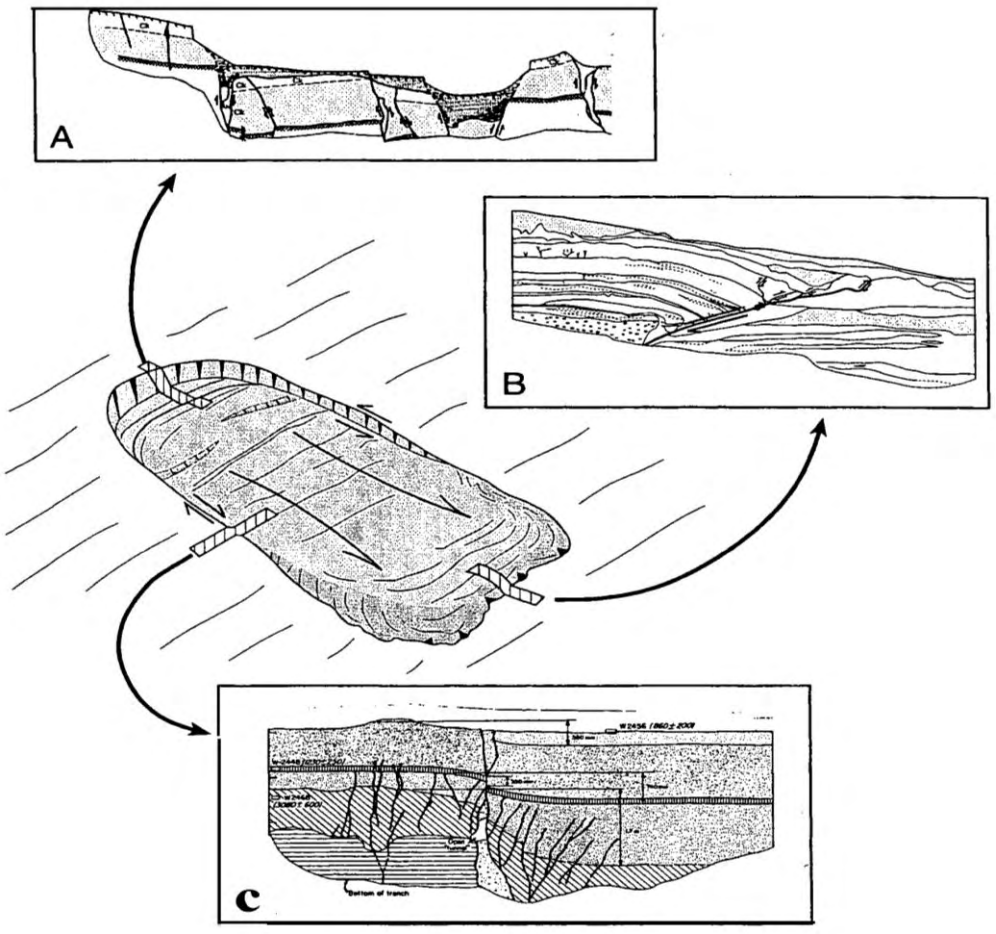

FIGURE 4-2
EXAMPLE OF A LANDSLIDE SHOWING ASSOCIATED STRUCTURES THAT APPEAR AS STRIKE-SLIP, THRUST, AND NORMAL FAULTS

A dominant characteristic of Libna Hill is its very steep flanks to the north, west, and south (***Exhibit 9***). Much of the steepness (orange color vs.

that of green or yellow) can be explained by the presence of fluvial scarps (i.e., risers), particularly in the west, which is likely the result of the Quaternary Sava River incision. Nevertheless, Libna Hill is an anomalously steep hill in the region, consistent with its interpretation as an anticline. The curvature highlights the mapped Libna Fault trace, and is consistent with and corroborates other maps, where it shows highest curvature adjacent to the proposed fault trace; but, as stated above and elsewhere, this can also be explained by various mass-wasting processes, including karstic collapse.

4.4.3 Orlica Fault Zone

The OFZ is a northeast trending strike-slip structure that is a part of the dominant northeast trending structural grain. The OFZ may represent the northern most extension of the Balaton Fault System (BRGM, 2010). The apparent truncation of the east-west structural trend indicates that the OFZ may offset the folds and faults suggesting that it may be younger than the east-west structural trend.

A series of lineaments define the most recent trace(s) of the OFZ. Some of the lineaments northeast of Krško are located differently from the current mapped trace of the OFZ (***Exhibit 7***). Both slope aspect and gradient maps support the delineation of these lineaments (***Exhibits 8 and 9***). The stronger lineaments can be traced from the eastern edge of the DEM to the Sava River. The lineament on the north side of Libna Hill is defined by a narrow curvilinear canyon and drainage. The drainage is significantly over-developed given its contributing area, which can be explained by either of the following: The drainage may represent a relict landform whose contributing area has been removed (e.g., tectonically offset), or the OFZ has fractured the local bedrock, allowing for high rates of dissolution in the carbonate rocks and subsequent erosion of the surface.

Either scenario is supportive of the currently mapped fault trace through the steep drainage. This narrow drainage has a more northerly trend that is different from the N75E trend of the fault to the northeast. The OFZ is thought to have a complex kinematic structure here, and the lineaments

support the hypothesis that it has step-over features that include a step-over to the northeast of Libna Hill (BRGM, 2010).

Approximately 6 km northeast of Krško town, the OFZ widens to as much as 2.5 km to 3 km. The most prominent lineaments occur in the upper portion of the narrow drainage northeast of Krško town and within this broad zone. These prominent lineaments are generally <4 km in length and possibly represent separate fault segments. These youthful-appearing segments may have had more recent activity than other segments, although the evidence is based entirely on geomorphic interpretations from remotely sensed data. These observations indicate that the OFZ, like many large faults, is segmented and that the youthful lineaments defining the segments may represent the most recent activity along the fault zone. Field reconnaissance performed by RIZZO geologists revealed shear zones in outcrops that are associated with the lineaments; however, the shearing was confined to the Miocene bedrock where they were observed.

Depending on the energy released in an earthquake and depth of the hypocenter, fault will rupture at the surface in segments. Typically one to four segments rupture in a seismic event, not the full, mapped fault length (DePolo et. al., 1991; Lettis et. al., 2002; and Manighetti et. al., 2006). The apparent youthful segments identified from the lineament analysis may represent past earthquakes where surface rupture has occurred.

Southwest of the Sava River the lineaments associated with the OFZ are moderate to weak and discontinuous (***Exhibit 7***); however, the possible continuation of the OFZ is evident in the slope aspect map (***Exhibit 8***). The aspect map provides another line of evidence for constraining the location of the OFZ, particularly on the southern edge of the Krško Hills, an area where the OFZ is poorly constrained by geological mapping and geophysics (BRGM, 2010).

4.4.4 Inferred Artiče Fault

A moderate to weak, single lineament consisting of south facing, aligned bedrock and alluvial escarpments is observed on the north side of the

Krško Basin at the base of the Artiče Hills. The sense of motion of the Artiče Fault is based on the geomorphic features making up the lineaments. The geomorphic expression suggests normal dip slip down to the south. This sense of motion is inconsistent with geophysical data (BRGM, 2010) that led to the interpretation that it as a reverse fault. The geomorphic expression would not necessarily appear different for reverse or normal fault kinematics, so this is not inconsistent with the geophysical interpretation. The lineaments, however, show strong evidence for an interpretation of fluvial terraces or erosional escarpments.

The Artiče Hills are highly dissected by fluvial incision especially when compared with the southern slope of the Krško Hills. There has been debate about the differential morphology between the Artiče Hills and Krško Hills, and the prevailing hypothesis is that there are ongoing differential rates of uplift between these two regions, with the Artiče Hills undergoing higher rates of uplift (GeoZS, 2010). The differential uplift has been suggested to be driven by the stepping over between the Orlica and Artiče faults (GeoZS, 2010); however, part of the basis for the conclusion of the recognition of the Artiče structure was based on a stream profile analysis, but the methods applied did not rely on the latest method of stream profile analysis for tectonic evaluation. Recent developments in tectonic stream profile analysis rely on a more robust filtering scheme for evaluating tectonic knickpoints (e.g. Snyder et al., 2000). The newer method relies on removing the bias associated with topographic steepening at tributary junctions due to fluvial processes.

The profile curvature map highlights differences between the two regions (***Figures 4-3 and 4-4***). Because profile curvature is the second mathematical derivative of topography, it can be used to identify components of the landscape showing the greatest rates of topographic change. This is important for deriving information about uplift rates, as regions with high uplift rates often display high curvature.

In soil-mantled landscapes, such as those within the Krško region, curvature may provide information about the time since tectonic deformation, or even the rates of steady tectonic deformation. Degraded soil-mantled landscapes often exhibit low curvature values, because the landscape is generally diffusive, and erosion is typically governed by the

one-dimensional diffusion equation. It predicts that areas of high curvature will degrade most rapidly. Therefore, regions of the landscapes with high curvature are more diagnostic for landscape evolution studies because they are more sensitive to the mechanisms that cause change (i.e., erosion, uplift) (Pelletier et al., 2006; Cline and Pelletier, 2007; Pelletier and Cline, 2007). It is apparent that the region defined by the Artiče Hills (***Figure 4-3***) has a higher curvature (enhanced white on black) than the southern slopes of the Krško Hills to the west (***Figure 4-4***).

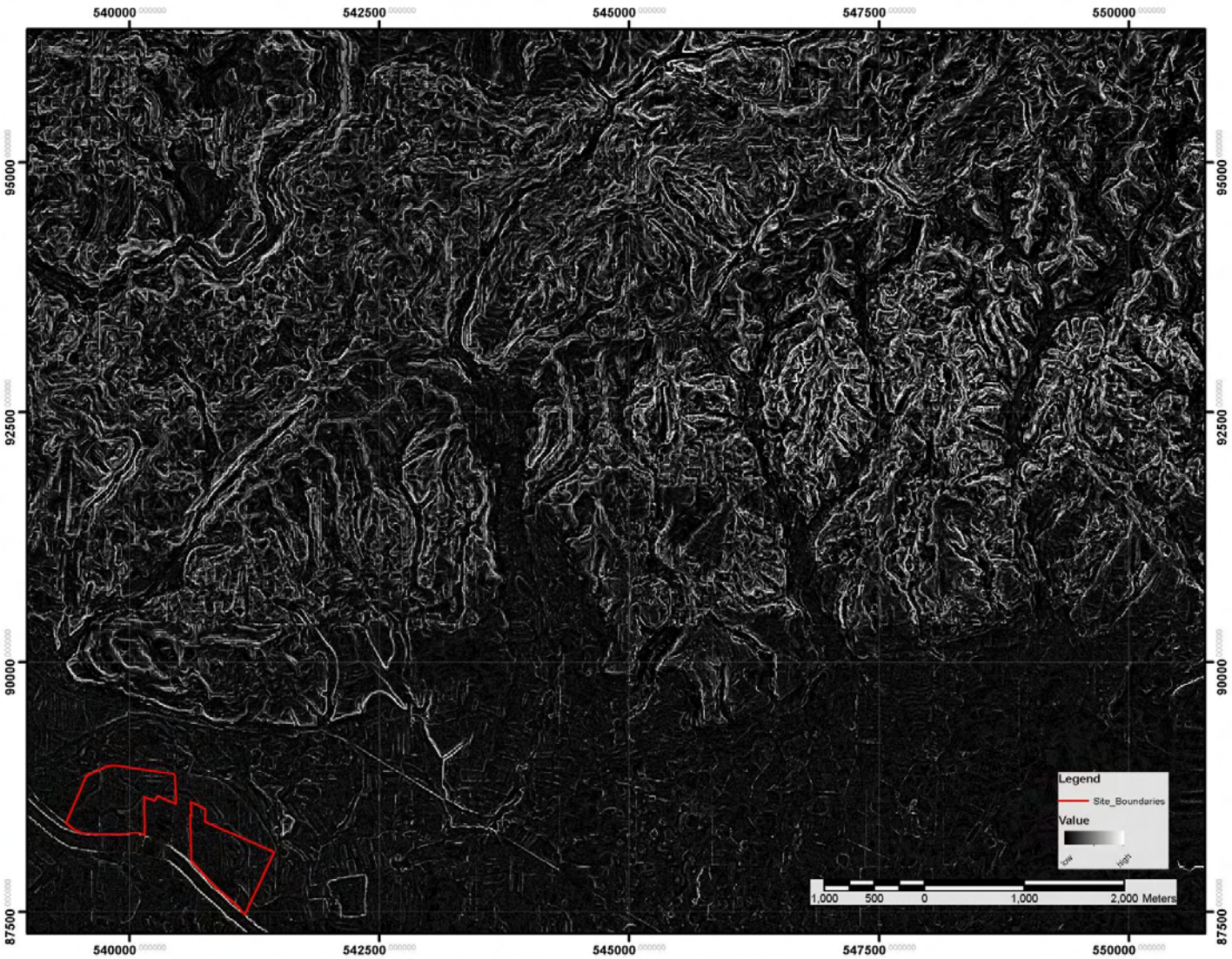

FIGURE 4-3
PROFILE CURVATURE MAP OF THE ARTIČE HILLS

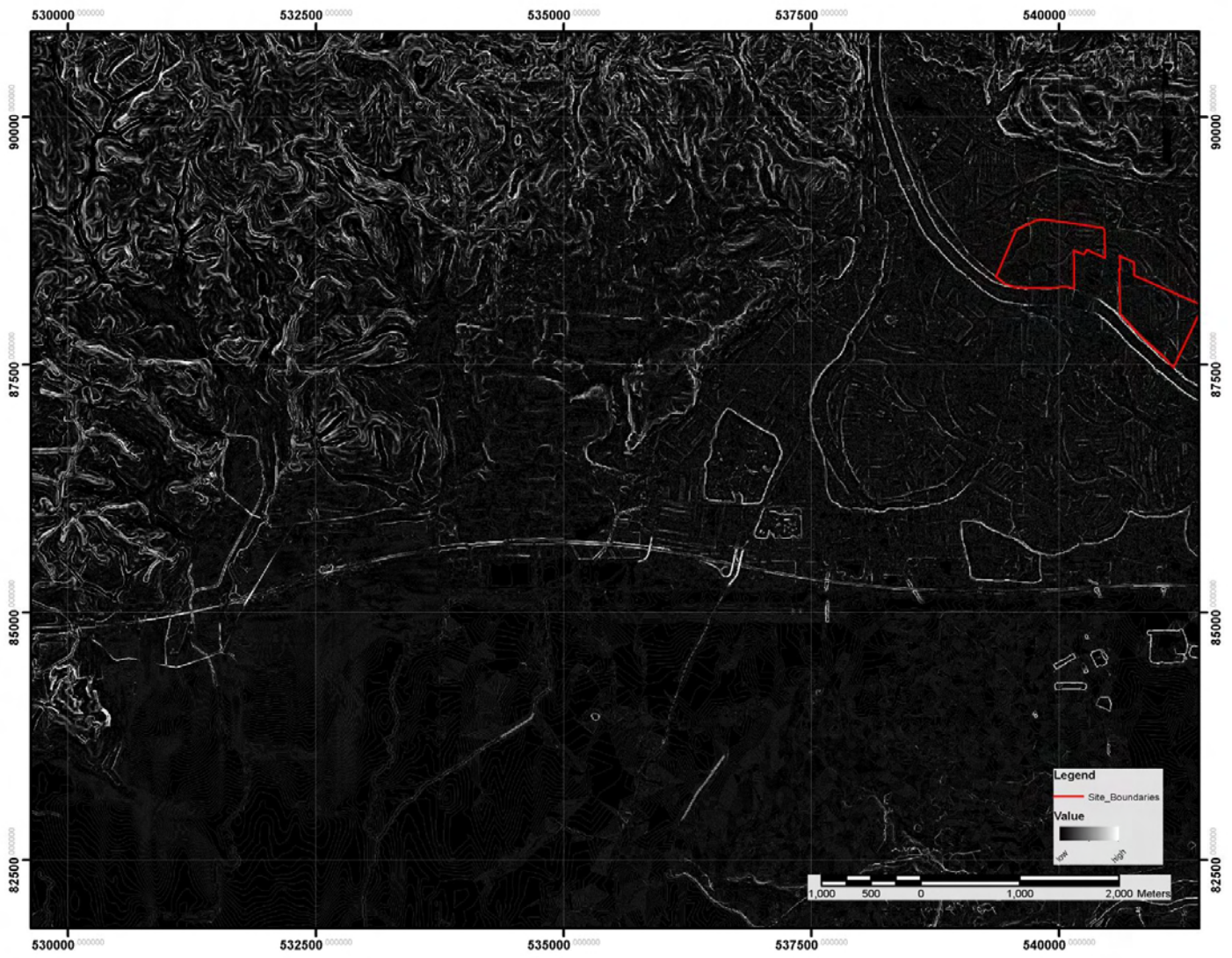

FIGURE 4-4
PROFILE CURVATURE MAP OF THE KRŠKO HILLS

4.5 BASIN MORPHOLOGY

Basin morphology is determined by a combination of the underlying lithology, climate, and tectonics. In relatively small regions such as the Krško Basin, the climate is a relative constant leaving only the lithology and tectonics to control basin morphology. Existing geologic maps allow one to constrain the underlying lithology and, therefore, the basin morphology is highly informative about the regional variability in tectonics.

Drainage basin density is constrained by matching the channel-head locations calculated from a DEM in ArcMap with the location defined by the actual channel head location. This ultimately leads to an empirically-driven definition of the landscape drainage density that is systematic and unbiased because it properly defines a channel head. Instead of drainage density (expressed as length divided by area), the channel head's distance from the hydrological divide was used ("channel density" expressed in length units). Using the length characteristics provides a better drainage density metric (the length from the divide is an inverse proxy for density). It also removes the bias toward purely upward migrating dendritic networks and allows for the relatively common channel initiation by mass wasting processes such as debris flow initiation and shallow (<3 m) landsliding (Montgomery and Dietrich, 1988). Although landsliding may add a stochastic element into the otherwise elegant definition of a channel head (i.e., the point where hillslope profiles transition from divergent to convergent), the length-based definition of Montgomery and Dietrich (1988) provides a more realistic model.

Hypsometric curves and their corresponding integrals are determined for three physiographically similar basins in the Artiče Hills (Basins 1 and 2) and Krško Hills (Basin 4) (***Figure 4-5***). (An additional basin [Basin 3] was discarded due to multiple DEM artifacts.) The curves suggest that the Artiče Hills are undergoing a (slightly) higher rate of uplift. There is a higher proportion of the landscape that is elevated, suggesting that fluvial dissection and landscape denudation is actively occurring. At Basin 4 in the Krško Hills, the landscape is already adjusted, suggesting that any periods of incision related to tectonics have passed. Differences between

the basin morphology of the Krško Hills and Artiče Hills may also be related, to some degree, to differences in underlying lithology.

The relationship between hypsometry and drainage density is often tenuous, given the comparison between a two-dimensional landscape metric (basin density) and a three-dimensional landscape metric (hypsometry). Nevertheless, the observed relationships between the Krško Hills and the Artiče Hills (***Table 4-1***) are consistent with expectations. In general, higher hypsometric integrals correspond with actively uplifting (aka "youthful") landscapes, and it is therefore expected that there would be shorter distances (i.e., higher drainage density) between the channel heads and the drainage divide. The higher drainage density corresponds with landscapes whose elevations are distributed at proportionally higher elevations, and are actively developing drainage configurations.

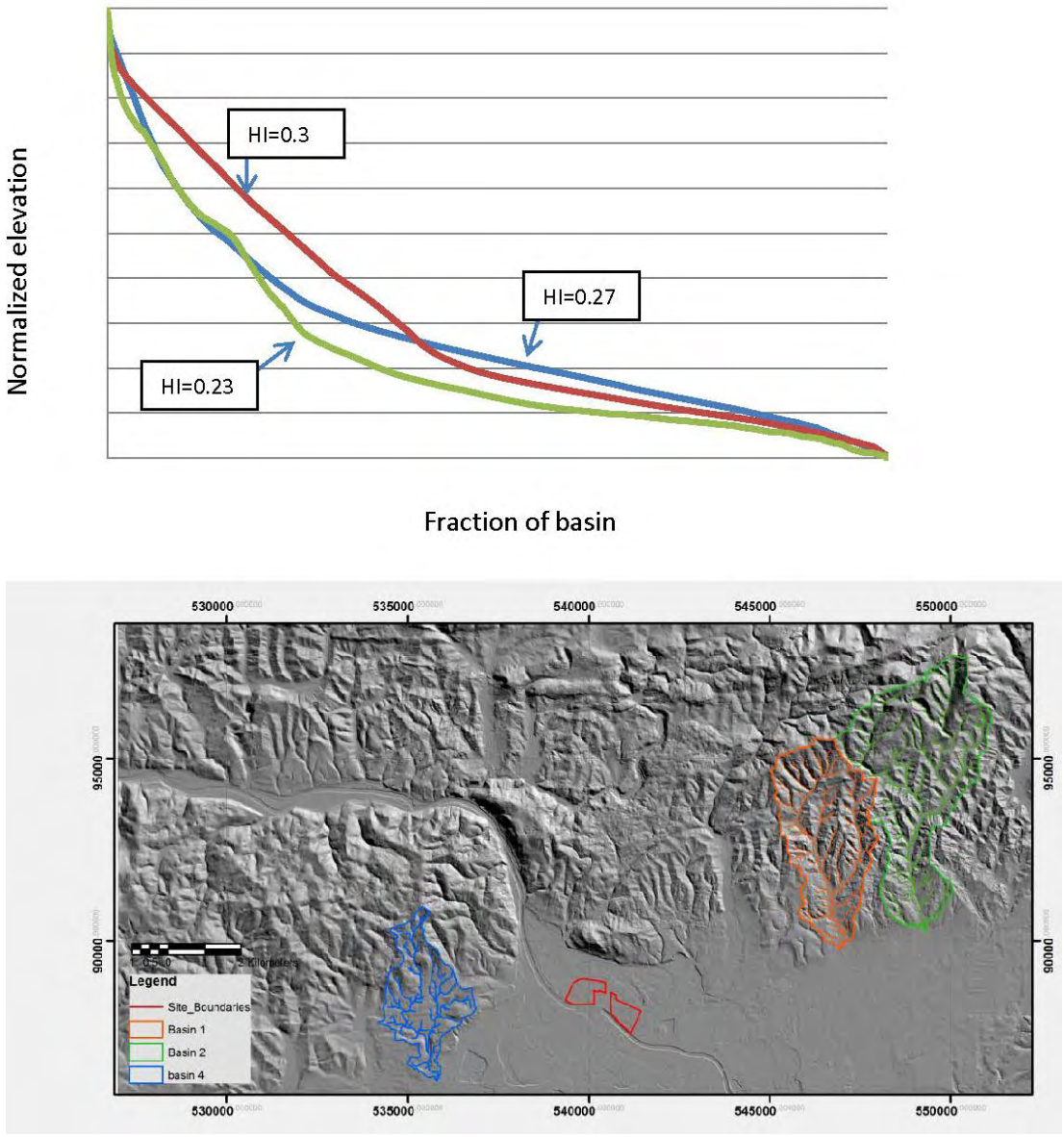

Notes:

The blue basin is in Krško Hills.

The orange, and green basins are in Artiče Hills.

Hypsometry Line colors relate to respective basins.

FIGURE 4-5
HYPSOMETRY BASIN MAP AND CURVES

TABLE 4-1
RELATIONSHIP BETWEEN HYPSOMETRY AND DRAINAGE DENSITY

REGION	DRAINAGE DENSITY (m)	HYPSOMETRIC INTEGRAL (DIMENSIONLESS)
Artiče Hills	120-150	0.27-0.30
Krško Hills	170-225	0.23

Note:

A hypsometric integral of <0.3 represents a relatively stable tectonic environment.

On the Artiče Hills, drainage densities of 120 m to 150 m (from hydrologic divide) correspond to roughly a 0.25 km^2 contributing area for the development of first-order streams within a catchment. So a stream does not incise the landscape where catchments are smaller than 0.25 km^2.

5.0 GEOCHRONOLOGY

5.1 BACKGROUND

An earlier effort to analytically date the sediments in the region, particularly the youngest sediment that may be displaced by the Libna Fault (i.e., the Globoko Formation) in the Libna Hill trench (BRGM, 2010) produced results that are at least one order of magnitude younger than anticipated (GeoZS, 2013). To assess these dates and to better constrain the ages of the regional Quaternary sediments, GEN requested RIZZO conduct geochronology investigations to constrain the age of the Globoko Formation using OSL, IRSL, and CRN (aka Terrestrial Cosmogenic Nuclide [TCN]) dating (RIZZO, 2013d).

Sampling for OSL and IRSL took place during a field campaign in October 2012 by representatives of RIZZO, GeoZS, and the University of Bern. Sampling for CRN took place in January 2013 by representatives from RIZZO and GeoZS.

5.2 APPROACH

RIZZO has provided independent age control for sedimentary units within the Krško region using OSL, IRSL, and CRN, at locations that provide critical, diagnostic information about the regional Quaternary geological history. Each method was specifically selected based on the sampling target's mineralogy (i.e., quartz for OSL and CRN, and feldspar for IRSL), as well as the target's depositional context (i.e., rate of deposition and/or erosional history). Combining these analytical methods provides a more robust geochronology because independent methods are being used to date the same deposit and each method targets a different age range. OSL and CRN have different (although overlapping) age limits (i.e., age capacity), so selecting the right method is important as well. OSL has a much lower age capacity than CRN. The capacity is not well defined, however, because the actual capacity of OSL is dependent upon both the environmental conditions, as well as the specific luminescence properties of mineral in the sample (Wintle, 2008). It is well-known that OSL has underestimated the age of known-age deposits. Therefore, applying multiple methods is critical. OSL typically targets Holocene and Late

Pleistocene sediments (<125 Ka), whereas CRN can target sediments ranging from the Holocene to the earliest Pliocene (<5 Ma). Applying multiple geochronology techniques provides a means to assess prior age dating efforts and constrain depositional ages.

Prior fault trenching and geochronology investigations of the Libna Fault by the BRGM Consortium (BRGM 2010; GeoZS, 2013) yielded ages for the post-Miocene (<5 Ma) sedimentary deposit within the fault zone on Libna Hill that were much younger than anticipated and inconsistent with the published findings (Verbič, 2005). These younger-than-anticipated dates led the BRGM Consortium to a position that the Libna Fault was capable under International Atomic Energy Agency (IAEA) guidelines. Due to the significant departure from the expected and previously accepted age (>2 Ma) for the Globoko Formation, GeoZS argued that the OSL-derived age is not representative, and provided several alternative explanations (GeoZS, 2013).

The intent of dating these Quaternary sediments is to identify the time of deposition, not the time of erosion or exposure time. The methods applied here are direct methods that date the actual material of interest. They are not proxy-depositional ages (i.e., radiocarbon dating of allochthonous or autogenous material or Uranium-Thorium dating of pedogenesis).

All of these methods rely on the very important assumption that the sediments have remained stable throughout their post-depositional lifespan, i.e., the modern depositional environment is representative and allows for meaningful interpretation of the sediment's age. This is a critical assumption because remobilization and subsequent deposition of the sediment will decrease the age — the age may be analytically correct, but may date the wrong depositional event. This makes careful interpretation of the geomorphic environment key for meaningful interpretation of ages.

Note also that the OSL method has a much younger upper limit to its age range than CRN does. Quartz OSL has a theoretical upper limit of roughly 2 Ma, although such an age has never been achieved. Saturation often occurs in <200 thousand years (Ka) (Murray et al., 2007).

As a result, ages that are older than the method's dating capacity (i.e., the oldest age a specific method's chronometer allows) will systematically result in the same age that must be considered a "minimum age."

5.3 SAMPLE COLLECTION

RIZZO and GeoZS geologists spent the weeks of 16 and 23 October 2012 and 7 and 14 January 2013 in the field selecting suitable sampling sites and collecting samples for both OSL and CRN methods. Ultimately, seven sites were selected: one for a 15.0 m borehole for CRN sampling and six for OSL sampling (***Exhibit 10***).

Initial sample site selection was based on the assigned mapped unit and accepted ages of the units based on the expertise of GeoZS staff and published literature from the region. Specific sample site selection was based on the following criteria:

- How diagnostic a landform is for interpreting regional tectonics (e.g., avoiding active slopes and ambiguous landforms)
- Degree to which bedding has been preserved
- Availability of appropriate materials (i.e., grain-size and mineralogy)
- Permissions from land owners and ease of access (e.g., road cuts, existing excavations)
- Designation of depositional unit (i.e., mapped unit designation)

For OSL sample collection, metal conduit tubes were hammered into exposed sand lenses with visibly preserved bedding and limited bioturbation. This method is necessary because OSL is sensitive to light and ensures that only the outer few millimeters are ever exposed to modern light. The method preserves the burial conditions at the time of sediment deposition and the luminescence properties at the time of sampling. Dose rate samples were collected as well. (i.e., the natural decay rate of Uranium [U], Thorium [Th], and Potassium [K]); representative samples were collected from the surrounding 10 centimeter (cm) from the sample tube.

For the CRN sampling, a 15 m borehole was drilled on the crest of Libna Hill to ensure the deepest samples were collected. For burial ages, a >8 m depth is required to ensure interpretable results. Site selection had to consider the need to use a small drill rig.

Ultimately, a site was selected on the eastern ridge of Libna Hill where there is minimal topographic shielding and where the Globoko Formation appeared to be intact and stable. The ridge at the crest is oriented in a general east-west direction. To the southwest, the crest has been subjected to mass wasting. To the north the slopes are likely more diffusive. The deposit at this location is mapped as the same unit that was encountered at the Libna Hill Trench (BRGM, 2010).

5.4 GEOCHRONOLOGY METHODS

The methods used for geochronology were OSL and CRN. These methods are briefly described below.

5.4.1 Optically Stimulated Luminescence (OSL)

OSL is used to determine the last time quartz or feldspar minerals were exposed to light (Huntley et al., 1985). Luminescence dating relies on the premise that sediment is exposed to light during fluvial or eolian transport. During that exposure time, trapped electrons within the crystal lattice (the "charge") are released and the luminescence charge is emptied. This process is known as "zeroing" of the mineral grain (Rittenour, 2008). The zeroing of the grains is dependent upon the light intensity and duration of light exposure, which are both functions of the transport mechanisms. Luminescence dating is, therefore, sensitive to the depositional environment and recent bioturbation.

When quartz or feldspar are buried and removed from light, ionizing radiation from the natural radioactive decay of the substrate produces free electrons that are trapped within imperfections of the quartz crystal lattice (i.e., "traps"). The accumulation of the trapped electrons (i.e., "charge") occurs at a rate proportional to the U, Th, and K decay (i.e., environmental dose rate). The calculated age of burial is a function of the

accumulated charge in the traps. When the traps in the lattice are filled, the charge can no longer accumulate and saturation is reached. At the point of saturation, the reported luminescence age will always be younger than the true age of sediment deposition. The time to saturation is dependent on both the properties of the unique crystal structure, as well as the environmental dose rate (high dose rates lead to early OSL saturation), but quartz OSL saturation often occurs in <200 Ka (Murray et al., 2007).

5.4.2 Cosmogenic Radionuclide (CRN)

CRN burial ages are used to determine the timing of sediment burial (Granger and Muzikar, 2001). In the simplest sense, for CRN burial dating to work, sediments must be buried deeply enough that that the in-situ production of cosmogenic radionuclides is negligible. CRN burial dating relies on the premise that cosmic rays bombard the Earth, producing CRNs. From these reactions, secondary particles are produced; the most relevant of which are neutrons and muons (Lal and Peters, 1967). When these reactions occur within minerals within the upper part of the Earth's near-surface (predominantly in the upper 4 m, but attenuates with depth), in-situ CRNs are produced. These are extremely useful for geological dating purposes if the CRN production rates and their respective half-lives are constrained (Granger and Muzikar, 2001); however, the site-specific in-situ production rates are complicated by geographic location (i.e., latitude and altitude) (Stone, 2000), as well as local scaling factors such as snow cover and topographic shielding (Vermeesch, 2007).

The scaling factors are not easily accounted for in the calculation of ages. For Quaternary geological timeframes, some of the more relevant cosmogenic radionuclides are ^{10}Be and ^{26}Al, both of which are produced in quartz, which is ideal for most dating purposes because quartz is both abundant in the natural sediment cycle and highly resistant to weathering (Granger and Muzikar, 2001). The production rates for both cosmogenic radionuclides are reasonably well constrained: the production ratio of ^{26}Al and ^{10}Be is ~6.8 (Balco and Rovey, 2008), and the ^{26}Al and ^{10}Be decay rates differ by a factor of ~2. Furthermore, the production rates of in-situ cosmogenic radionuclides attenuate with depth in a predictable manner,

making it possible to model the expected CRN production rate at any depth using a series of exponentials (Granger and Muzikar, 2001).

The simplest method of sediment burial dating with CRNs is simple burial dating (Granger and Muzikar, 2001). For this method, it is assumed that sediment is buried deeply enough to where CRN production rates are negligible. As a result, many of the assumptions and scaling factors are unnecessary for the age calculation and both surface erosion and inheritance do not need to be considered. The only necessary assumption is that the CRN inventory (i.e., the accumulated ^{26}Al and ^{10}Be concentration per gram of quartz) in the sediment is derived from a steadily eroding basin upstream, in which the CRN production reaches equilibrium with the erosion rate, and that the sample is rapidly transported and well mixed, as is the case for most fluvial settings (Balco et al., 2012). The final age of burial (i.e., deposition) is then determined from the ^{26}Al and ^{10}Be ratio because both the production and decay rates are known. In the case of deep burial, the production rate is negligible and assumed to be zero, so only the decay rate is needed. The final age is derived from ^{26}Al and ^{10}Be and relies on the known differential decay rates (higher ^{26}Al and ^{10}Be is a younger age).

5.5 SAMPLE ANALYSIS

The PRIME Laboratory (USA) was contracted for the CRN dating and the University of Bern (Switzerland) was contracted for OSL dating. Both laboratories were qualified under RIZZO's Quality Assurance Program.

5.5.1 PRIME Laboratory

Physical and chemical preparations of the CRN samples were performed by PRIME Laboratory at their physical and chemical pre-treatment laboratory. At that lab, they isolated pure quartz targets for ^{26}Al and ^{10}Be measurements. Actual measurements of the ^{26}Al and ^{10}Be were performed on their accelerator mass spectrometer (AMS), which can measure very low levels of long-lived, stable, and unstable nuclides.

5.5.2 Bern OSL Laboratory

Physical and chemical preparation of samples was performed at the OSL lab at the University of Bern. Pure quartz and feldspar were isolated so that their luminescence signal could be measured. OSL measurements were performed on quartz, and for samples that showed signs during measurement of approaching saturation, on feldspar as well. Background dose rate measurements of U, Th, and K were completed at the University of Bern as well using mass spectroscopy to measure dose rate-contributing radioactive elements.

Due to the controversial young ages derived from the Libna Trench (GeoZS, 2013), it was necessary to determine the methodological limitations present with OSL in the Krško Basin sediments. At the request of GEN, RIZZO led an independent technical review to evaluate the data and methods used by the University of Bern lab. Dr. Rittenour from the USU Luminescence Laboratory conducted the independent review. Dr. Rittenour's review (which can be found in ***Appendix 3***) and key statements, are referenced below in the discussion.

5.6 RESULTS

The sample sites and respective ages are shown on ***Figure 5-1***. Results from OSL are internally consistent, although when compared with CRN results, the OSL samples from the inferred Plio-Quaternary (Globoko) samples are an order of magnitude younger. Reconciliation of these differences and their implications for regional tectonics are discussed in ***Section 6.1 and 6.2***. Results from the OSL testing are presented in ***Appendix 4*** and synthesized in ***Table 5-1***. ***Appendix 5*** is the data report provided by PRIME for CRN results. Results derived from the CRN method (RIZZO, 2013e) are presented in ***Table 5-2***.

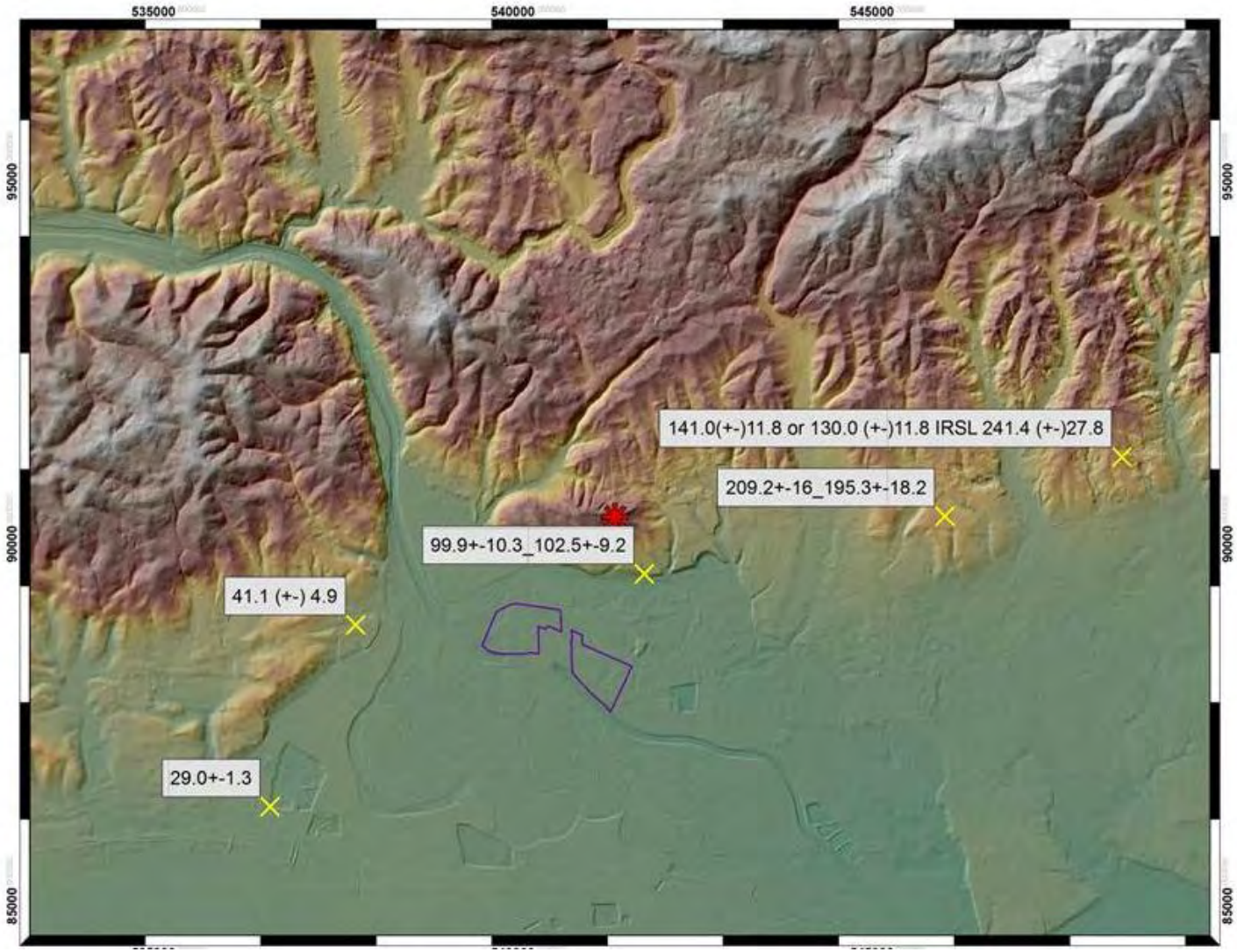

FIGURE 5-1
GEOCHRONOLOGY SAMPLE LOCATION MAP WITH AGES

TABLE 5-1
AGE DATING RESULTS OF CRN ANALYSES

AMS (CRN) sample ID	Cosmogenic ^{26}Al Atoms Per Gram SiO2	Relative Uncertainty (%)	Cosmogenic ^{10}Be Atoms Per Gram SiO2	Relative Uncertainty (%)	^{26}Al/^{10}Be	*Minimum Burial Age (Ma)
RIZZO-CRN-JAN2013-15.0	-	NA	49,505	23.8	NA	NA
RIZZO-CRN-AUG-2013-14-14.2	150,475	64.4	28,933	9.6	5.2 (+4.26/-3.51)	0.65 (+2.33/-1.24)
RIZZO-CRN-AUG-2013-12.7-12.9	112,411	56.7	37,522	6.6	3.00 (+2.03/-1.79)	1.79 (+1.86/-1.07)
RIZZO-CRN-JAN2013-10.5	158,359	47.6	51,814	7.3	3.06 (+1.81/-1.56)	1.75 (+1.48/-0.96)
RIZZO-CRN-JAN2013-8.0	136,726	225.6	52,546	22.2	NA	NA
RIZZO-CRN-JAN2013-6.0	146,534	111.0	66,279	19.8	NA	NA
RIZZO-CRN-AUG-2013- 3.4-3.55	NA	NA	76,797	6.5	NA	NA
RIZZO-CRN-AUG-2013-2.75-2.9	NA	NA	62,668	5.8	NA	NA
RIZZO-CRN-JAN2013-1.0	1,244,389	33.8	246,741	5.4	5.04 (+2.09/-1.88)**	0.68 (+0.94/-0.71)**
RIZZO-CRN-AUG-2013-0.45-0.6	NA	NA	308,763	3	NA	NA

Notes:

* Muon production at depth is not accounted for.

** Sample too near surface; it is too shallow to be treated as a burial age due to high CRN productions rates.

TABLE 5-2
SUMMARY OF AGE DATING RESULTS FROM OSL ANALYSES

OSL SAMPLE ID	OSL AGE (KA)	IRSL AGE (KA)	PREVIOUSLY EXPECTED AGE
BERN-01-Libna	99.9 ± 10.3	-	<125 Ka
BERN-02-Libna	102.5 ± 9.2	-	<125 Ka
BERN-03-Libna	31.9 ± 2.4	-	<125 Ka
BERN-05-Libna	209.2 ± 16.0	-	Plio-Quaternary (>2 Ma)
BERN-06-Libna	195.3 ± 18.2	-	Plio-Quaternary (>2 Ma)
Krsk1	41.1 ± 4.9	-	Late Pleistocene (<125 ka)
USU-01-Libna	140.0 ± 11.8	241.4 ± 27.8	Plio-Quaternary (>2 Ma)
GBL2	130.1 ± 11.8		Plio-Quaternary (>2 Ma)

5.6.1 Discussion of the OSL Results

The OSL chronology constrains the aggradation and incision rates within the middle-late Pleistocene sedimentary deposits of the Krško Basin. Based on landform morphology, it is apparent that many of these sediments are derived from tributaries as opposed to the Axial River (i.e., Sava River). The OSL data suggest several samples suffered from saturation issues (***Appendix 4***), particularly the two samples at the Globoko Mine site that were dated at roughly 130 Ka (Sample GBL-2) and 140 Ka (Sample USU-01-Libna); however, other sediments, such as those located near Artiče Terrace (BERN-05-Libna and BERN-06-Libna) returned ages of ~200 Ka and the sediment's level of saturation at Artiče Terrace was not as evident. If the Artiče Terrace OSL ages are in fact, non-saturated, true ages, they suggest that the two locations comprise different sediment provenances, or at a minimum, that the deposits at the Globoko Mine site and the Artiče Terrace site are composed of mixed sediment sources from different provenances.

From a morphological perspective, it is feasible that both sites may originate from tributary sources and not the Axial River; however, a detailed geomorphic investigation to determine the local provenance was not conducted.

It is also important to note that OSL saturation is not always readily detectable using standard methods (Zander and Hilgers, 2013). For this study, numerous methods were applied that tested the OSL saturation. IRSL was applied to feldspar grains. Feldspar can typically extend the

ages of OSL because the mineralogy allows for a larger charge than quartz, although the absolute ages from IRSL may not be as reliable. For this study, IRSL was applied to test for saturation and the measured IRSL ages were significantly higher (***Table 5-1***), suggesting the quartz OSL was saturated. Details are described in ***Appendix 4***.

The possible saturation of the OSL signal in the quartz grains suggests that OSL may not be appropriate for constraining the ages of the Plio-Quaternary deposits because any sediment deposit with a true age >150 Ka to 200 Ka will then return an age that maximizes at 200 Ka. This finding is consistent with published works globally (Murray et al., 2007), where maximum OSL ages rarely reach 500 Ka, and in many cases, quartz OSL reaches saturation in <200 Ka. As a result, most published OSL ages are from the late Quaternary (i.e., ~125 Ka). This has further implications to the ages returned from OSL in the Libna Trench (GeoZS, 2013), where saturation was also suspected, although not as rigorously tested. Because the sediments are likely saturated, the reported ages should only be treated as minimum ages.

The independent technical review provided by Dr. Rittenour of USU (***Appendix 3***) reported several key findings as follows:

- There are strong technical merits of the OSL analysis completed at the University of Bern.
- The results from the OSL analysis do suggest that oversaturation is an issue, as was described in the OSL report from the University of Bern.
- Based on stratigraphic relationships and sample elevation differences, it is highly probable that some of the younger-than-expected ages are a function of mis-mapping of the sediments. This is implied by GeoZS in ***Appendix 6***, based on a comparison of lithological data from a 30m borehole on the Brežice Terrace with surface exposure samples. The OSL method does an adequate job at constraining the ages of the Late Pleistocene (<125 Ka) sediments.
- The OLS method becomes saturated when it approaches ~130 Ka to 200 Ka. The detectability of the saturation is not straight-forward, although the samples from the Globoko Mine are likely 20 to 30 percent saturated based on evidence from the IRSL tests.

- The merits of the OSL samples from the trench on Libna Hill (GeoZS, 2013) cannot be assessed. Nevertheless, the elevation differences suggest they are likely of a different age than the sediments at the Globoko Mine and Artiče Terrace.

RIZZO strongly agrees with Dr. Rittenour's position that there are issues with the way the so-called Globoko Formation is currently mapped. Some of the sediments with similar lithology that are presently mapped as the Globoko Formation may be reworked Globoko Formation sediments or simply a younger, inset terrace within the Sava River system. It is also important to reiterate that Dr. Rittenour was not able to comment directly on the OSL ages from the Libna Trench because the data were not available; however, the ages derived from the trench do not allow for a reasonable interpretation of the landscape evolution in the Krško Basin and broader region. This topic is expanded upon below, where we discuss the geomorphic conditions required to reconcile the geochronology, including the OSL ages from Libna Hill.

5.6.2 Discussion of the CRN Results

Eleven CRN burial samples were collected from a borehole on the Libna Hill between 1 m and 15 m. Each was measured for ^{26}Al and ^{10}Be inventories (atoms per gram of quartz) using AMS. ^{10}Be measurements were successful for all but the 3.0 m depth sample due to an unexpectedly low quartz yield. As a result of the low yield, ^{26}Al results were only obtained from three samples at 10.5 m depth. The extremely low yield was unexpected, given that prior mapping revealed very high quartz content in the samples.

^{26}Al and ^{10}Be simple burial ages were calculated from three samples at various depths (i.e. 14.2 m, 12.9 m and 10.5 m). The depth of the borehole allowed for the age calculation using the simple burial method (Granger and Muzikar, 2001). The method produces the most reliable bracket for the young age (minimum age) because it relies on the well-constrained decay ratio of ^{26}Al and ^{10}Be (~2:1), and limits assumptions and interpretations. The minimum ages based on the ^{26}Al and ^{10}Be are ~1.8 Ma (analytical uncertainty shown in ***Table 5-2***). This suggests that deposition of the Globoko Formation on top of Libna Hill occurred as

recently as ~1.8 Ma but most likely occurred at a much older date because the reported age does not account for the CRN production by muons at 10.5 m depth. This usually pushes ages 10-30% older than the minimum calculated age. The results of the CRN dates are presented in ***Table 5-2*** (from ***Appendix 5***)***.***

The only critical assumption when applying the simple burial method is that the sample was adequately mixed prior to burial. This assumption is validated because the sample is composed of fluvial gravel (Matmon, et al., 2012). ***Figure 5-2*** presents the burial plot of the samples showing the ^{26}Al and ^{10}Be ratios plotted against the total ^{10}Be inventories. The plotting method graphically illustrates the time since burial (burial age), as well as prior exposure history of the sediment. The advantage of simple burial dating is that the initial CRN inventory (inheritance) does not need to be known; it only needs to be high enough to allow for radionuclide decay. Additionally, the ^{26}Al and ^{10}Be are insensitive to surface erosion provided the sample is buried deeply enough. That is because the production of CRNs reaches a point where it is low enough to not significantly impact the decay rate; however, when a sample is not buried deeply enough, the production of in-situ ^{26}Al and ^{10}Be continue at a rate proportional to their production ratio, attenuated by its depth of burial while simultaneously decaying at the known ratio of ~2:1. This increases the ^{26}Al and ^{10}Be and, consequently, causes a younger-than-true age to be calculated (i.e., "naïve age") (Granger and Muzikar, 2001). As a result, the simple burial age of a ^{26}Al and ^{10}Be should always be considered a minimum age.

There is significant analytical uncertainty associated with the ^{26}Al measurements that lead to ^{26}Al/^{10}Be ratios (Table 5-1) with large (but similar) analytical uncertainty; however, there is good precision for the calculated ^{26}Al/^{10}Be burial ages from 10.5 m and 12.9 m depth. Furthermore, ***Figure 5-3*** shows the well-behaved ^{26}Al and ^{10}Be depth profiles that attenuate with depth in a predictable manner although the CRN depth profile could not be used to calculate an age due to high erosion totals. Very high erosion totals add significant uncertainty to the interpretation of the ages, the site where the CRN samples were collected has undergone at least 23 m of erosion. Approximately 1.2 km to the west, there is a mapped Globoko Formation deposit at an elevation of

~345 m on top of Libna Hill and the Elevation of the CRN borehole is 322 m. While the depth profile cannot be used to provide an analytical age with confidence, it does provide a basis for qualitatively evaluating the burial age's quality.

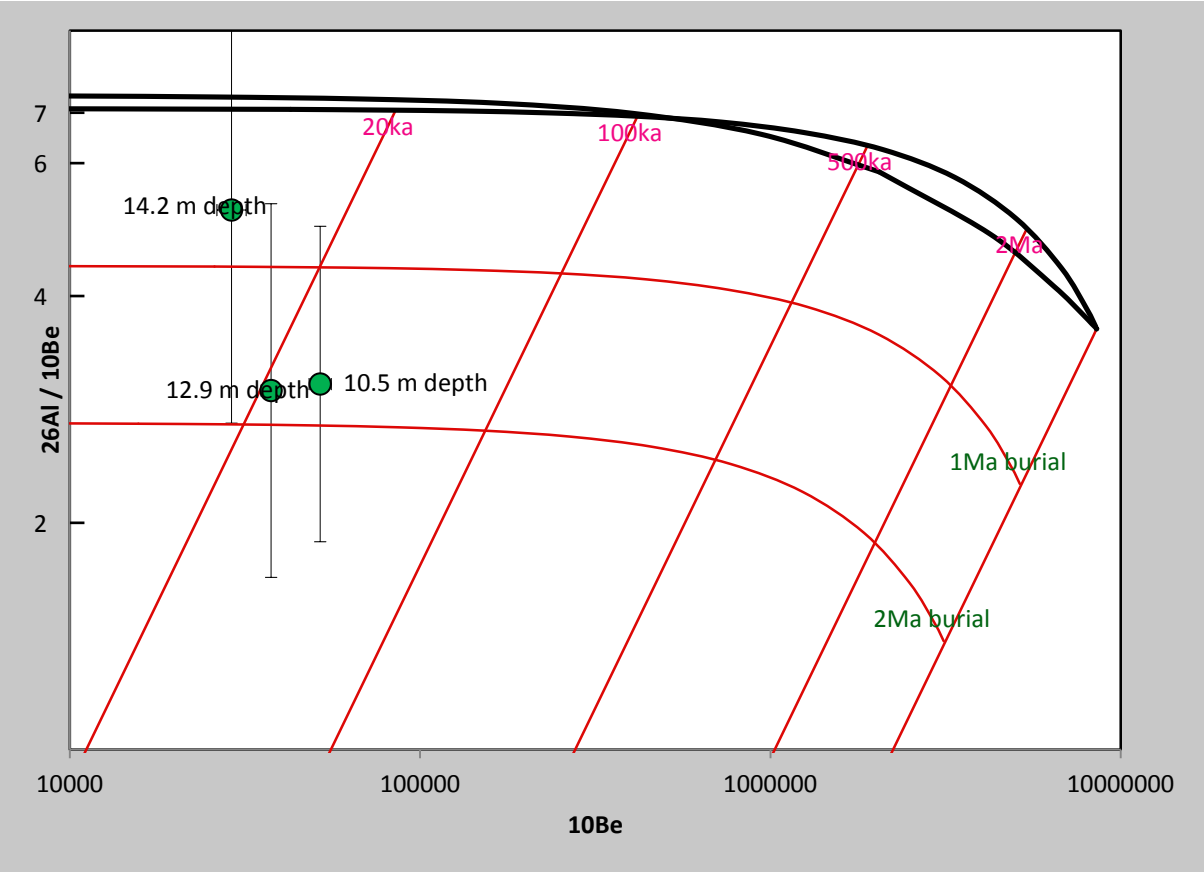

Notes:

Minimum (no muon production calculated) burial ages from CRN borehole at different depths. Deepest calculated depth suggests a minimum age of roughly 1.8 Ma. 1-sigma (standard deviation) of the $^{10}Al/^{10}Be$ and ^{10}Be are shown by the vertical and horizontal error bars, respectively.

FIGURE 5-2
"BANANA" PLOT OF CRN MINIMUM BURIAL AGE

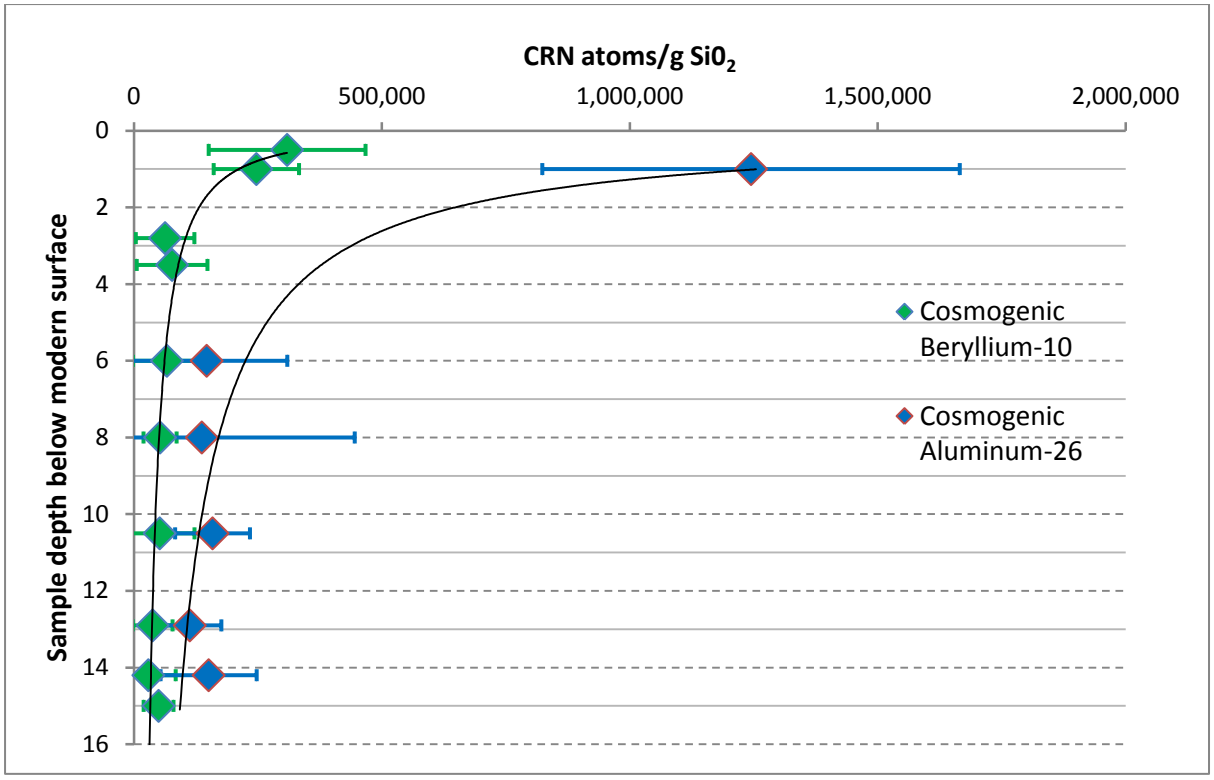

FIGURE 5-3
^{26}AL AND ^{10}BE DEPTH PROFILES

5.6.3 Reconciling the OSL and CRN Chronologies

There is significant disparity between the depositional ages derived from OSL and those of the CRN method for the same mapped unit. To resolve these differences it is important to first recognize that OSL in the Krško Basin may have a saturation limit of 150 ka to 200 ka. ***Figure 5-4*** shows a possible limit for the OSL in the Krško Basin, as evidenced from the dramatic limiting constraint on the age, regardless of the elevation of the sediment being dated. Earlier efforts at dating the Globoko Formation on Libna Hill may have overlooked this, thus returning a saturation age instead of a depositional age (GeoZS, 2013).

Using principles of geomorphology, it is expected that the sediments on top of the Libna Hill (i.e., from the Trench) would be significantly older than those located 100 m below them. Alternatively, the upper elevation sediments could be younger if the units were massive, undergoing steady aggradation, but they should not be the same age.

A straight-forward explanation for the elevation-age relationship is shown on ***Figure 5-4***. Saturation may be limiting the OSL method's capability with sediments older than 140 Ka to 200 Ka. This is supported by the Bern Laboratory's analysis as well as Dr. Rittenour's expert review (***Appendix 3***). While saturation was briefly discussed in the Libna Trench report (GeoZS, 2013), the samples dated did not undergo rigorous saturation testing as was done for this iteration of age dating. The strong evidence for OSL saturation at the Globoko Mine (***Appendix 4***), combined with a reliable simple burial CRN age on Libna Hill, further supports the likelihood of saturation of OSL samples from the Libna Trench. It is also well known that CRN has the ability to date older sediments than OSL, making CRN a more suitable method for dating the Globoko Formation, which has long been thought to be older than 2 Ma.

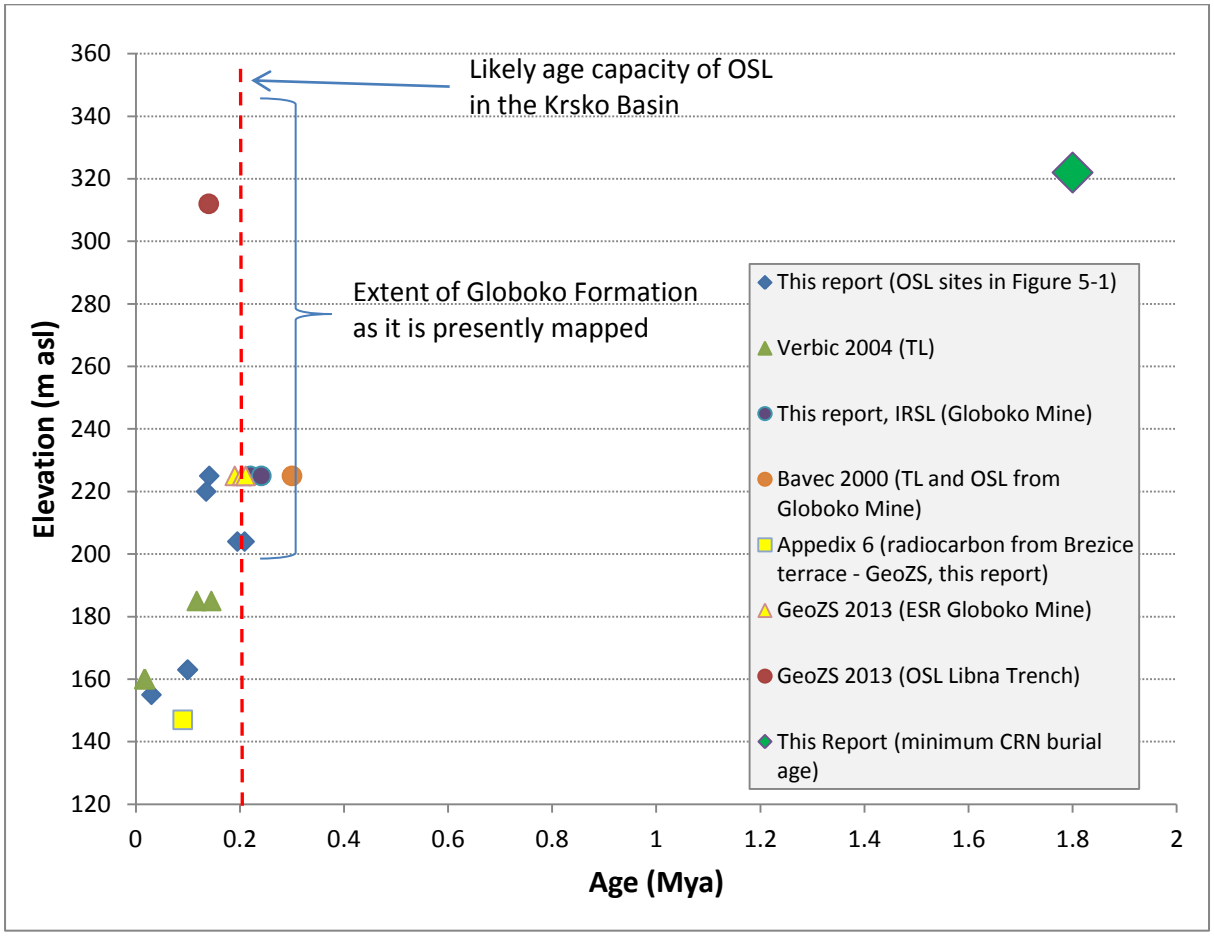

FIGURE 5-4
POSSIBLE LIMIT OF OSL METHOD IN THE KRŠKO BASIN

In addition to selecting age-appropriate methods, reconciling the differences between the different methods needs to consider the

geomorphic processes that have formed the regional landscape. There is morphological evidence that some small refinements may be necessary to constrain the geological model, specifically, to constrain the extent of the true Plio-Quaternary deposits and the processes that may have resulted in alteration.

The presently mapped Plio-Quaternary sediment from the Artiče Terrace was dated with OSL at ~200 Ka. The OSL ages do not show strong evidence for saturation, suggesting they may be representative ages. If this is the case, the sediments may have been reworked by fluvial processes, thus resetting the OSL "clock." Therefore, we would not expect the ages on Libna Hill or any other true, in-situ Globoko Formation to be the same, although the lithological content of the sediment is similar (lack of carbonate clasts which discriminate these sediments from the ones deposited in Quaternary by the Sava river; see ***Appendix 6***). It is feasible that many of the Plio-Quaternary gravels mapped at lower elevations are, in fact, reworked Globoko Formation, having been re-deposited by tributaries, as opposed to the axial paleo Sava River (as is currently implied). From a morphological perspective, they appear to take the form of eroded alluvial fans. Refining the map of the Plio-Quaternary sediments from a process geomorphic and landscape evolution perspective will shed a great deal of light on these disparities. Furthermore, constraining the extent of the in situ Plio-Quaternary has implication about regional uplift patterns in the Krško Basin.

5.7 IMPLICATIONS FOR THE AGES DERIVED FROM THE LIBNA TRENCH AND OVERALL LANDSCAPE EVOLUTION

OSL results appear to constrain ages for middle-late Quaternary deposits in the Krško region, but they lack the ability to date sediments older than about 200 Ka. Therefore the OSL geochronology from the last 100 Ka helps to constrain the rates of aggradation (infill of sediment to the Krško Basin), as well as Sava River incision, which acts as the local base level (control) for regional incision patterns. The CRN geochronology constrains the aggradation and fluvial abandonment of the Plio-Quaternary terraces and highlights the issues associated with applying the incorrect geochronology techniques to older sediments.

The OSL ages from the Libna Trench should not be considered representative of the age of the Globoko Formation's sediment on top of Libna Hill. The top of Libna Hill is nearly 100 m above the Globoko Mine site and Artiče Terrace. If the ages from the Trench site and the 200 Ka age for the Artiče Terrace are accurate, then a series of unlikely events would have had to occur.

The following unlikely "catastrophic" scenarios would need to be considered to describe the fluvial history of the Sava River. They are inconsistent with the current understanding of landscape evolution in regions that are not undergoing significant orogenic uplift (Montgomery and Brandon, 2002).

- ***Scenario 1***: A very significant aggradation event would have had to deposit >120 m of sediment in less than 60 ka (to the top of Libna Hill). It would have been followed by a very dramatic period of "catastrophic" incision, where more than 100 m of sediment would have been eroded across the entire basin nearly instantaneously, before returning to more reasonable rates of incision and aggradation (***Figure 5-5***).

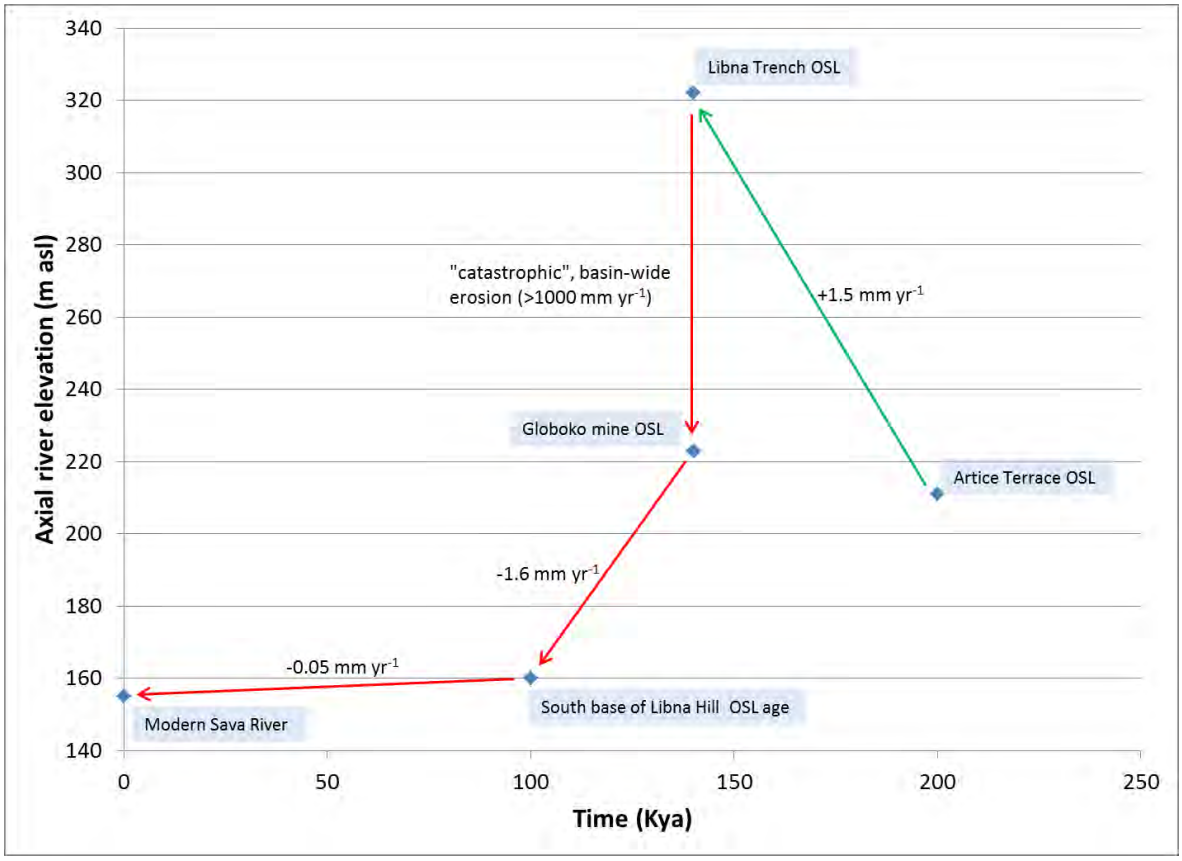

FIGURE 5-5
CATASTROPHIC INCISION SCENARIO

- ***Scenario 2***: An aggradation event would have had to deposit ~10 m of sediment over 60 Ka, followed by a nearly instantaneous "catastrophic" aggradation event where >100 m of sediment would have been deposited beyond the top of Libna Hill (***Figure 5-6***). Following the instantaneous aggradation of sediments within the entire Krško Basin to an elevation of >320 m, the entire basin would have had to have undergone an episode of rapid erosion and sediment evacuation to an elevation of ~160 m (roughly >160 m incision in only 40 Ka).

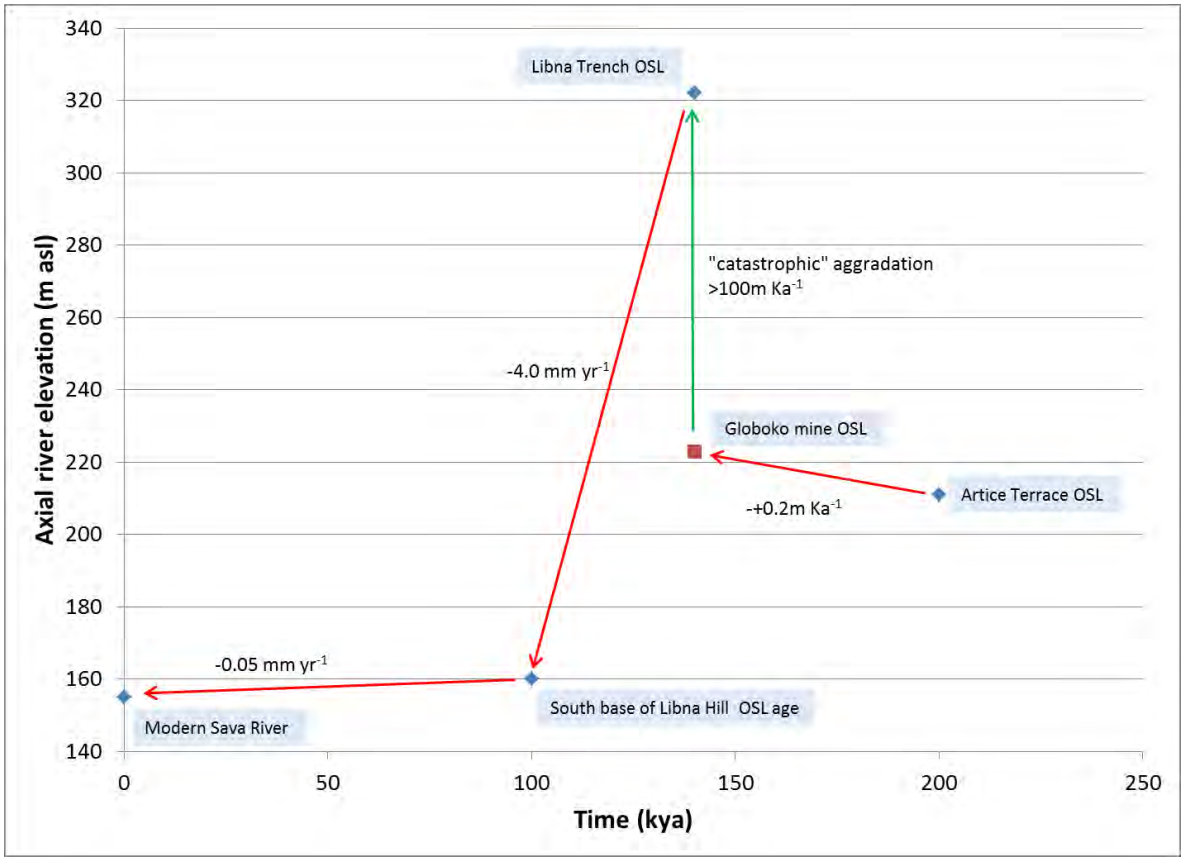

FIGURE 5-6
CATASTROPHIC AGGRADATION SCENARIO

Incision rates greater than 1.0 mm yr^{-1} (1.0 m Ka^{-1}) are typically reserved for areas undergoing high uplift rates or for areas of very high relief that are within constrained valleys and canyons. For example, the Drac River in the Alps is incising at a rate of ~0.8 mm $year^{-1}$, a value that is consistent with exhumation landscape erosion rates in regions of the Alps experiencing higher uplift rates (Robl et al., 2008). To accept the value of 4 mm yr^{-1}, which is required for Scenario 2, would make it consistent with rates measured in the New Zealand Alps. The New Zealand Alps are one of the more rapidly uplifting regions in the world—the landscape erosion rates range from ~1 mm yr^{-1} to 9 mm yr^{-1} (Montgomery and Brandon, 2002). In order to accept the Sava River incision rates of 4 mm yr^{-1} or higher, a dramatic reduction of base level is required (e.g. rapid sea level decline, orogenic uplift or local factors such as temporary lake drainage). There is no geological evidence for any of these factors near the time indicated by the OSL ages from the Libna trench. A rapid lowering of the base level would force knickpoint migration upstream on the Sava River and its tributaries to a relatively

nearby location. Published works (Roble et al., 2008) have demonstrated that rivers in the southeastern Alps, including the Sava River, have very little tectonic signature, and no abrupt knickpoints, such as those required to generate massive episodes of incision. In addition, the field reconnaissance disclosed no evidence of a knickpoint. A more likely explanation is given below as Scenario 3.

- ***Scenario 3***: between the Miocene (i.e., end of Pontian) and >1.7 Mya (millions of years ago), the Globoko Formation's sediments were deposited in the Krško Basin to an elevation greater than the modern crest elevation of Libna Hill. Subsequent incision of the Sava River began just prior to ~1.8 Ma (minimum age) and by a series of episodic incision and aggradation events, eroded the majority of the sediments from the Basin. By roughly 100 kya (thousands of years ago) the Sava River was within 15 m elevation of where it is today (***Figure 5-7***), suggesting the net incision of the Sava River is probably less than 0.1 m ka^{-1} (0.1 mm yr^{-1}).

  The rates required to incise and aggrade for this "reasonable" scenario are consistent with published reports of rivers in tectonically active areas with similar relief from around the world (Montgomery and Brandon, 2002). Hence, this scenario is credible and supportable.

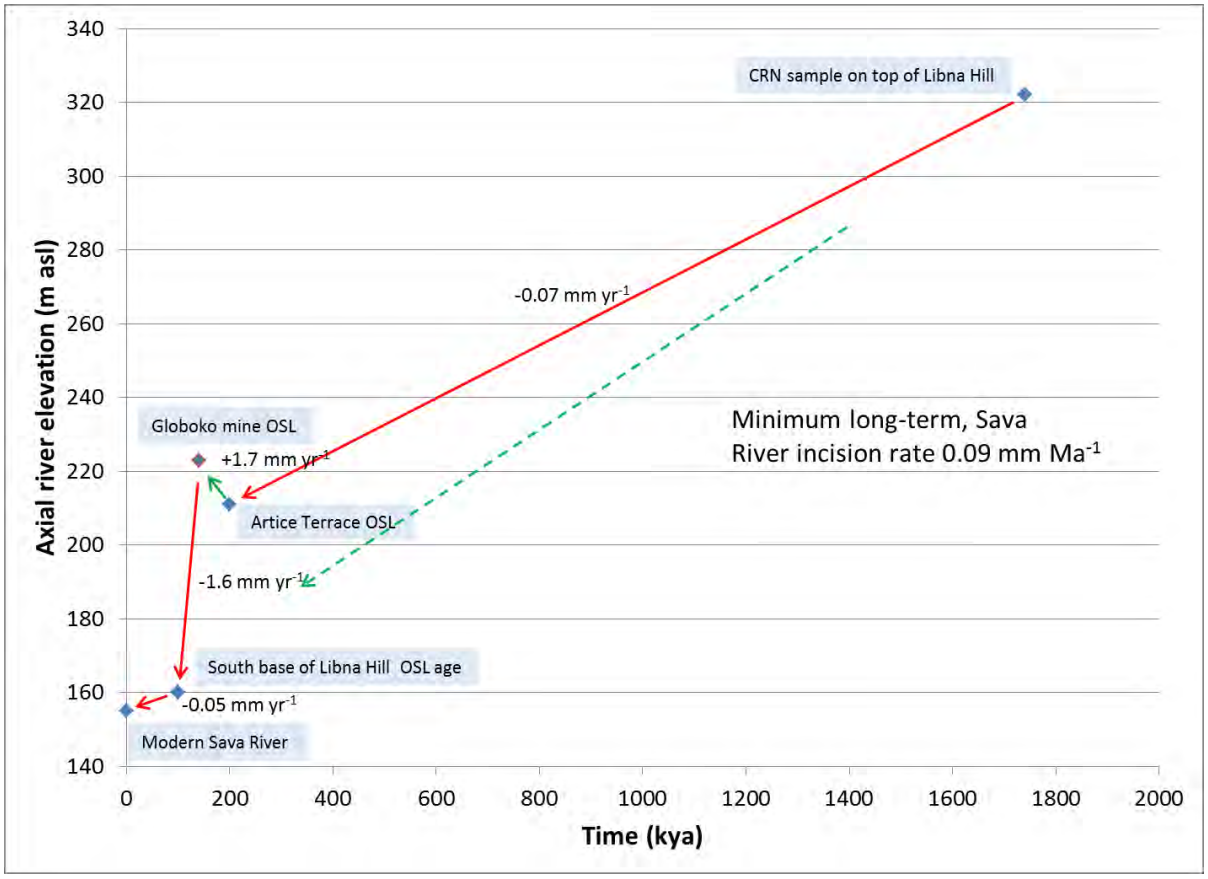

FIGURE 5-7
REALISTIC INCISION/AGGRADATION MODEL

The Libna Hill trench was excavated in the periphery of a karst sinkhole and/or landslide, as demonstrated by the geomorphic study (***Figure 4-1***). This location casts significant doubt on the OSL dated sediments from the trench. This being the case, a careful reconsideration of the tectonic displacement of the Plio-Quaternary sediments by the Libna Fault is warranted.

6.0 CONCLUSIONS

This Section presents the conclusions of the three investigations (HRS surveys, geomorphic characterization, and geochronology) summarized in this Report in terms of characterizing the faults within the Krško 2 NPP Site vicinity and the tectonic framework of the Krško Basin. This Section also addresses the impact of these conclusions on the fault parameters used in the Krško PFDHA and the resolution of the PFDHA peer review comments related to the faults addressed in this Report.

6.1 CHARACTERIZATION OF FAULTS WITHIN THE KRŠKO NPP SITE AREA

6.1.1 Postulated Stara Vas Fault

The geomorphologic investigation revealed no geomorphic evidence for the postulated Stara Vas Fault. A small outcrop on the western flank of Libna Hill exhibits fractures in the Miocene bedrock, but no evidence of displacement is observed. The HRS Profile Lines 12K-2 and 08K-5 are very noisy, but did identify a fault (inferred) within the Miocene bedrock. The geological and geophysical data forming the basis to postulate the existence of the postulated Stara Vas Fault is very weak. There is no evidence for displacement on the postulated Stara Vas Fault Because of the lack of evidence for displacement and the weakness of the case that the fault exists, the postulated Stara Vas Fault should be given no further consideration as a potential fault displacement hazard or source of ground motion at the Krško Site.

6.1.2 Libna Fault

6.1.2.1 Age of Faulting

The maximum age of faulting, if tectonic, is estimated to be less than the minimum calculated age of ~1.8 Ma based on the minimum CRN age of the Globoko Formation (RIZZO, 2013d). This is in contrast to the OSL ages (120 Ka to 200 Ka) derived from the Libna Trench study (BRGM, 2010); which are more than a full order of magnitude younger than the previously published age of > 2 Ma (Verbič, 2005) for the Globoko Formation. There are numerous lines of evidence supporting the RIZZO

and GeoZS position that the OSL dates in the trench are not accurate ages:

1. The landscape evolution possibilities that would be necessary to support the validity of the OSL ages from the Libna Trench require a "catastrophic" aggradation or incision scenario (***Section 5.6***). The long- and short-term rates implied by these scenarios to explain the age-elevation relationships are too high for the tectonic setting of the Krško Basin. This is also indicated in the Libna Hill report. The degree to which the incision rates are unreasonable is supported by published studies of river incision and landscape erosion rates in tectonically uplifting areas in the French Alps (e.g. Brocard et al., 2003; Montgomery and Brandon, 2002).

2. The new >1.8 Ma CRN burial age, which is incompatible with the absolute OSL ages from the Libna Trench, allows landscape scenarios with incision and aggradation rates that are reasonable for the tectonic setting of the Krško Basin, and are consistent with published works from the Alps (e.g. Brocard et al., 2003).

3. The new OSL geochronology suggests that OSL oversaturation is occurring between >140 Ka and 200 Ka. This strongly suggests that the Libna Trench OSL sample ages of ~140 ka are due to the sediment's antiquity, and thus should only be treated as minimum ages.

4. The displacement of the Globoko Formation by the Libna Fault is questionable because Libna Trench No. 2 was excavated on the edge of mass wasting features. As discussed in ***Section 4.4.2,*** the presence of karst and landsliding brings into question any tectonic displacement of the Globoko Formation.

6.1.2.1 Length of the Libna Fault

There is moderate geomorphic expression of the Libna Fault on Libna Hill; however, there is no geomorphic expression of the Libna Fault to the south within the Krško Basin or to the north of Libna Hill. The absence of geomorphic expression is expected in the Basin because it is almost entirely covered by young Holocene to upper Pleistocene fluvial deposits related to the meandering of the Sava River (GEN, 2012). The absence of geomorphic expression north of Libna Hill and geologic mapping (GeoZS, 2010) indicates that the Libna Fault does not project north of Libna Hill.

Although there is an apparent absence of faulting in HRS Profile Lines 12K-1, 12K-2, 08K-5, and 08K-9, there is evidence of offsets in HRS Profile Lines 08K-8a, 08K-10c, and 12K-3. On this basis, one can legitimately postulate that the Libna Fault projects south of Libna Hill as a discontinuous structure between HRS Profile Lines 08K-8a, 12K-3, and possibly 12K-4. This suggests that the cumulative length of the Libna Fault is 4.5 km. The interpreted possible faults observed further south in HRS Profile Lines 12K-6 and 12K-7 occur well within the Miocene limestone and are likely related to the Balaton Fault System, not the Libna Fault or any other northwest trending faults. It is also important to note that all of the faults identified with HRS terminate within the Miocene bedrock.

6.1.2.2 Capability of the Libna Fault

A previous interpretation of Plio-Quaternary tectonic activity on the Libna Fault was based on the Libna Hill Trench and its associated OSL geochronology. Trench mapping was performed in a technically proficient manner (GeoZS, 2013); however, only one trench was successfully mapped, providing limited and inconclusive data. The mapped trench was excavated into the side of a karst or landslide landform, making any determination of tectonic displacement of Plio-Quaternary sediments problematic and highly questionable.

Landsliding and karst processes are significant agents of landscape change in the Krško Region (***Figures 2-3 and 4-1***). Based on the recommendations of Hart et al., (2013), and taking into account the new data and interpretations from geomorphic investigations summarized in this report, observations in the Libna Hill trench have been reinterpreted considering the possible effects of both tectonic faulting and non-tectonic landslides and mass-wasting processes. Hart et al., (2013) note that the geologic interpretation of faults should consider:

1. Geological context: e.g., is the fault in question consistent with the tectonic setting? Is the age of the displacement (if known) consistent with the tectonic history of the region? Is the regional geology and topography conducive to landsliding?

2. Multiple working hypotheses: e.g., always consider that multiple processes that may have formed the observed displacement or

lineament. Field investigations should be aimed at testing these hypotheses.

3. Use geomorphic and geological judgments: e.g., it must be acknowledged that there are multiple processes that can produce nearly identical landforms and apparent displacements. This is clearly demonstrated on ***Figure 4-2***.

There is no reliable evidence that Plio-Quaternary deposits were repeatedly displaced through the action of tectonic movement along the fault. Given the location of the Libna Hill trench near a karst-related sinkhole and probable landslide feature, Plio-Quaternary movement along the fault is interpreted to be due to the stated non-tectonic processes.

Based on the body of information compiled in this report, it is highly unlikely that the Libna Fault is capable under both the Criterion 3 (g) of Appendix A in 10 Code of Federal Regulations Part 100(NRC 2013) and the International Atomic Energy Agency's (IAEA) Specific Safety Guideline (SSG) 9, Section 8.4 and 8.8 (IAEA, 2010) as stated below:

- 10 CFR Part 100 Appendix A
  - No evidence of movement is exhibited within the past 35,000 years and no recurring movement within the past 500,000 years has occurred on the Libna Fault.
  - There is no related historical seismicity.
  - There is no evidence to suggest that the Libna Fault is related to another capable fault.
- SSG-9, Section 8.4
  - The Libna Fault shows no evidence of past movement or movements (such as significant deformations and/or dislocations) of a recurring nature within such a period that it is reasonable to conclude that further movements at or near the surface may occur.
  - There is no evidence of a structural relationship between the Libna fault and another capable fault.
- SSG-9, Section 8.8
  - There is no reliable evidence along the Libna Fault to demonstrate that it may be a capable fault with the potential to affect the safety of a plant at a site, the feasibility of design, construction and safe operation of a plant at the proposed Krško 2 NPP sites.

6.1.3 Orlica Fault Zone

The N30-45^{o}E trending OFZ is marked with prominent geomorphic features reflected as moderate to strong lineaments in analysis of the DEMs developed from LiDAR data (***Exhibit 7***). Lineaments associated with the OFZ northeast of the Sava River project to the town of Krško. This is consistent with the BRGM interpretation of the OFZ (GeoZS, 2010).

The OFZ has a mapped length of 25 km northeast of Krško (BRGM, 2010). It is expressed as a narrow sinuous drainage basin immediately northeast of where it crosses the Sava River near Krško. 6 km to the north and east, the OFZ widens up to 3 km. Youthful appearing lineaments have been identified in the upper section of the narrow drainage and within the broader section northeast of the narrow drainage, suggesting the fault is more segmented than previously believed.

The OFZ is considered a seismogenic source in the GeoZS seismotectonic model (GeoZS, 2010) as regards a Probabilistic Seismic Hazard Analysis (PSHA). Based on the lineament analysis the fault zone consists of multiple segments with geomorphic features suggestive of different ages of activity. This implies from a seismogenic perspective that the fault is not a single segment and that future earthquakes would occur on one or more segments, not along the full length of the OFZ. This is supported by recent investigations that suggest the number of segments that rupture is an indication of the magnitude of the maximum earthquake (M_{max}). Typically one to four segments rupture in a seismic event, not the full, mapped fault length (DePolo et. al., 1991; Lettis et. al., 2002; and Manighetti et. al., 2006). A thorough analysis of the OFZ has not yet been performed, but it may result in additional seismogenic segmentation.. If seismogenic segmentation results from a detailed analysis of the OFZ, it may reduce the estimate of the maximum earthquake (RIZZO, 2012) the Fault Zone can generate in the future.

6.1.4 Inferred Artiče Fault

The Artiče Structure is a flexure associated with an inferred fault that has been identified from geophysical survey lines (BRGM, 2010). The warping can be interpreted as either a depositional feature over an existing

escarpment or deformation from faulting. Weak to moderate lineaments are observed at the base of the Artiče Hills (***Exhibit 7***). These lineaments are likely associated with fluvial erosion of the paleo Sava River as discussed in ***Section 4.0***, not faulting associated with the Artiče Structure.

The Artiče Hills are highly dissected by fluvial incision, especially when compared with the southern Krško Hills on the south and west side of the Sava River. The prevailing hypothesis is that there are ongoing differential rates of uplift between these two regions, with the Artiče Hills undergoing higher rates of uplift as a result of faulting. However, the hypsometric analysis does not support this interpretation—the hypsometric integrals are low and the differences between the integrals from the Krško Hills and Orlica Hills are very similar. The differences in dissection between the Orlica and Artiče Hills are likely related to the differences in the underlying lithology, and the higher elevation of the Orlica Mountains. This is further supported by the absence of lineaments suggestive of Plio-Quaternary activity. Very little evidence exists to support a case for Plio-Quaternary faulting along the inferred Artiče Fault.

6.2 IMPLICATIONS OF INVESTIGATION CONCLUSIONS TO THE KRŠKO PFDHA

The Krško PFDHA (RIZZO, 2013a) provides information that is relevant to risk-informed decision making in a regulatory environment, both for the existing NPP site and for the proposed alternative sites for a new NPP. The results from the Krško PFDHA (RIZZO, 2013a) indicate that fault displacement of engineering significance is very low. The probability of future surface fault displacement within the footprint of the proposed NPP 2 sites is nearly the same and extremely low; a mean annual probability of exceedance of less than $1X10^{-6}$ for 0.001 m (1 millimeter [mm]). The exceedance probabilities are below typical regulatory levels of concern. Some parameters used in the Krško PFDHA for the faults considered are conservative based on the results of the investigations presented in this Report. The parameters addressed in this Report are compared to those from a Krško PFDHA in ***Table 6-1.*** The basis for revising the parameters is given in ***Section 6.2.2.***

TABLE 6-1
COMPARISON OF RELEVANT PARAMETERS BETWEEN THIS INVESTIGATION AND THE KRŠKO PFDHA

Fault	Original PFDHA Fault Parameters		Fault Parameters Based on these Investigation Results	
	Probability of Activity	Fault Length	Probability of Activity	Fault Length
Postulated Stara Vas	0.3	1.0 and 2.5 km	0	0 km
Libna	1	4.6, 5.9, and 10.5 km	0.5	1.25 to 4.5 km
Orlica Fault Zone	1	25 and 15 km	1	8 to 12 km
Artiče	1	11.6 and 16.4 km	0.5-1	3 km
Other North-West Trending Faults	0.5	4.8 to 7.2 km	< 0.5	< 4.8 km

6.2.1 Implications for Fault Parameters used in the Krško PFDHA

The findings of the geomorphological investigations presented in ***Section 4.4.1*** indicate that no geomorphic evidence exists on or surrounding Libna Hill to support Plio-Quaternary fault activity along the postulated Stara Vas Fault. The evidence for the existence of the Fault is limited to one small bedrock outcrop on Libna Hill and a weak inferred fault observed in the re-interpretation of HRS profile line 12K-2 (RIZZO, 2013f) that crosses the projection of the postulated Stara Vas Fault. Because Plio-Quaternary activity of the postulated fault is not indicated by the geomorphic analysis, it is concluded that the fault, if it exists, is currently inactive and, therefore, should not be included in a PSHA or PFHDA.

Geomorphic investigations along the Libna Fault on Libna Hill (***Section 4.4.2***) demonstrate that the dominant surface processes responsible for forming the escarpment are mass wasting movements that include karstic collapse and landsliding. Field reconnaissance supports this finding. The CRN age of the Globoko Formation on the crest of Libna Hill suggests that, if tectonic displacement has occurred on the Libna Fault, it is younger than 1.8 Ma or more, not 140 Ka. The HRS survey indicates that

the Libna Fault extends into the Krško Basin, at most, as a discontinuous structure for approximately 4.5 km.

The geomorphic investigations of the OFZ identified a number of strong lineaments representing aligned geomorphic features (***Exhibit 7*** and ***Section 4.4.3***); however, these lineaments are typically < 4 km. Some of the lineaments identified by this investigation indicate that the OFZ is a highly segmented fault zone and should be treated as such when estimating its potential as a seismic source..

The RIZZO PFDHA divided the OFZ into two segments (15 km and 25 km) on the basis of the GeoZS (2010) seismotectonic model. Based on the geomorphic evidence, limited field checking, and published information of fault segmentation, a more reasonable rupture length is 8 km to 12 km (2-3 segments).

The inferred Artiče Fault has limited geomorphic (***Section 4.4.4***) and geophysical information to support it being a tectonic feature. It was identified as a possible fault based on seismic profiles that suggest warping of interpreted Plio-Quaternary units. There was also a suggestion that the Artiče Hills are going through differential uplift (i.e. BRGM, 2010); however hypsometry analysis suggests this is not the case.

Geomorphic expression of the other faults that are parallel to the north-west structural grain represented by the Libna Fault is very weak to nonexistent. The north-northwest trending mapped faults that bound the slope of the Artiče Hill drainages have moderate to weak geomorphic expression and are very short (1 km to 2 km) (***Exhibit 6***).

6.2.2 Addressing Peer Review Comments

The Krško PFDHA peer review comments were originally addressed in the Krško PFDHA sensitivity analysis (RIZZO, 2013b). The conclusions of this investigation further address their overall theme of conservatism as expressed by the Peer Review Panel in the fault parameter values used in the Krško PFDHA. The conclusions of this investigation (***Section 6.1***) reinforce observations of the Peer Review Panel that some inputs to the

Krško PFDHA are conservative, now probably viewed as overly conservative.

Peer Review Comment No. 8 addresses slip rates of faults and suggests that "it could be useful to calculate the sedimentation and or deformation rate(s) using the thickness and the deformation of the different Miocene period horizons visible in the seismic reflection profile lines." Assessing either sedimentation or deformation rates based on the HRS profiles is difficult because much of the material overlying the eroded Miocene marls and limestone is very young (Holocene and upper Pleistocene).

A compilation of borehole data from the vicinity of the Krško 2 NPP Sites indicates that the Holocene/Pleistocene fluvial gravels are 3 m to 5 m thick and immediately cover Miocene marls and limestones. Basin morphology analyses (i.e., hypsometry and drainage density) suggest that the hypothesis of Pleistocene uplift of the Artiče Hills is very weak. Knick points indicative of Pleistocene uplift that would be expected in the drainages of the Artiče Hills are not present. More prominent dissection of the Artiče Hills relative to the Krško Hills are interpreted to be associated with differences in the underlying lithology and upstream areas (catchment size and elevation), as opposed to tectonic uplift of the Artiče Hills.

Conclusions of this investigation should be considered in any revision to the PFDHA or the seismic source characterization element of any planned PSHA as suggested in Peer Review Comment No. 10. As the results of this investigation confirm the statements of the Peer Review Panel that some input parameters used in the original PFDHA were conservative, an updated PFDHA will yield lower probability of exceedance curves than reported in the report reviewed by the Peer Review Panel. The results of the investigations also allow some of the ranges of uncertainty included in the PFDHA to be narrowed.

6.3 Implications of New Information on Seismotectonic Model

New information presented in the interim reports (RIZZO 2012, 2013c, 2013d, and 2013e) and this report address postulated, known and inferred faults within the proposed Krško NPP 2 vicinity. These reports also address the age of Quaternary units and erosion rates within the

Krško Basin. Based on this information it is apparent that the tectonic processes within the Krško region are less dynamic than previously implied (BRGM, 2010) and that additional investigations will likely further constrain the level of tectonic activity. Incorporating the fault parameters presented in ***Table 6-1*** and considering new information on the geochronology and erosion rates will lead to an updated seismotectonic model that will be more representative of the neotectonic framework of the Krško Basin. Incorporating new information to update the seismotectonic model will provide more robust inputs to the planned PSHA.

7.0 REFERENCES

Bavec, M., 2000, "Poročilo o določanju starosti kvartarnih sedimentov v Krški kotlini z metodo termoluminescence (TL) in optično stimulirane luminescence (OSL)," Projektna naloga: Neotektonske raziskave na območju JE Krško, Naročnik Uprava RS za jedrsko varnost, Tipkano poročilo, Geološki zavod Slovenije.

Bavec and Rižnar, 2013, Personal Communications, 26 April 2013.

Balco, G., and C.W. Rovey II, 2008, "An Isochron Method for Cosmogenic-Nuclide Dating of Buried Soils," *American Journal of Science 308*, pp. 1083-1114.

Balco G., Soreghan G.S., Sweet D.E., Marra K.R., Bierman P.R., 2012. "Cosmogenic-Nuclide Burial Ages for Pleistocene Sedimentary Fill in Unaweep Canyon, Colorado, USA," Quaternary Geochronology, 2012.

BRGM, 2010, "Geotechnical, Geological and Seismological (GG&S) Evaluation of the New Nuclear Power Plant at the Krško Site: Phase 1 Summary Report," Final Report, Bureau de Recherches Géologiques et Minières Consortium, France, June, 2010.

Brocard, G.Y., P.A. van der Beek, D.L. Bourles, L.L. Siame, J.L. Mugnier. 2003. Long-term fluvial incision rates and post-glacial river relaxation time in the French western Alps from ^{10}Be of alluvial terraces with assessment of inheritance, soil development and wind ablation effects. ESPL, V. 209, p 197-214.

Bull, W. B., and L.D. McFadden, 1977, "Tectonic Geomorphology North and South of the Garlock Fault, California," A Proceedings Volume of the Annual Geomorphology Symposia Series, (8), pp. 115-138.

Cline M.L., J.D., Pelletier, 2007, "Cinder Cone Hillslope Modeling at the San Francisco Volcanic Field, Arizona," In the paper session: Volcanic and Aeolian Geomorphology and Geothermal Systems, *American Geophysical Union Annual Meeting.*

Cotton, W.R., 1999, "Faults Aren't Always What They're Cracked Up To Be," in K.L. Hanson, K.I. Kelson, M.A. Angell, and W.R. Lettis, (eds.), Identifying Faults and Determining their Origins, U.S. Nuclear Regulatory Commission (NRC), NUREG/CR-5503, Appendix A, p. A27-A50NUREG/CR-5503, Appendix A, p. A27-A50.

Cunningham, D., S. Grebby, K. Tansey, A. Gosar, and V. Kastelic, 2006, "Application of Airborne LiDAR to Mapping Seismogenic Faults in Forested Mountainous Terrain, Southeastern Alps, Slovenia," Geophysical Research Letters, 33(20), 0-L20308.

DePolo, C., D. Clark, B. Slemmons, and A. Ramelli, 1991, "Historical Surface Faulting in the Basin and Range Province, Western North America: Implications for Fault Segmentation," Journal of Structural Geology, 13(2), PP 123-196.

DeLong, S., G.E. Hilley, M. Rymer, and C. S. Prentice, 2011, "Fault Zone Structure from Topography: Signatures of en échelon Fault Slip at Mustang Ridge on the San Andreas Fault," Monterey County, California, USA, Tectonics, i29.

DeLong, S. B., C. S. Prentice, G. E. Hilley, and Y. Ebert, 2012, "Multi-temporal ALSM Change Detection, Sediment Delivery, and Process Mapping at an Active Earth Flow," Earth Surface Processes and Landforms, 37(3), pp. 262-272.

Dietrich, W. E., D.G. Bellugi, L. S. Sklar, J. D. Stock, A. M. Heimsath and J. J. Roering, 2003, "Geomorphic Transport Laws for Predicting Landscape Form and Dynamics," Geophysical Monograph, 135, pp. 103-132.

GEN, Energija, d.o.o., 2012, "Summary of Historical Reports on Sava River Fluvial Migration," Provided to Paul C. Rizzo Associates, Inc.

GeoExpert a.g., 2013, "Report - Seismic Data Acquisition and Processing, Sava Plain, Krško - Brežice Area, High-Resolution Seismic Survey," GeoExpert, a.g., Switzerland, February 2013.

Geomatrix, 2004, "Revised Seismotectonic Model of the Krško Basin", Geomatrix, Oakland, California, (Reference PSR-NEK-2.7.1 (Rev. 1), January 2004.

GeoZS, 2010 "Geotechnical, Geological, and Seismological (GG&S) Evaluations for the New Nuclear Power Plant at the Krško Site (NPP Krško II): Seismic Source Models," Geološki Zavod Slovenije, Ljubljana, Slovenia, June 2010

GeoZS, 2013, "Geotechnical, Geological, and Seismological (GG&S) Evaluation of the New Nuclear Power Plant at the Krško Site (NPP Krško II): Paleoseismological Trenches on the Libna Hill," Revision 1.1, Geološki Zavod Slovenije, Ljubljana, Slovenia, April 2013.

Gosar, A., 1998, "Seismic-Reflection Surveys of the Krško Basin Structure – Implications for Earthquake Hazard at the Krško Nuclear Power Plant," SE Slovenia, Journal of Applied Geophysics, v. 39, pp. 31-153.

Granger, D.E., and P.F. Muzikar, 2001, "Dating Sediment Burial with in Situ-Produced Cosmogenic Nuclides: Theory, Techniques, and Limitations," *Earth and Planetary Science Letters* 188, pp. 269-281.

Hart, M.W., P.J. Shaller, G.T. Farrand, 2013, "When Landslides Are Misinterpreted as Faults: Case Studies from the Western United States," *Environmental and Engineering Geoscience,* v. 19, p. 97-98, February, 2013.

Hilley, G. E., S. DeLong, C. Prentice, K. Blisniuk, and J. R. Arrowsmith, 2010, "Morphologic Dating of Fault Scarps Using Airborne Laser Swath Mapping (ALSM) Data," Geophysical Research Letters, 37(4), 0-Citation L04301.

Huntley, D. J., D.I. Godfrey-Smith, and M.L.W. Thewalt, 1985, "Optical Dating of Sediments," Nature 313, pp. 105–107.

International Atomic Energy Agency, 2010 "Seismic Hazards in Site Evaluation for Nuclear Installations," IAEA Safety Standards Series, Specific Sfety Guide No. SSG-9, Section 8.0.

Lal, D. and B. Peters, 1967, "Cosmic Ray Produced Radioactivity on the Earth," in Sitte, K., ed. Handbuch der Physik, New York, Springer-Verlag, pp. 551-612.

Lettis, W., J. Bachhuber, R. Witter, C. Brankman, C. Randolph, A. Barka, W. Page, and A. Kaya, 2002, "Influence of Releasing Step-Overs on Surface Fault Rupture and Fault Segmentation: Examples from the 17 August 1999 Izmit Earthquake on the Noerth Anatolian Fault, Turkey," Bulletin of the Seismological Society of America, 92(1), pp. 19-42.

Manighetti, I., M. Campillo, S. Bouley, and F. Cotton, 2007, "Earthquake Scaling, Fault Segmentation, and Structural Maturity," Earth and Planetary Letter 253, pp 429-438.

Markič, M., and D. Rokavec, 2002, "Geološka Zgradba, Nekovinske Mineralne Surovine in Lignit Okolice Globokega (Krška kotlina)," RMZ – Materials and Geoenvironment, Ljubljana, 49 (2), pp. 229-226.

Matmon, A; G. Stoc; D. Gosar; K. Howard, 2012, "Dating of Pliocene Colorado River Sediments: Implications for Cosmogenic Burial Dating and the Evolution of the Lower Colorado River," Geological Society of America Bulletin, V. 124 No. 3-4 pp. 626-640.

Montgomery, D. R., and W. E. Dietrich, 1988, "Where do Channels Begin?" Nature (London), 336(6196), pp. 232-234.

Montgomery, D.R. and M.T. Brandon, 2002, "Topographic Controls on Erosion Rates in Tectonically Active Mountain Ranges, Earth and Planetary Science Letters 201 (2002) 481-478.

Murray, A., J. Buylaert, M. Henriksen, J. Svendsen, and J. Mangerud, 2007, "Testing the Reliability of Quartz OSL Ages Beyond the Eemian," *Radiation Measurements*, Proceedings of the 15th Solid State Dosimetry 43, 2-6 pp. 776-780.

NRC, 2013, "Seismic and Geologic Siting Criteria for Nuclear Power Plants," Appendix A of the Title 10 of the Code of Federal Regulations Part 100, Criterion 3, July 2013 update, U.S. Nuclear Regulatory Commission, Washington, DC.

Pelletier, J. D., S. B. DeLong, A. Al-Suwaidi, M. Cline, Y. Lewis, J. L. Psillas, and B. Yanites, 2006, "Evolution of the Bonneville Shoreline Scarp in West-Central Utah; Comparison of Scarp Analysis Methods and Implications for the Diffusion Model of Hill Slope Evolution," Geomorphology, 74(1-4), pp. 257-270.

Pelletier, J. D., and M. L. Cline, 2007a, "Nonlinear Slope-Dependent Sediment Transport in Cinder Cone Evolution," Geology (Boulder), 35(12), pp. 1067-1070.

Pelletier, J. D., M. Cline, and S. B. DeLong, 2007b, "Desert Pavement Dynamics; Numerical Modeling and Field-Based Calibration," Earth Surface Processes and Landforms, 32(13), pp. 1913-1927.

Pelletier, J. D., T. Engelder, D. Comeau, A. Hudson, M. Leclerc, A. Youberg, and S. Diniega, 2009, "Tectonic and Structural Control of Fluvial Channel Morphology in Metamorphic Core Complexes; The Example of the Catalina-Rincon Core Complex," Arizona. Geosphere, 5(4), pp. 363-384.

Perron, J. T., J. W. Kirchner, and W. E. Dietrich, 2009, "Formation of Evenly Spaced Ridges and Valleys, Nature, 460(7254), pp. 502-505.

Persoglia, S. (ed.), 2000, "Geophysical Research in the Surrounding of the Krško NPP," Final Report and Annexes, Contract No. 98-0286.00 for European Commission Directorate General IA Tacis Procurement Unit.

Placer, L., 1999, "Structural Meaning of the Sava Folds," Geologija, v. 41, pp. 191-221.

Poljak, M., L. Placer, B. Stojanov and, H. Rifelj, 1997, "Geološka reambulacija hriba Libne pri Krškem in okolice, "Unpublished Report prepared by the Inštitut za geologijo geotehniko in geofiziko (IGGG), št. dok. ŠGGS15, p. 21.

Poljak, M, A. Gosar, and M. Zivic, 2010, "Active Tectonics in Slovenia," Geology of the Adriatic Area, GeoActa, Special Publication 3 (2010), pp. 15-24.

Prelogov, E., B. Saft, V. Kuk, J. Veli, M. Dragaš, and D. Lui, 1998, "Tectonic BRGM," GeoZS, IRSN, ZAG. Geotechnical, Geological, and Seismological (GG&S) Evaluations for the New Nuclear Power Plant at the Krško Site (NPP Krško II) Geology – Phase 1, p. 163.

Rittenour, T.M., 2008, "Luminescence Dating of Fluvial Deposits: Applications to Geomorphic, Palaeoseismic, and Archaeological Research," *Boreas*, v. 37, pp. 613-635.
RIZZO, 2010, "Final Report: Reprocessing of High Resolution Seismic Data, Krško II Nuclear Power Plant, Slovenia," Revision 0, Paul C. Rizzo Associates, Inc., Pittsburgh, PA, USA, 17 December 2010.

RIZZO, 2012, "Interim Technical Report: Geomorphic Analysis of Tectonic Features in the Krško Basin," Slovenia, Revision 0, Paul C. Rizzo Associates, Inc., Pittsburgh, PA, USA, 21 December 2012.

RIZZO, 2013a, "Technical Report: Probabilistic Fault Displacement Hazard Analysis, Krško East and West Sites, Proposed Krško 2 Nuclear Power Plant, Krško, Slovenia," Revision 1, Paul C. Rizzo Associates, Inc., Pittsburgh, PA, USA, 13 May 2013.

RIZZO, 2013b, "Final Technical Report: Sensitivity Analysis, Probabilistic Fault Displacement Hazard Analysis, Krško East And West Sites, Proposed Krško 2 Nuclear Power Plant, Krško, Slovenia, Revision 1, Paul C. Rizzo Associates, Inc., Pittsburgh, PA, USA, 31 May 2013.

RIZZO, 2013c, "Interim Report: Interpretation of High Resolution Seismic Data Compiled in October 2012, Krško 2 Nuclear Power Plant, Krško

Slovenia," Revision 1, Paul C. Rizzo Associates, Inc., Pittsburgh, PA, USA, 15 April 2013.

RIZZO, 2013d, "Interim Report: Geochronology Investigations to Constrain the Age of the Libna Fault near the Propose Krško 2 Nuclear Power Plant, Krško, Slovenia," Revision 1, Paul C. Rizzo Associates, Inc., Pittsburgh, PA, USA, 30 September 2013.

RIZZO, 2013e, "Reinterpretation of 2008 and 2012 High-Resolution Seismic Data Compiled in the Krško Basin, Proposed Krško 2 Nuclear Power Plant, Krško, Slovenia," Revision 1, Paul C. Rizzo Associates, Inc., Pittsburgh, PA, USA, 30 October 2013.

Roebl, Jorg, S. Hertgarten, and K Stuwe, 2008, "Morphological Analysis of the Drainage System in the Eastern Alps, Tectonophysics, 460, pp. 263-2777.

Roering, J. J., J. W. Kirchner, and W. E. Dietrich, 1999, "Evidence for Nonlinear, Diffusive Sediment Transport on Hillslopes and Implications for Landscape Morphology," Water Resources Research, 35(3), pp. 853-870.

Snyder, N. P., Whipple, K. X., G. E. Tucker, and D.J. Merritts, 2000, "Landscape Response to Tectonic Forcing: Digital Elevation Model Analysis of Stream Profiles in the Mendocino Triple Junction Region, Northern California," Bulletin of the Geological Society of America, 112(8), pp 1250-1263.

Stone, J. 2000, "Air Pressure and Cosmogenic Isotope Production," J. Geophys. Res., 105, 23,753-23,759.

Tucker, G. E., and R. L. Bras, 1998, "Hillslope Processes, Drainage Density, and Landscape Morphology," Water Resources Research, 34(10), pp. 2751-2764.

Vermeesch, P., 2007, "CosmoCalc: An Excel Add-In for Cosmogenic Nuclide Calculations," G^3: Geochem., Geophys., Geosyst 8, Q08003.

Verbič, T. 2004, "Stratigrafija kvartarja in neotektonika vzhodnega dela Krške kotline, 1 del stratigrafija," (Quaternary Stratigraphy and Neotectonics of the Eastern Krško Basin, Part 1: Stratigraphy), Razprave IV Razreda SAZU XLV-3, 171-225, Ljubljana (Abstract in English).

Verbič, T., 2005, "Quaternary Stratigraphy and Neotectonics of the Eastern Krško Basin – Part 2: Neotectonics - Razprave IV. Razreda Sazu," Vol. XLVI-1, (Abstract in English), pp. 171-216.

Whipple, K. X., C. Wobus, E. Kirby, and N. P. Snyder, 2003, "Tectonics from Topography; Methods, Application, and Limitations," EOS, Transactions, American Geophysical Union, 84(46), Abstract T22E-08.

Whipple, K. X., 2009, "The Influence of Climate on the Tectonic Evolution of Mountain Belts," Nature Geoscience, 2(2), pp. 97-104.

Wintle A G., 2008, "Luminescence Dating: Where it has Been and Where it is Going," Boreas 37(4), pp. 471-482.

Wintle, A.G., 2010, "Future Directions of Luminescence Dating of Quartz," Geochronometria, 37 (1) pp. 1-7.

Zander A, and A. Hilgers, 2013, "Potential and Limits of OSL, TT-OSL, IRSL and pIRIR290 Dating Methods Applied on a Middle Pleistocene Sediment Record of Lake El'gygytgyn, Russia," Climate of the Past, 9-2, pp. 719-733.

EXHIBITS

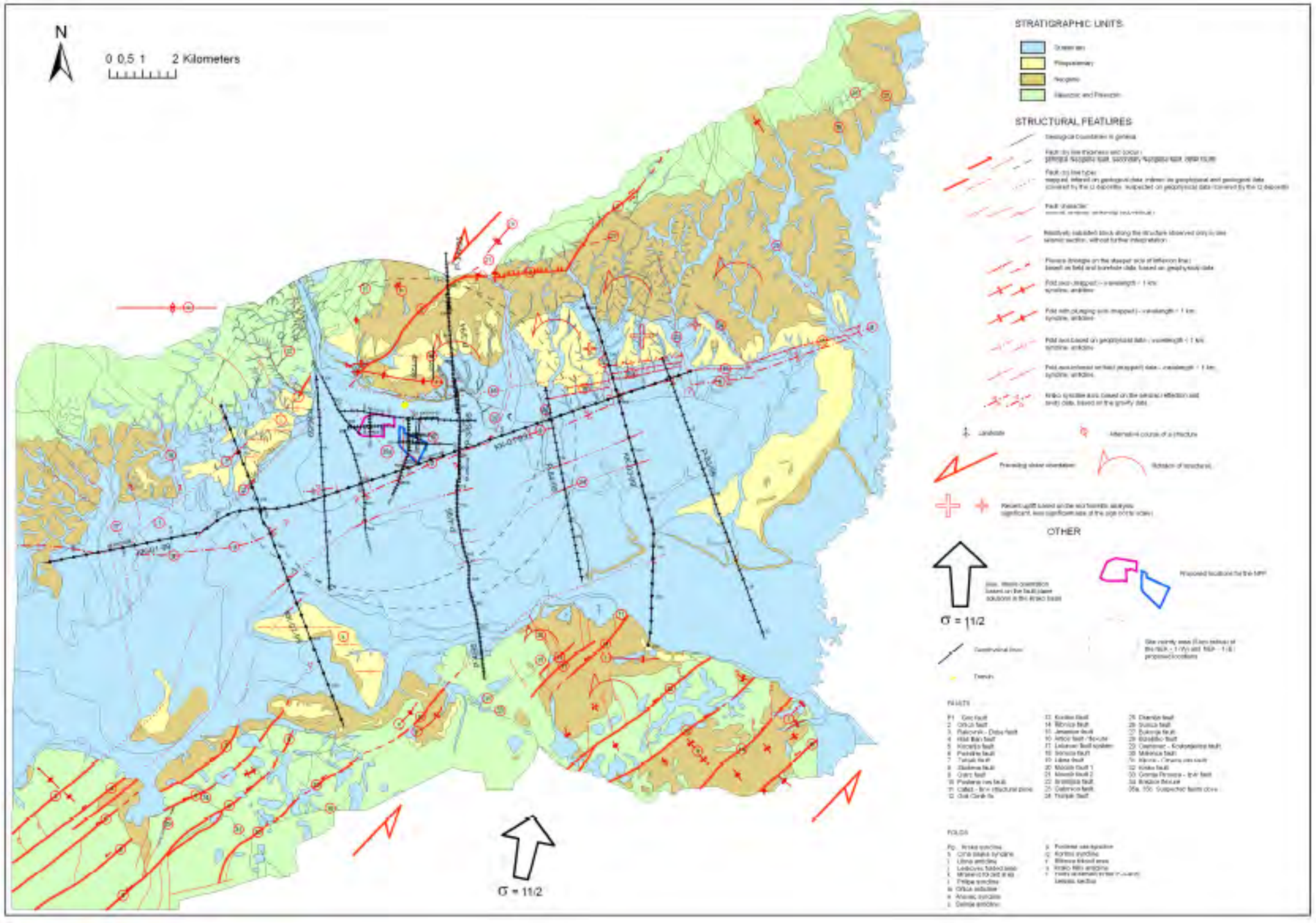

EXHIBIT 1
SEISMOTECTONIC MODEL OF THE KRŠKO BASIN (GeoZS, 2010)

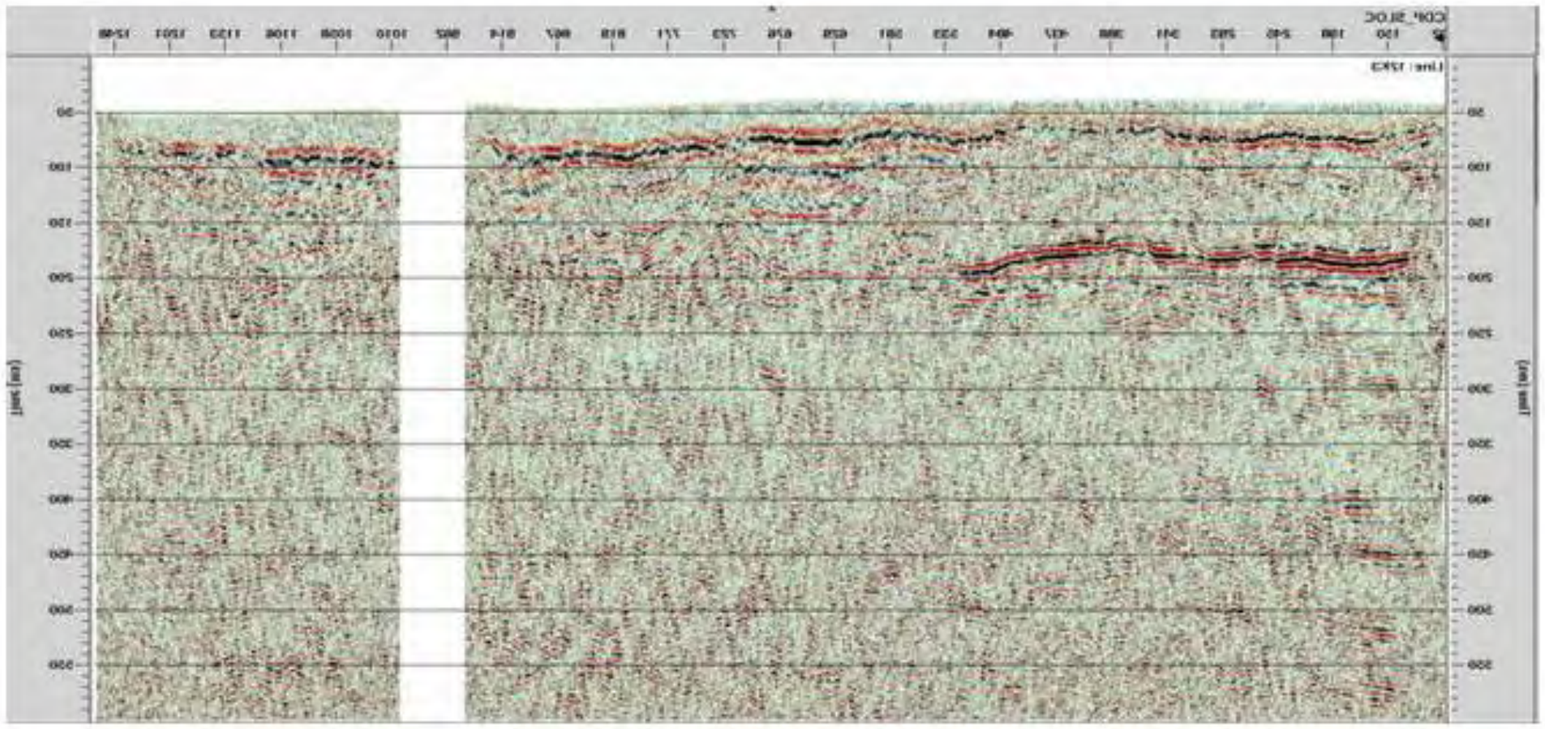

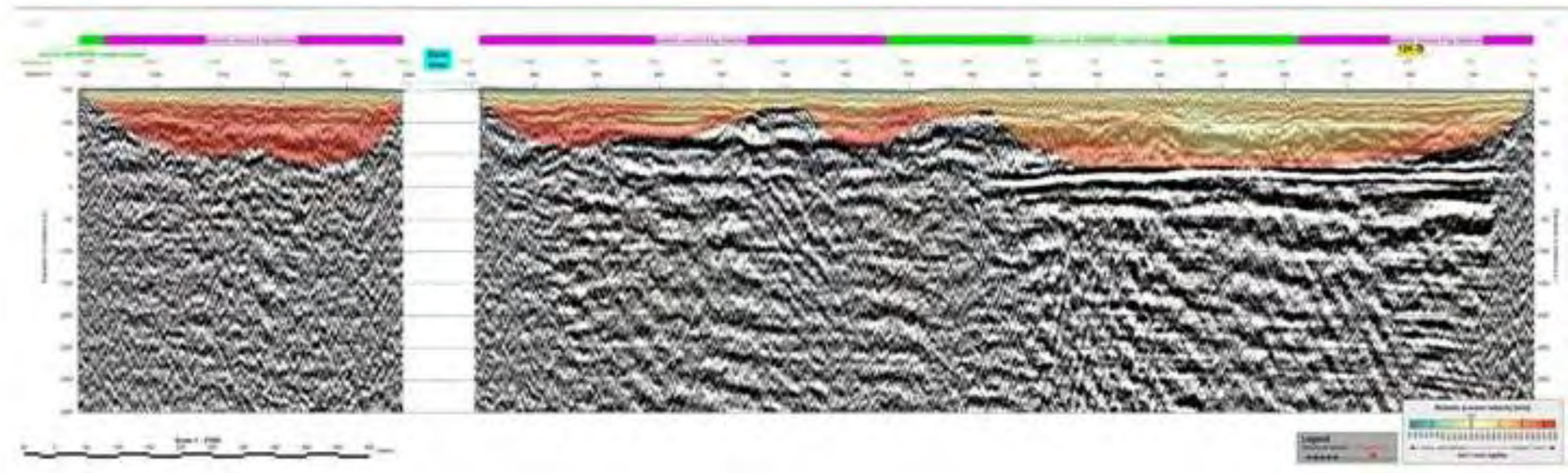

EXHIBIT 2
PROMAX VERSUS HYBRID REFRACTION/REFLECTION PROCESSED PROFILE LINE 12K-3

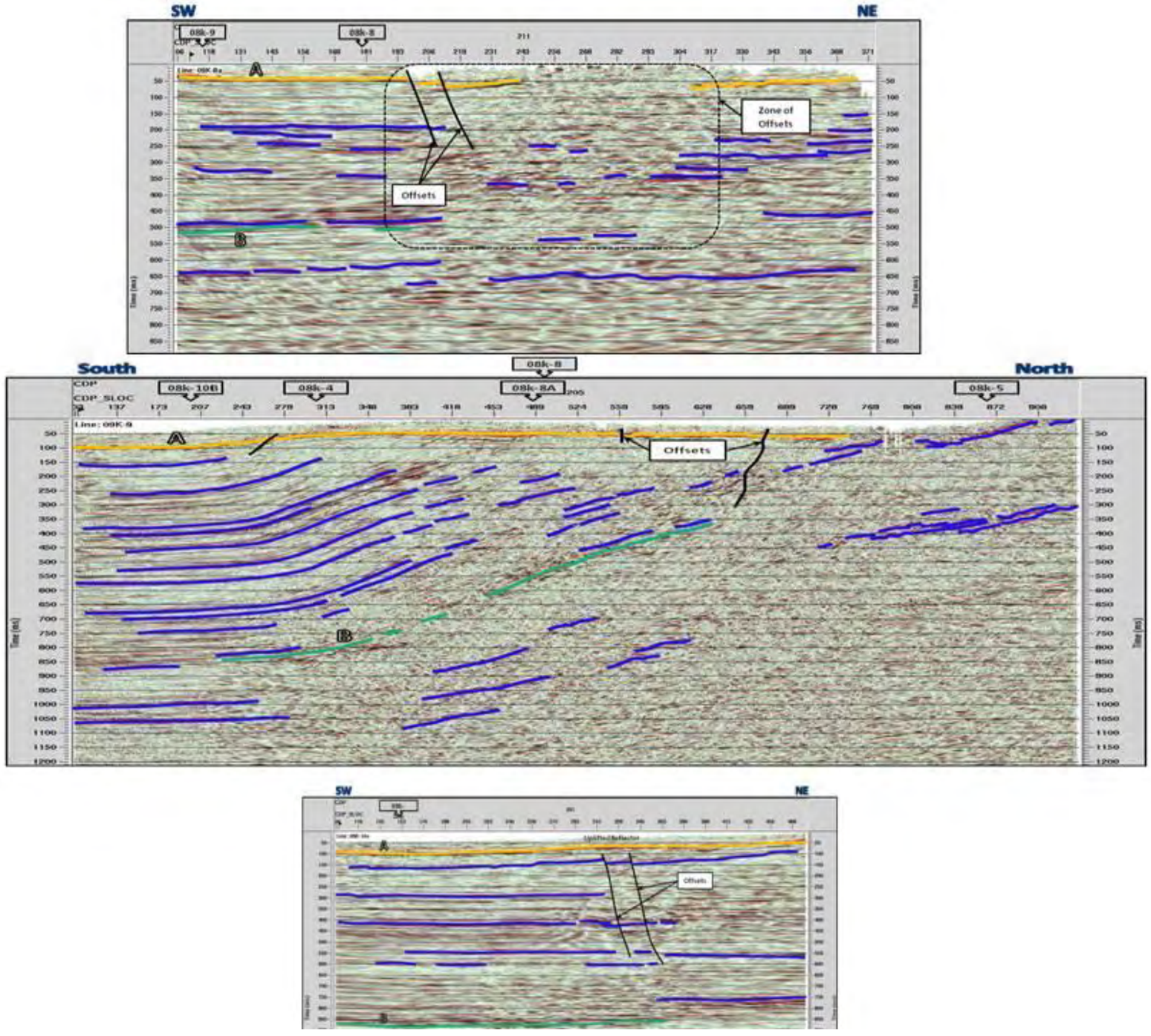

EXHIBIT 3
STERLING-PROCESSED HRS PROFILES 08K-8a, 08K-9, AND 08K-10c

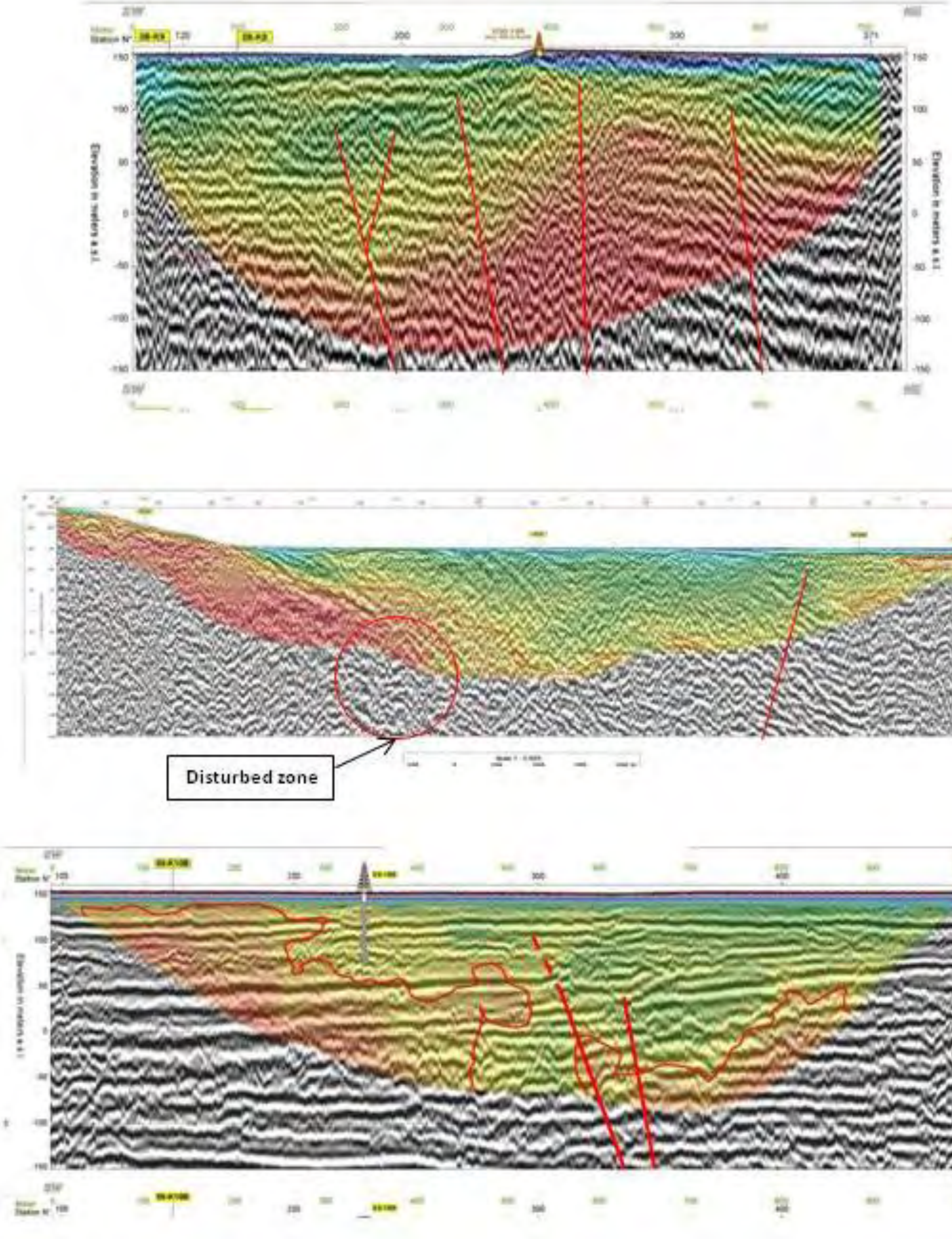

EXHIBIT 4
HYBRID REINTERPRETATION OF 08K-8a, 08K-9, AND 08K-10c

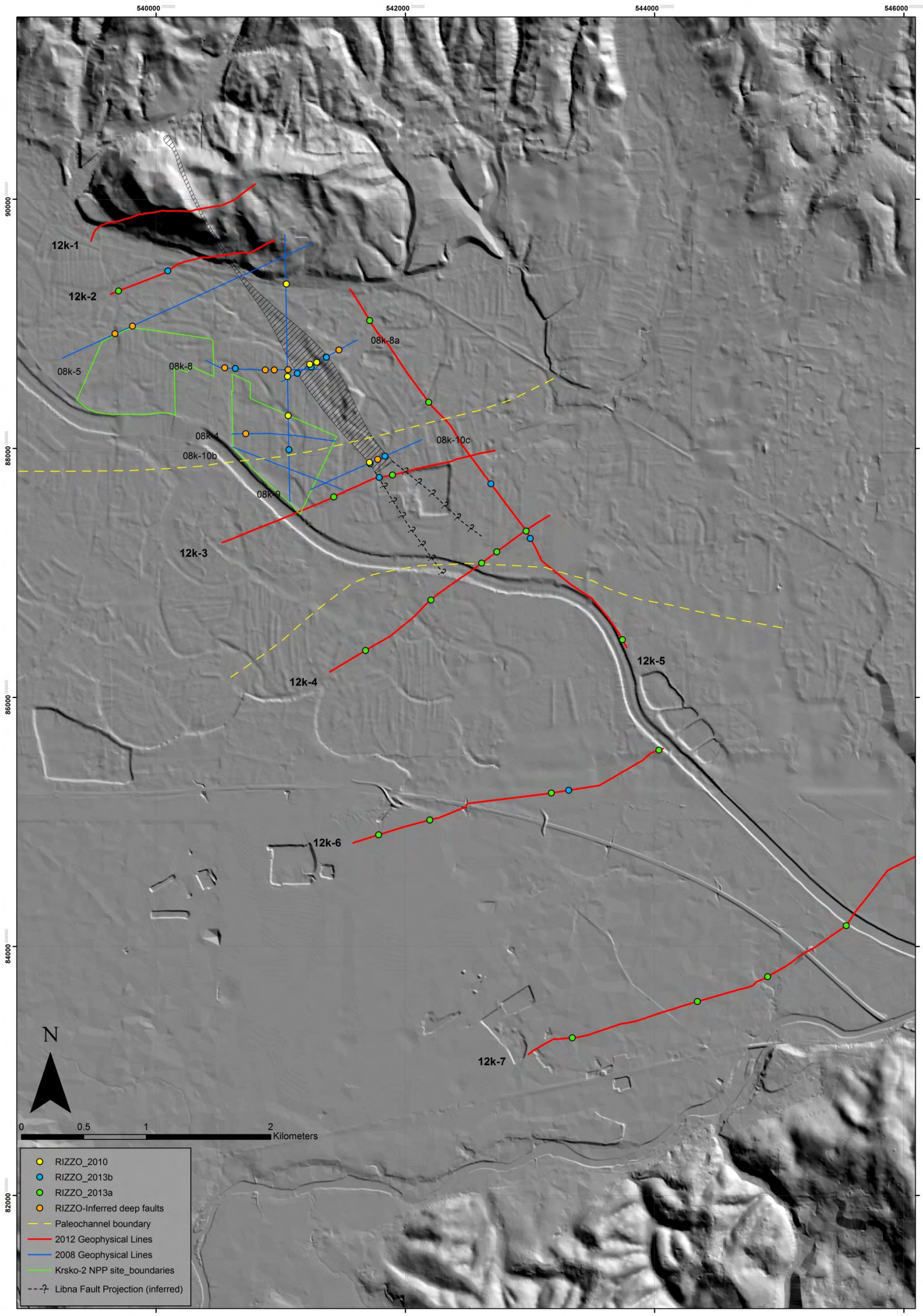

EXHIBIT 5
INTERPRETED FAULTS IN PLAN VIEW

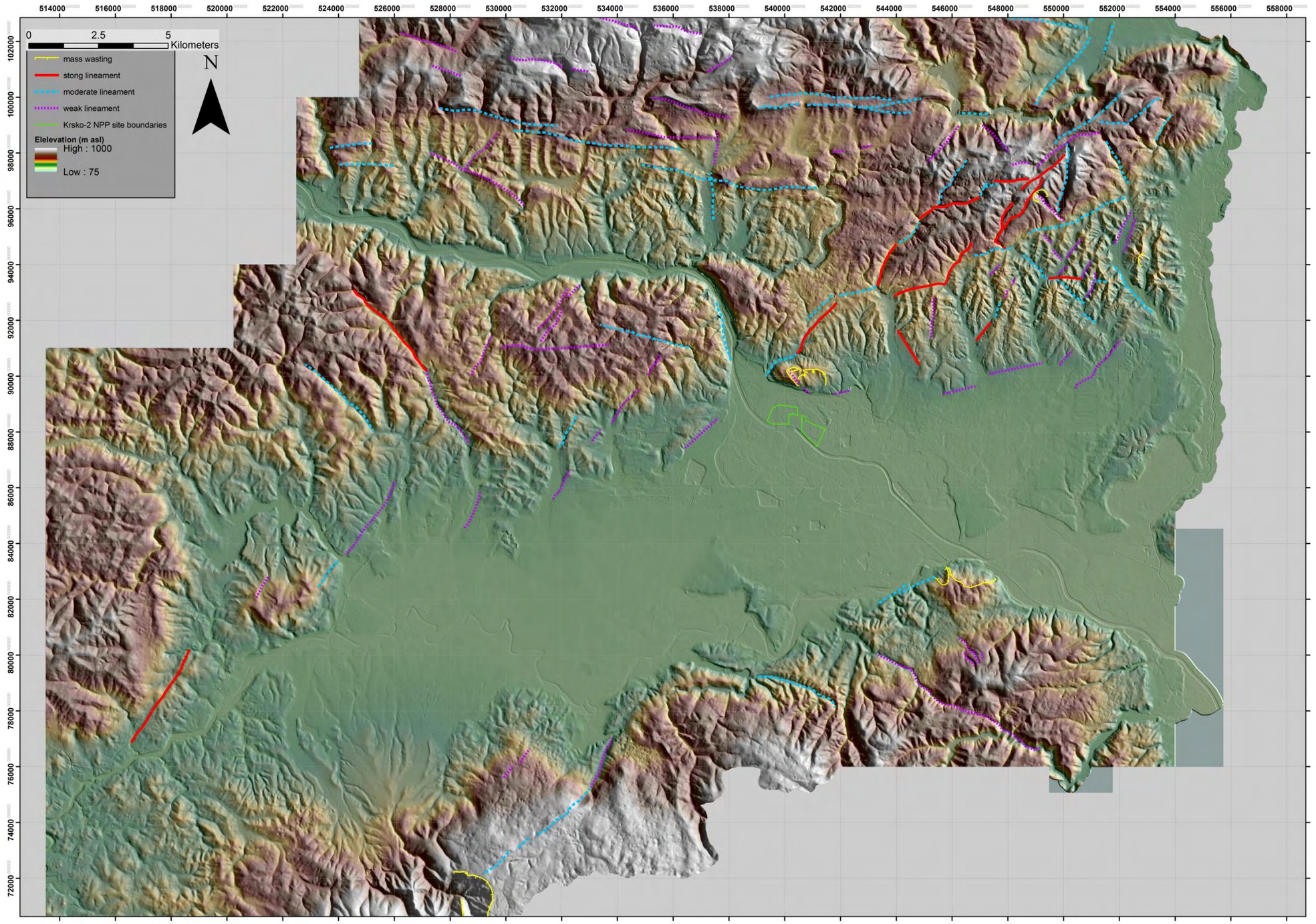

EXHIBIT 6
1.0 M AND 5.0 M HILLSHADE WITH COLOR DEM OVERLAY

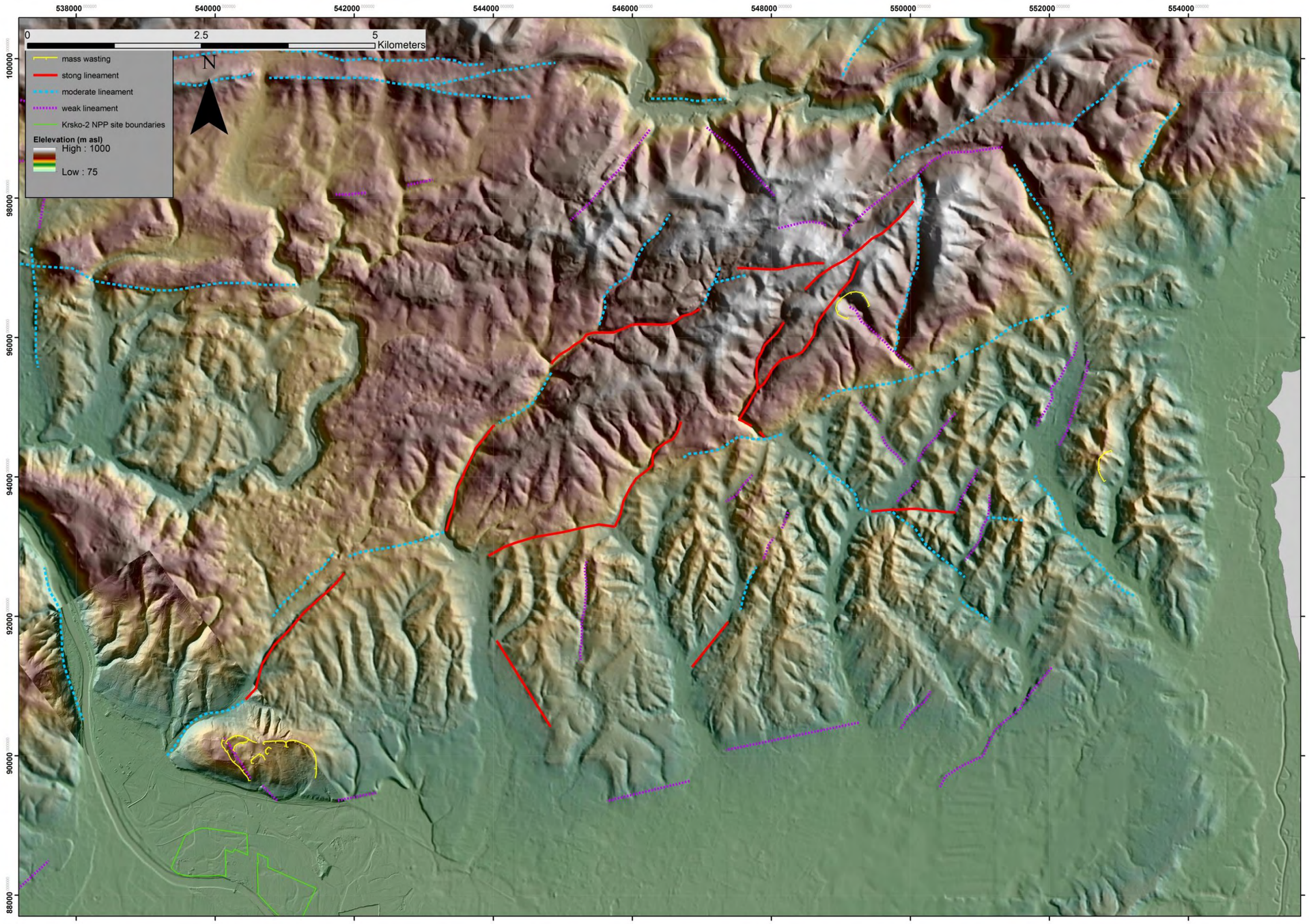

EXHIBIT 7
LINEAMENTS OF THE ORLICA FAULT ZONE AND INFERRED ARTIČE FAULT

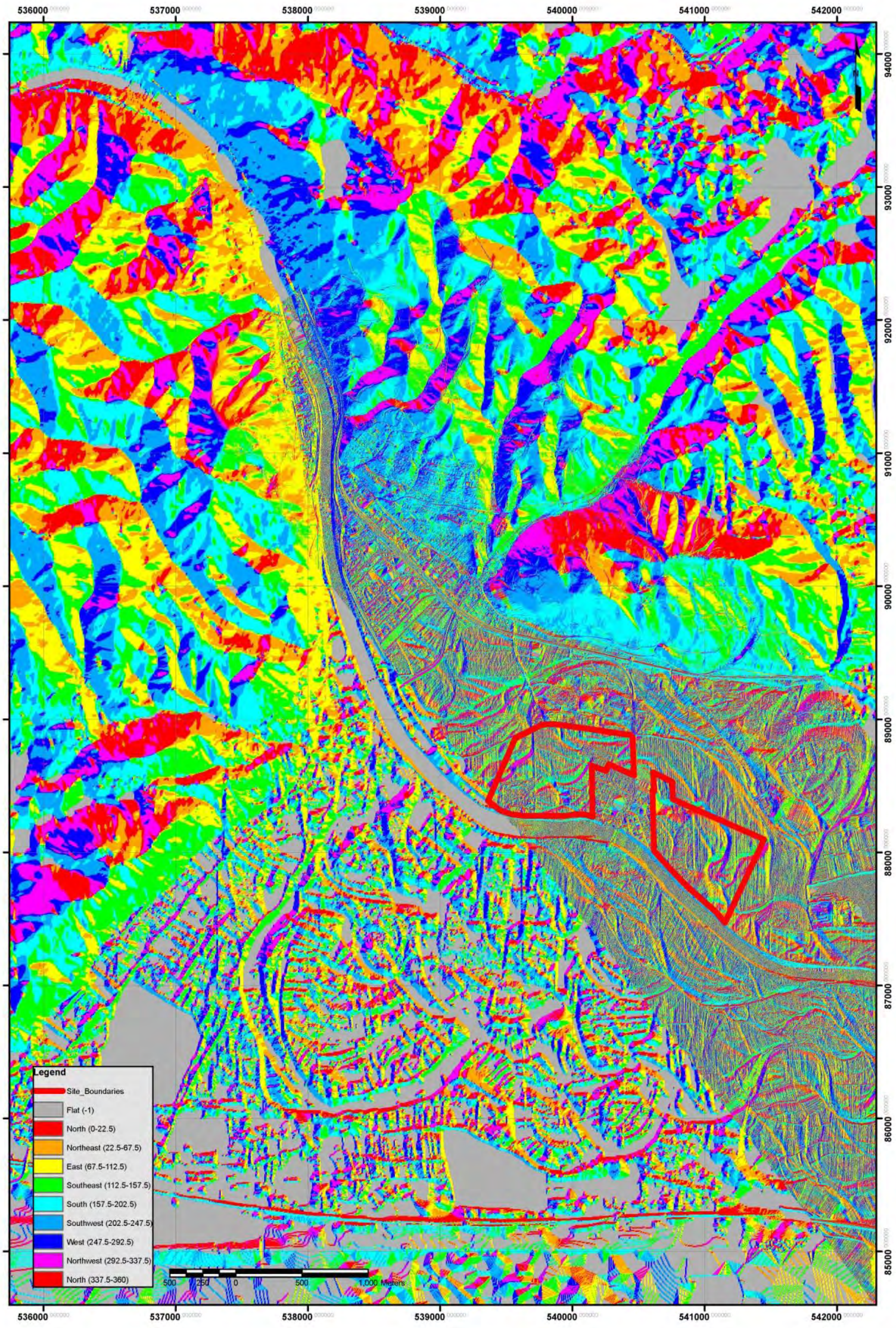

Note:
Slope gradient is the rate of topographic changes.

EXHIBIT 8
SLOPE ASPECT MAP

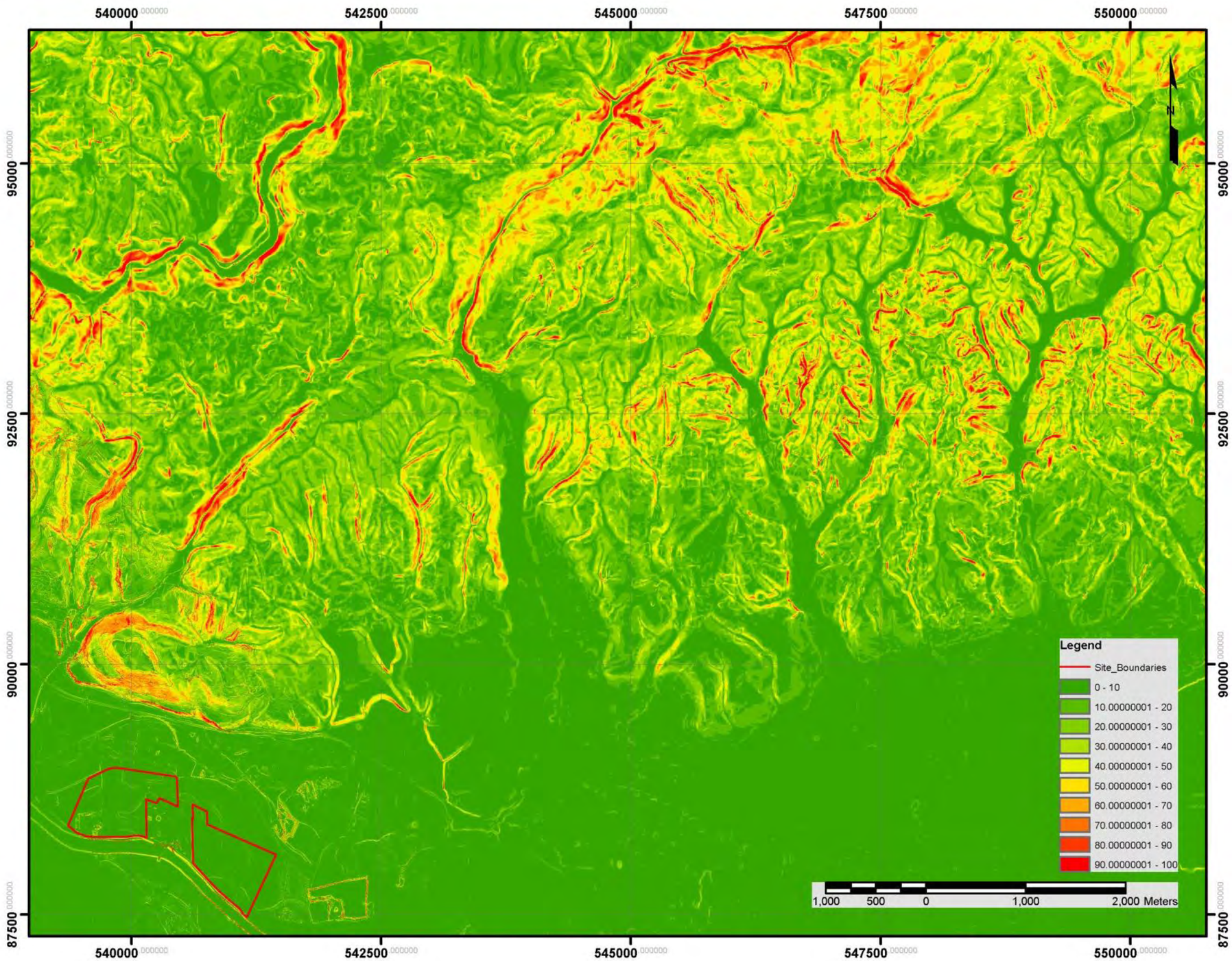

EXHIBIT 9
SLOPE GRADIENT MAP

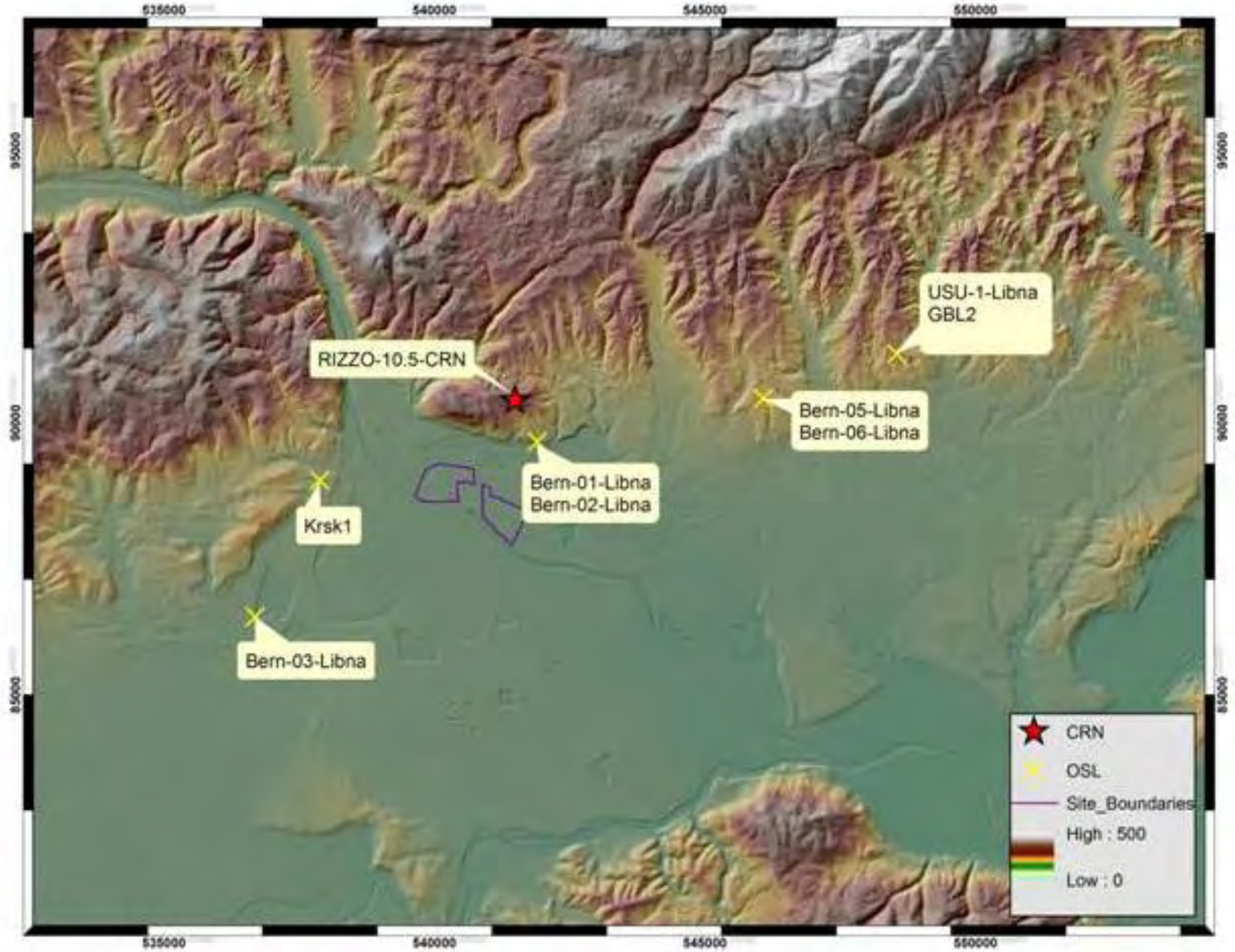

Note:
Color relief designation is in meters.

EXHIBIT 10
GEOCHRONOLOGY SAMPLE LOCATION MAP

APPENDIX 1

STERLING PROCESSED 2012 HRS PROFILES

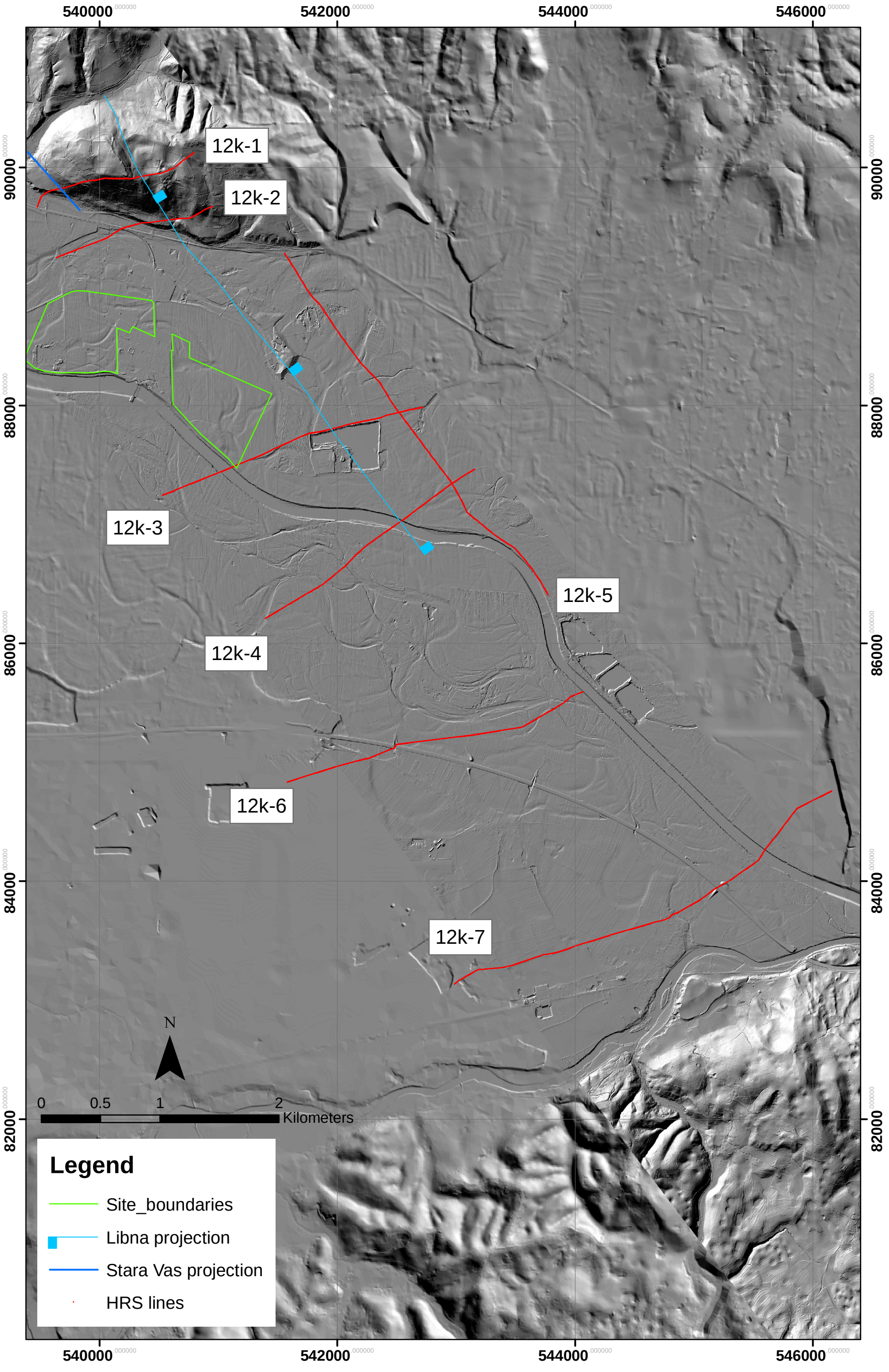

FIGURE 1-HRS layout

Figure 2: Raw Field Record - Filter: 28-300Hz with 50 Hz

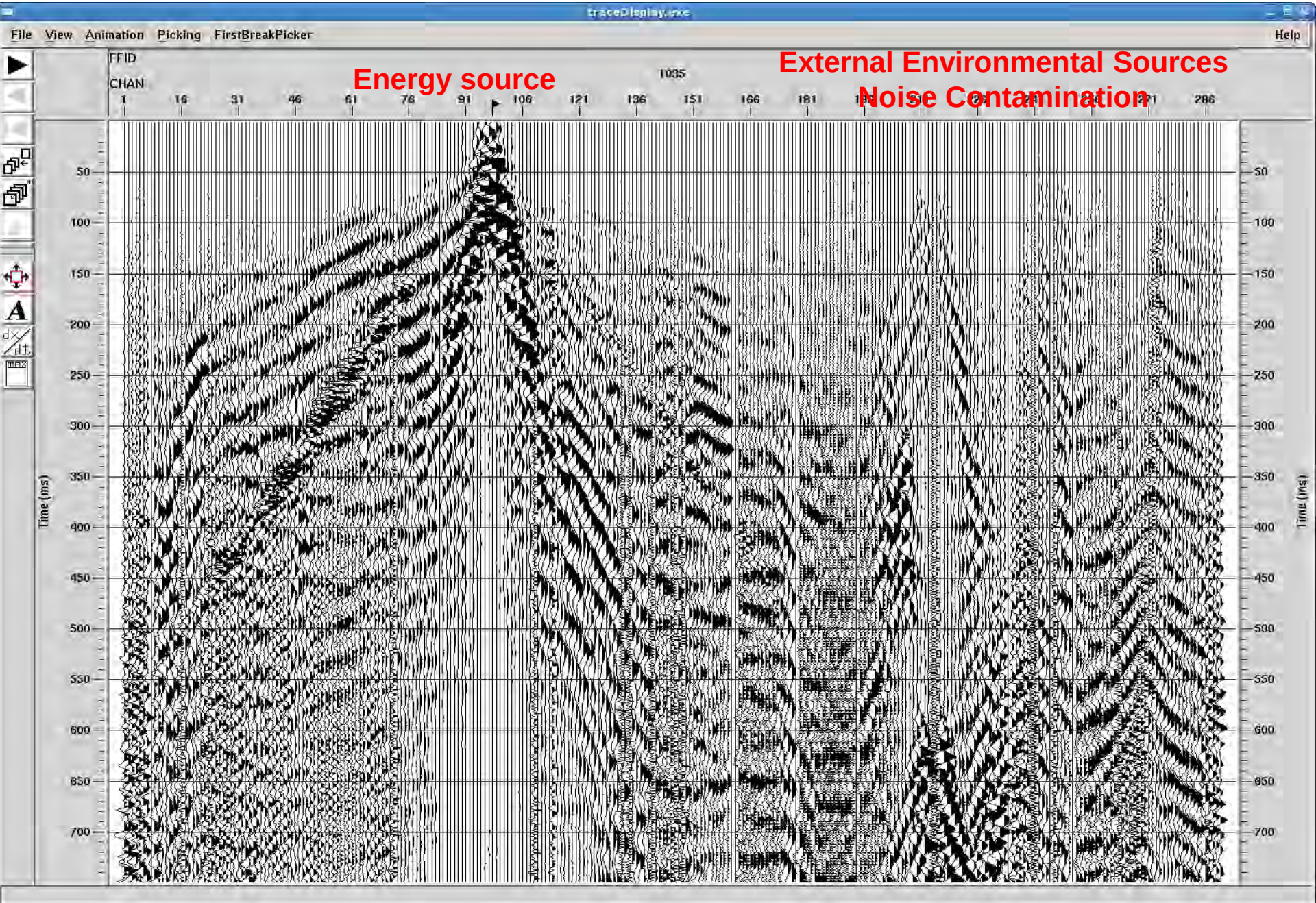

Figure 3: Line 12K- 1 - Final Stack - 30-300 Hz Filter

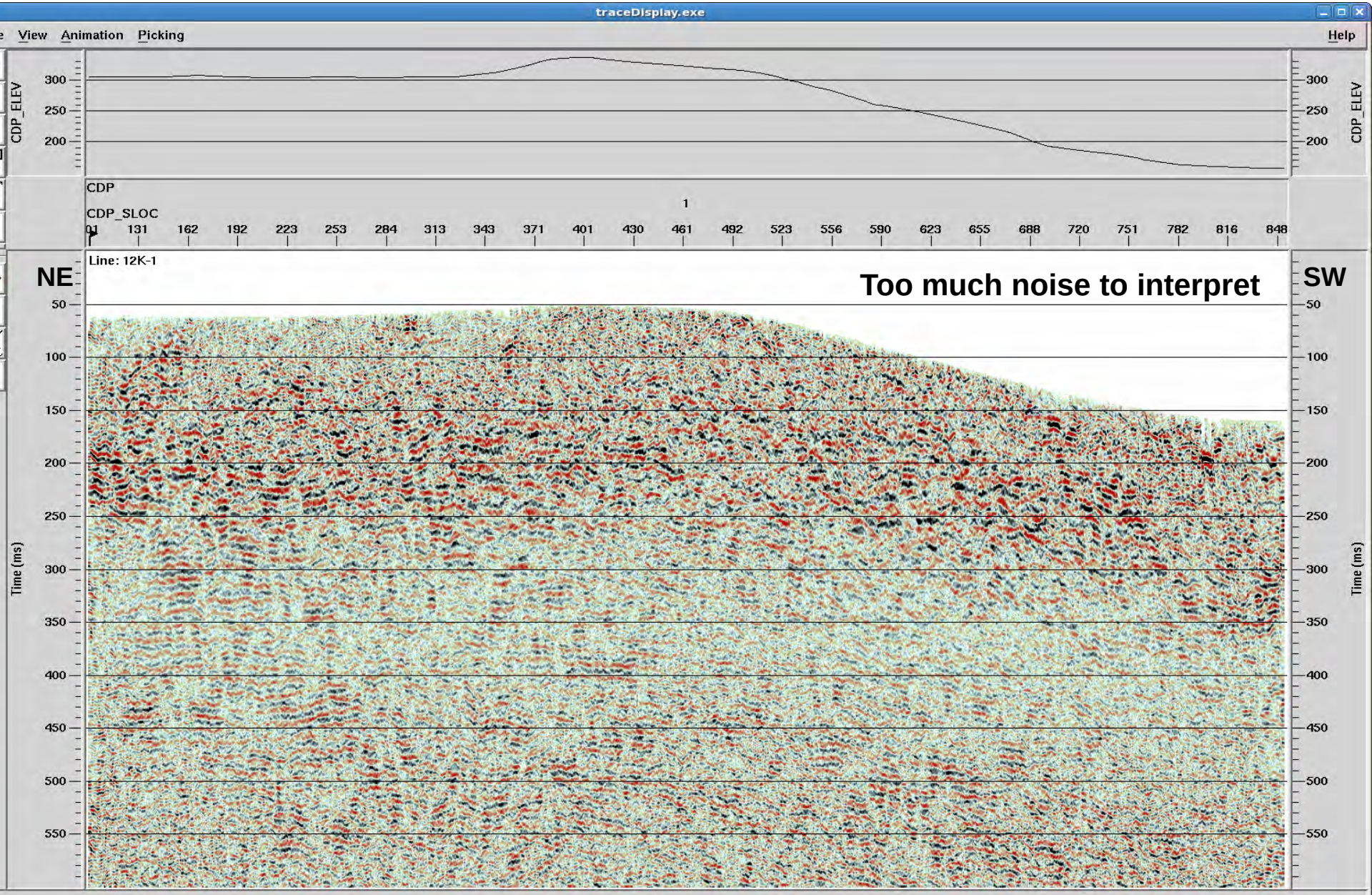

Figure 4: Line 12K- 2 - Final Stack - 30-300 Hz Filter

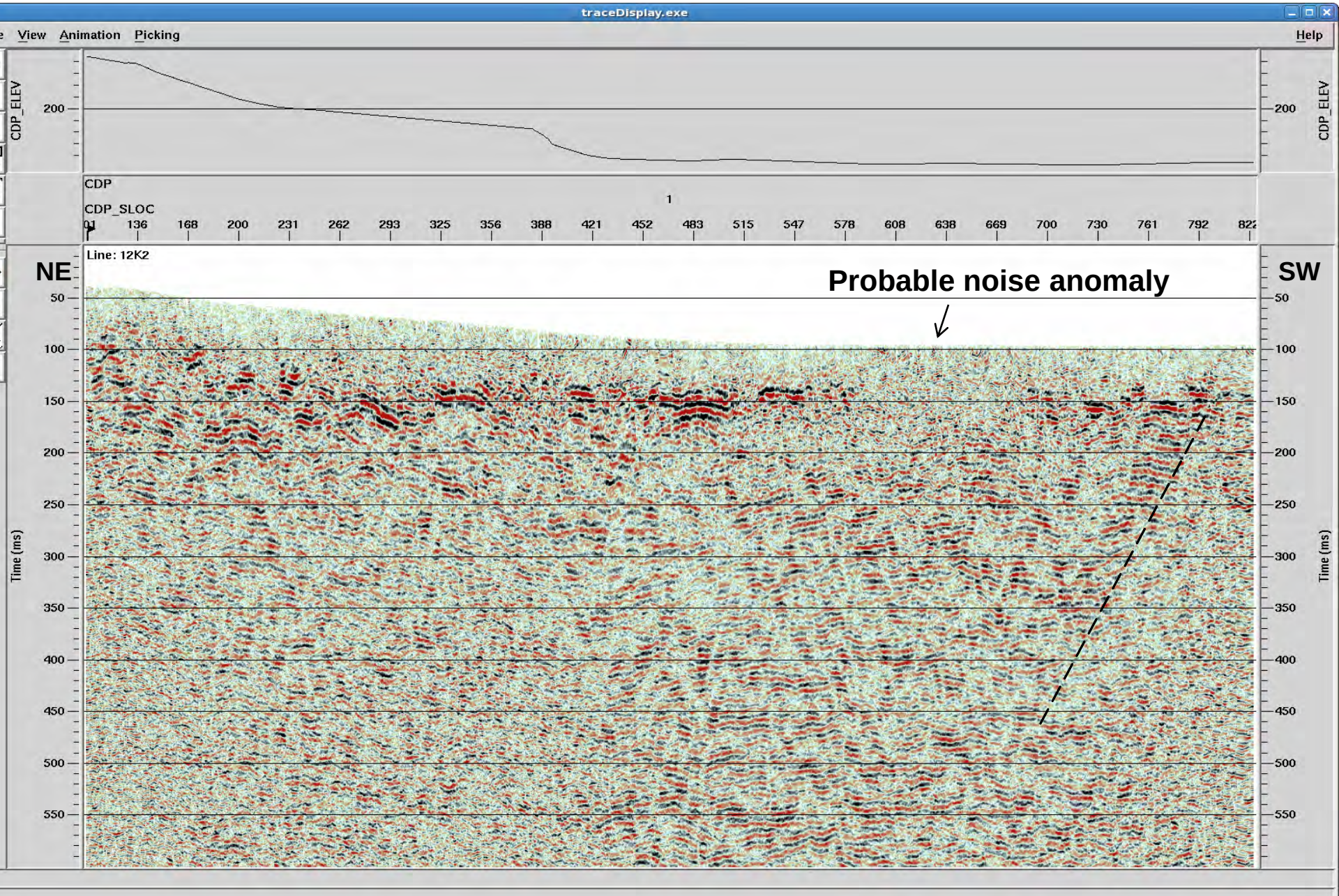

Figure 5: Line 12K- 3 Final Stack 30-300 Hz Filter

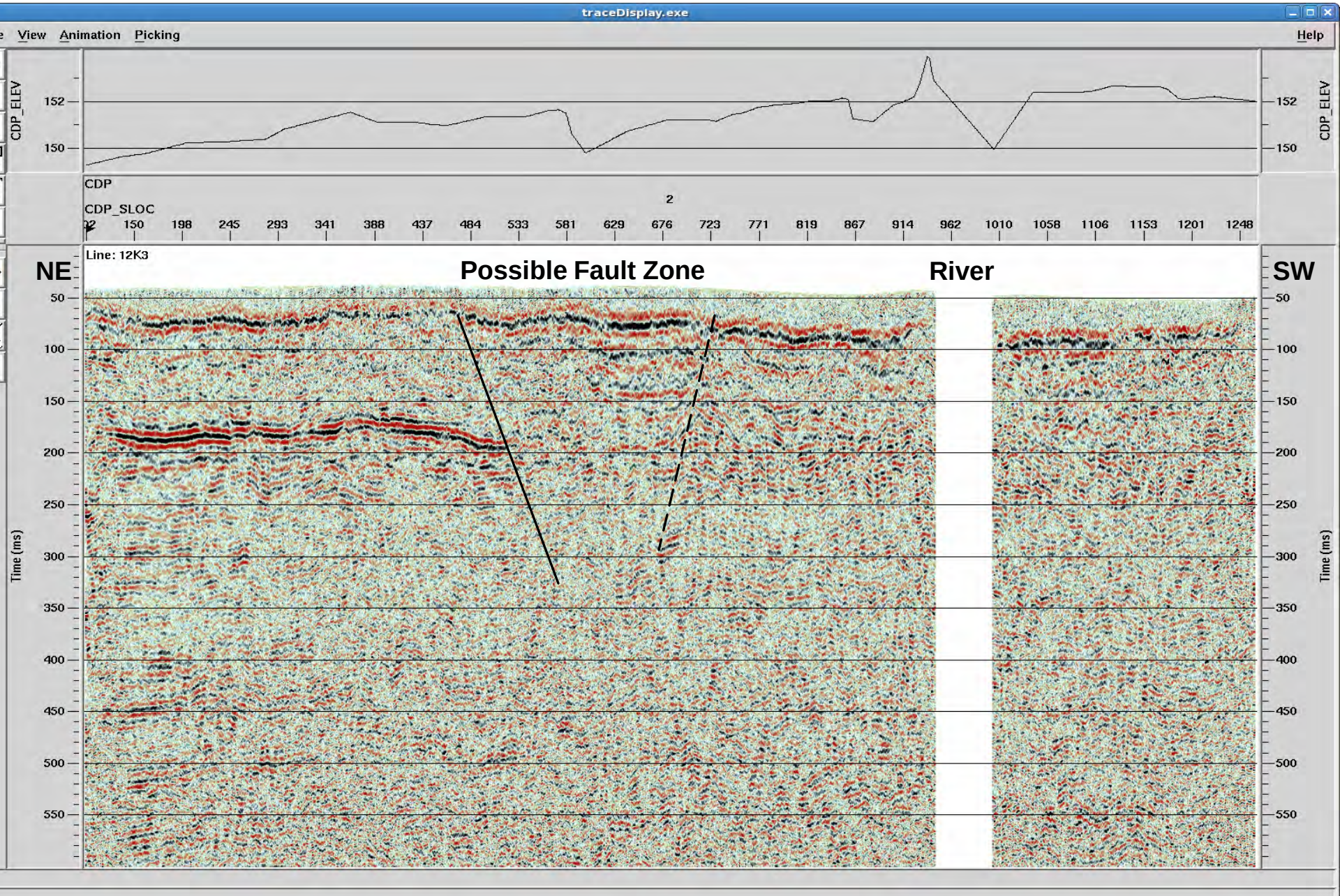

Figure 6: Line 12K- 4 - Final Stack - 30-300 Hz Filter

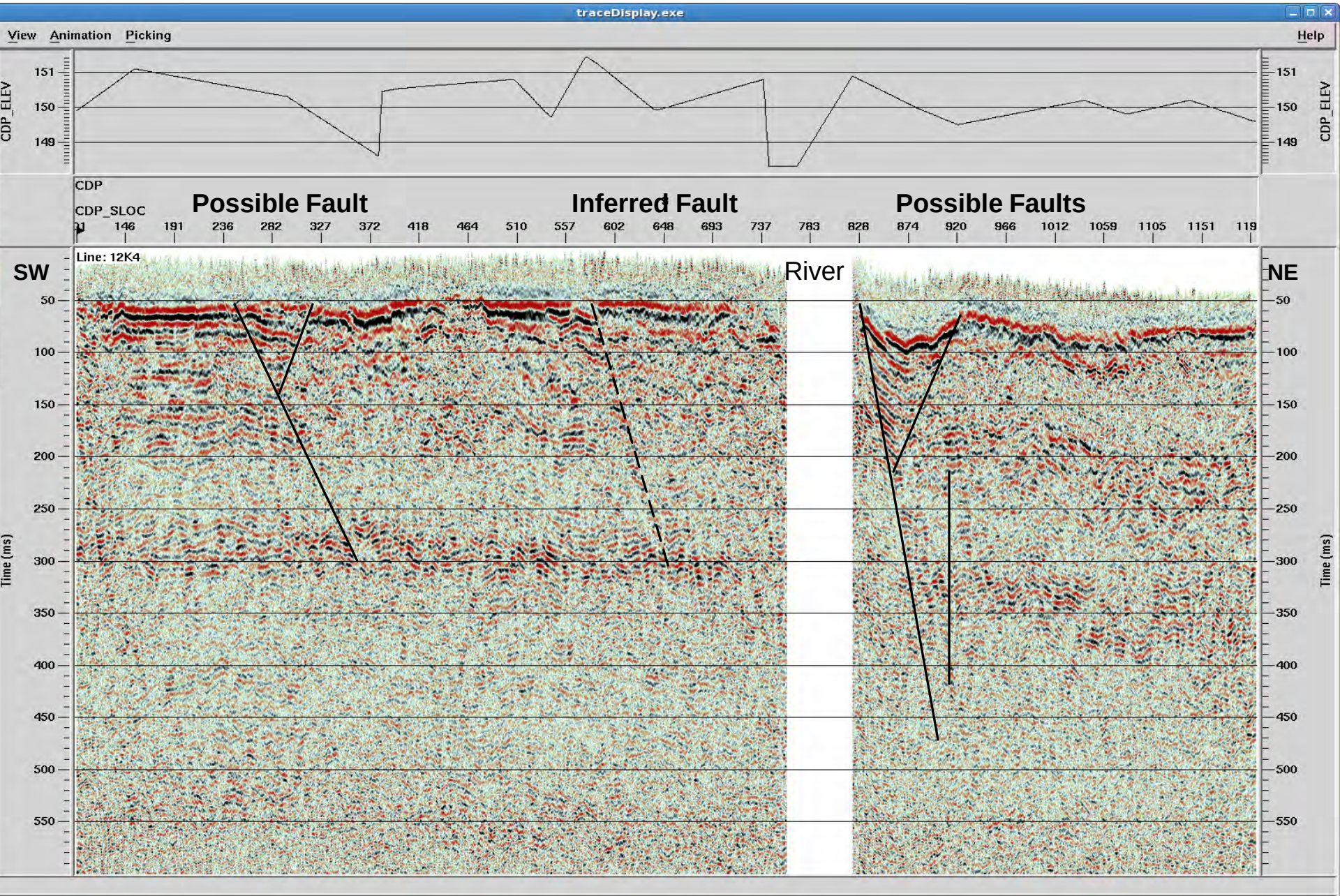

Figure 7: Line 12K- 5 - Final Stack - 30-300 Hz Filter

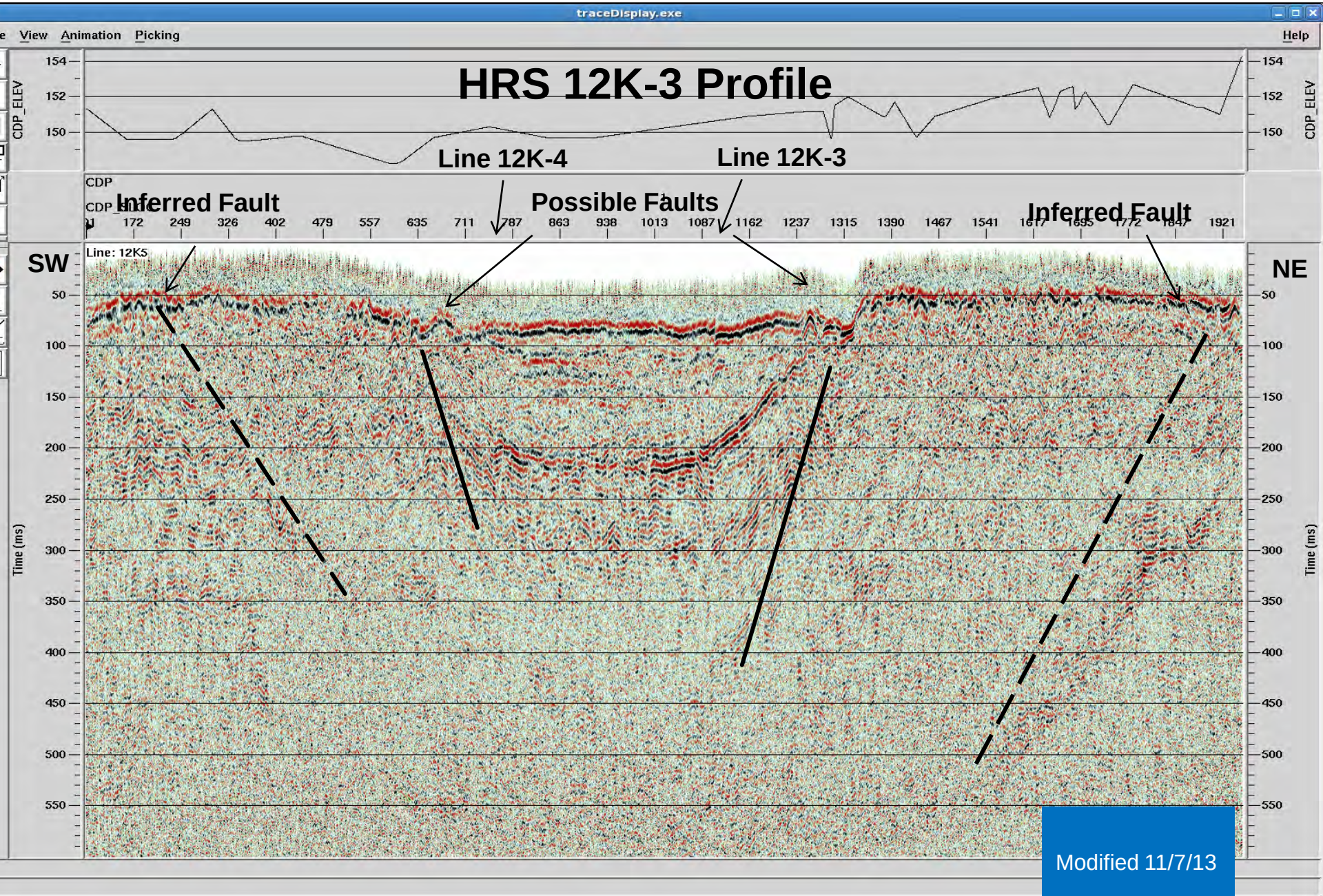

Modified 11/7/13

Figure 8: Line 12K- 6 - Final Stack - 30-300 Hz Filter

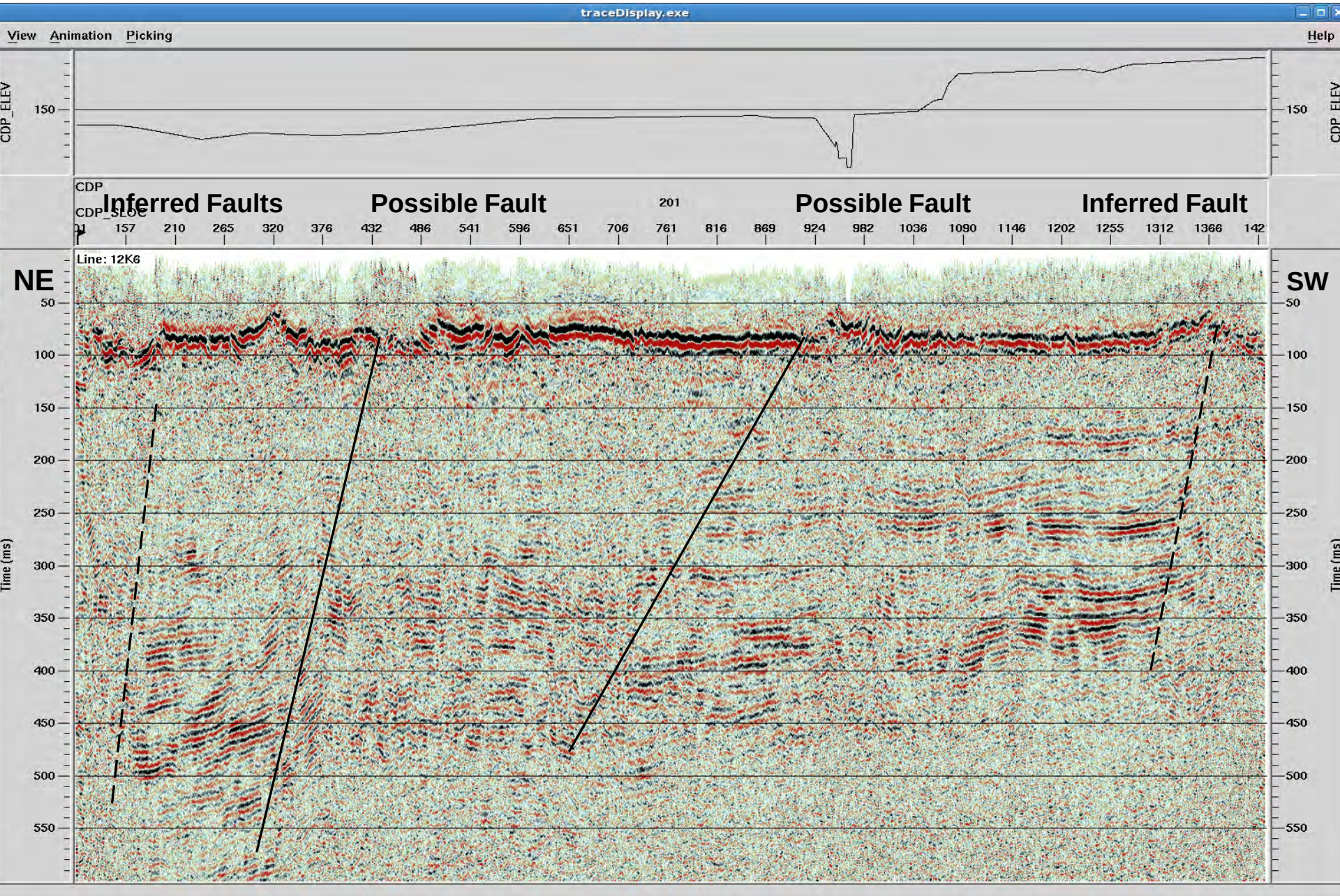

Figure 9: Line 12K- 7 - Final Stack - 30-300 Hz Filter

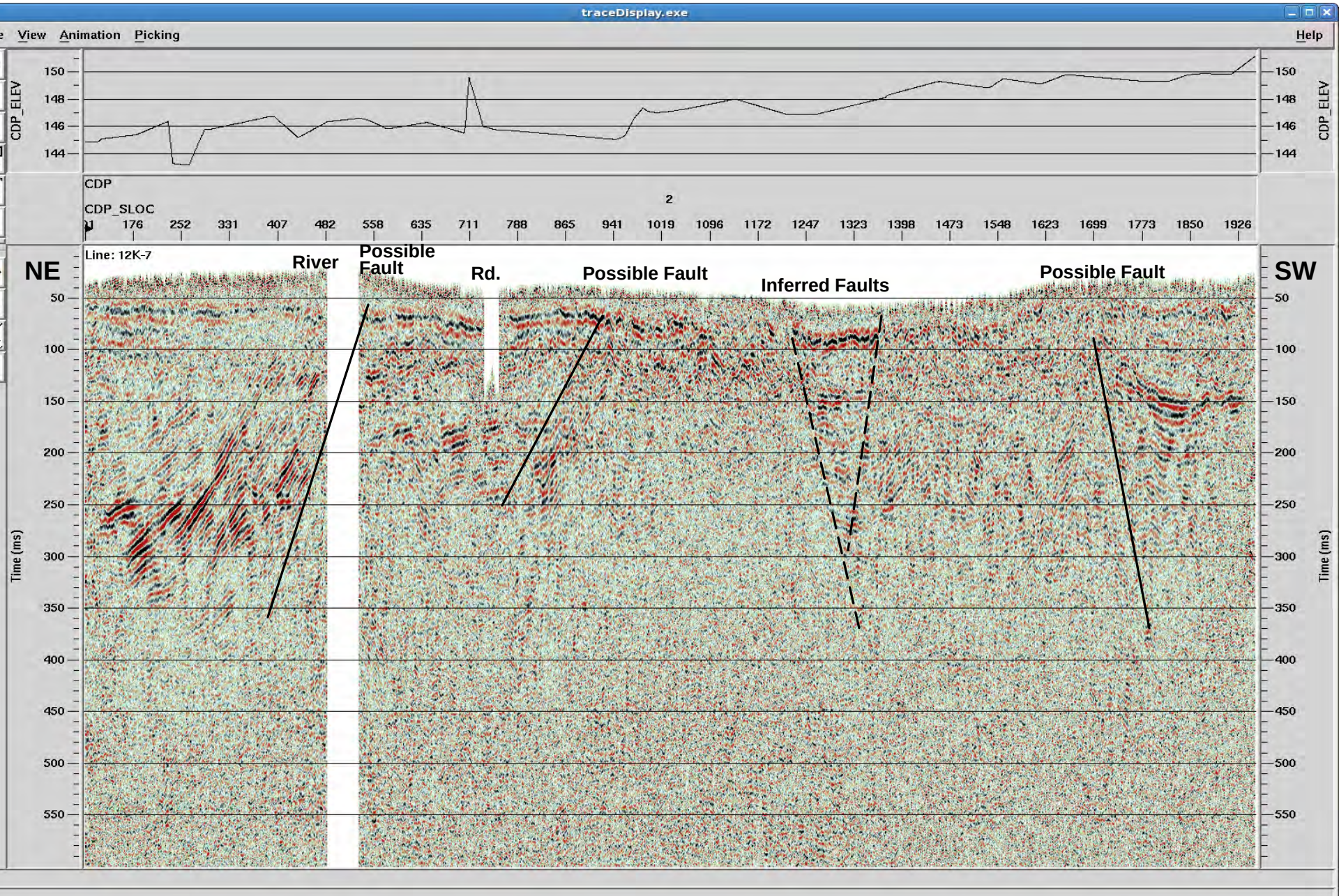

APPENDIX 2

GEOEXPERT HYBRID REFRACTION/REFLECTION FOR SELECTED 2008 AND ALL 2012 HRS PROFILES

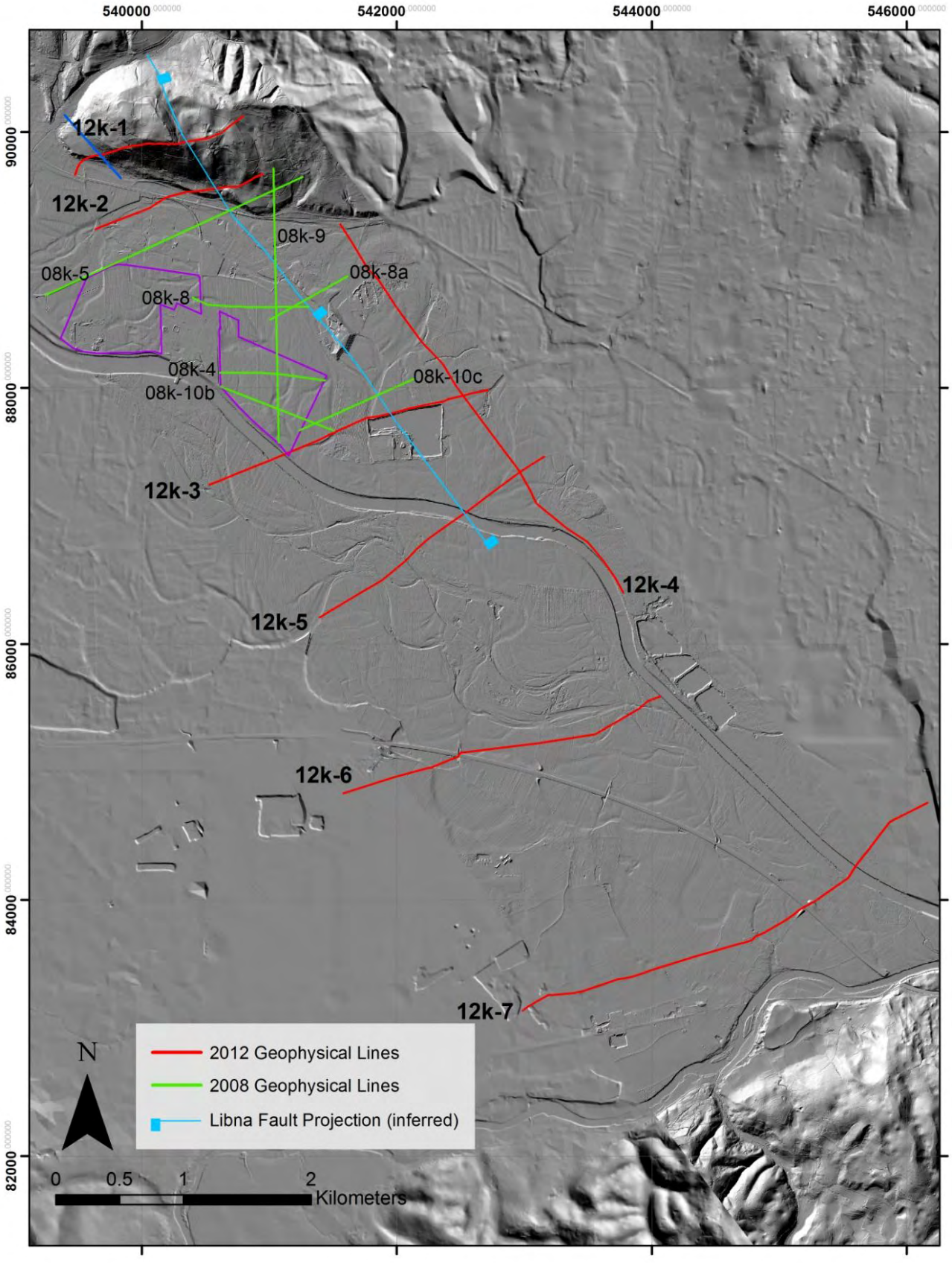

FIGURE 1
PLAN VIEW IMAGE SHOWING HIGH RESOLUTION SEISMIC SURVEY LINE PROFILES RE-INTERPRETED IN THIS REPORT

GEN ENERGIJA, d. o. o.
Vrbina 17, 8270 Krško

GEN ENERGIJA

Characterization of the Libna feature
Sava Plain, Krško - Brežice Area, Slovenia
High Resolution Seismic Survey

LINE 12K-1

Refraction tomography derived seismic velocity field

Field acquisition parameters

Spread layout	split-spread of varying asymmetry	CDP-distance	1 m
Number of channels	340	Coverage	56-fold (nominal)
Group interval	2 m	Instrumentation	Seismic Instruments Inc.
Geophone type	10 Hz	Sampling rate	0.5 ms
Geophone pattern	1 Geophone / Station	Recording time	750 ms
Source interval	4 - 6 m	Field filters	LC 4 Hz / HC anti-alias
Source type	Hammer 8 kg	Recorded by	D. Martin
Seismic crew	W.Frei	Date	15-16.10.2012

Data verification and survey geometry assignment

1 Reformatting and gain recovery
2 Line geometry and survey data assignment
3 Data verification, editing and analysis

Refraction seismic processing sequence (diving wave tomography)

1-3 dto.
4 Refraction arrival picking
5 CMP-sort of first break picks
6 Derivation of the refraction seismic velocities for the initial model by using the Delta-t-V method
7 Refinement by iterative modelling of the velocity-depth-profile by WET-tomography (30 iterations)
8 Display of velocity field

Scale 1 : 5'000

Processed by Ph. Corboz, November 2012

GeoExpert ag
Seismic Surveying
P.O. Box 325;Tannenstrasse 93
8424 Embrach / Switzerland
Tel. +41 71 652 60 70
info@geoexpert.ch; www.geoexpert.ch

Project management
Paul C. Rizzo Associates, Inc. ENGINEERS/CONSULTANTS/CM

Enclosure **1a**
report 4. February 2013

Fig. 1a: Seismic velocity field derived by refraction diving wave tomography

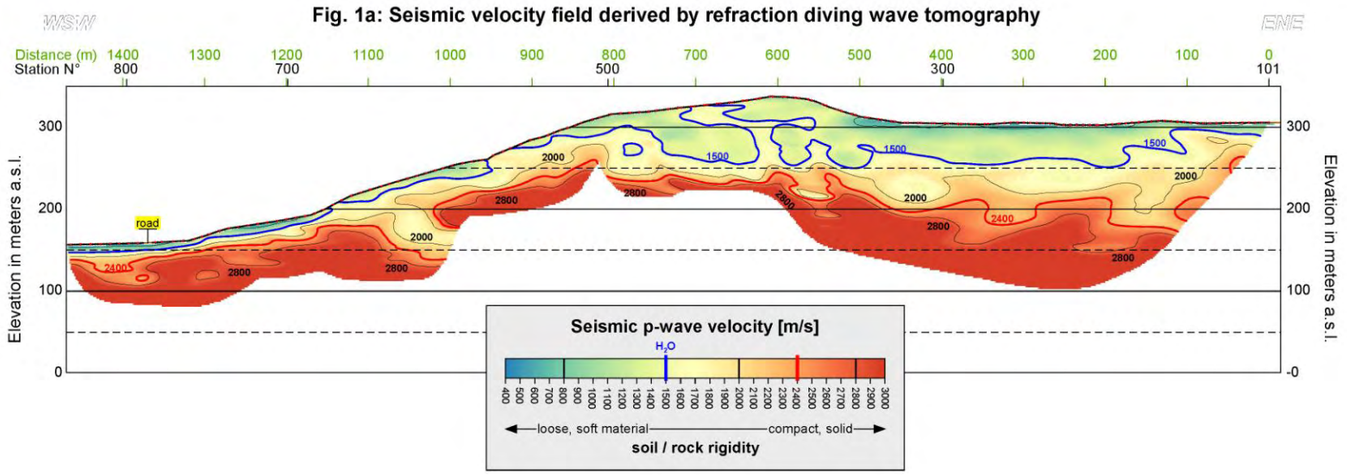

Fig. 1b: Refraction raypath density per m²

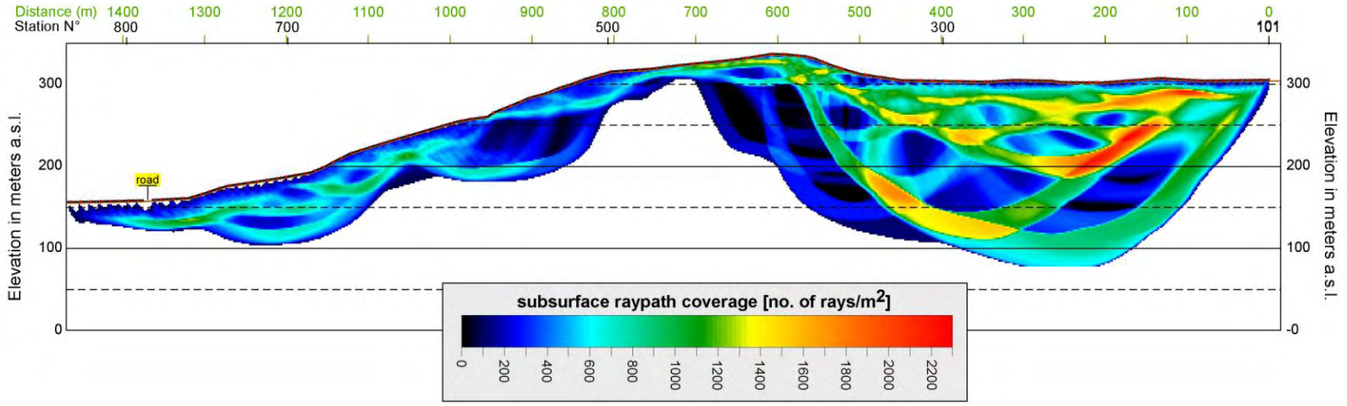

FIGURE 2
DETAILS OF SEISMIC VELOCITY AND REFRACTION RAYPATH DENSITY SHOWING 12K-1 AS AN EXAMPLE

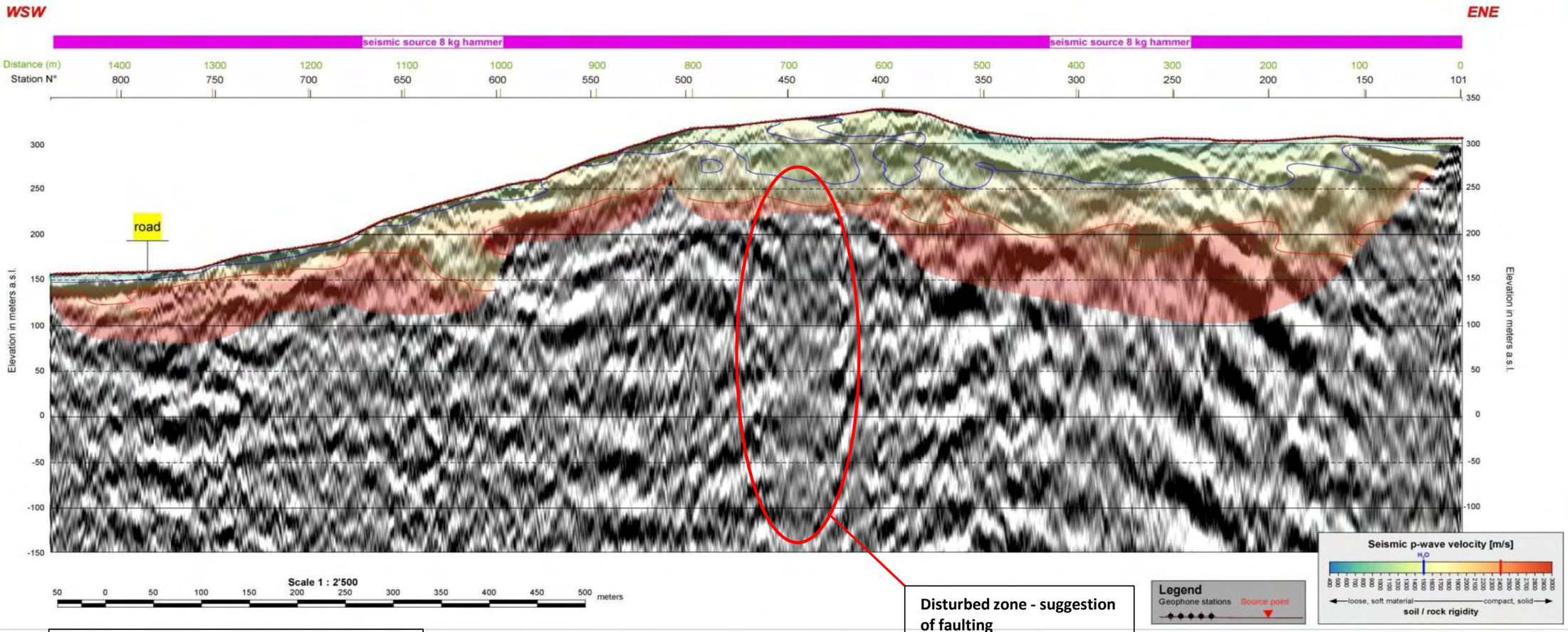

FIGURE 3
INTERPRETATION OF HRS HYBRID PROFILE 12K-1

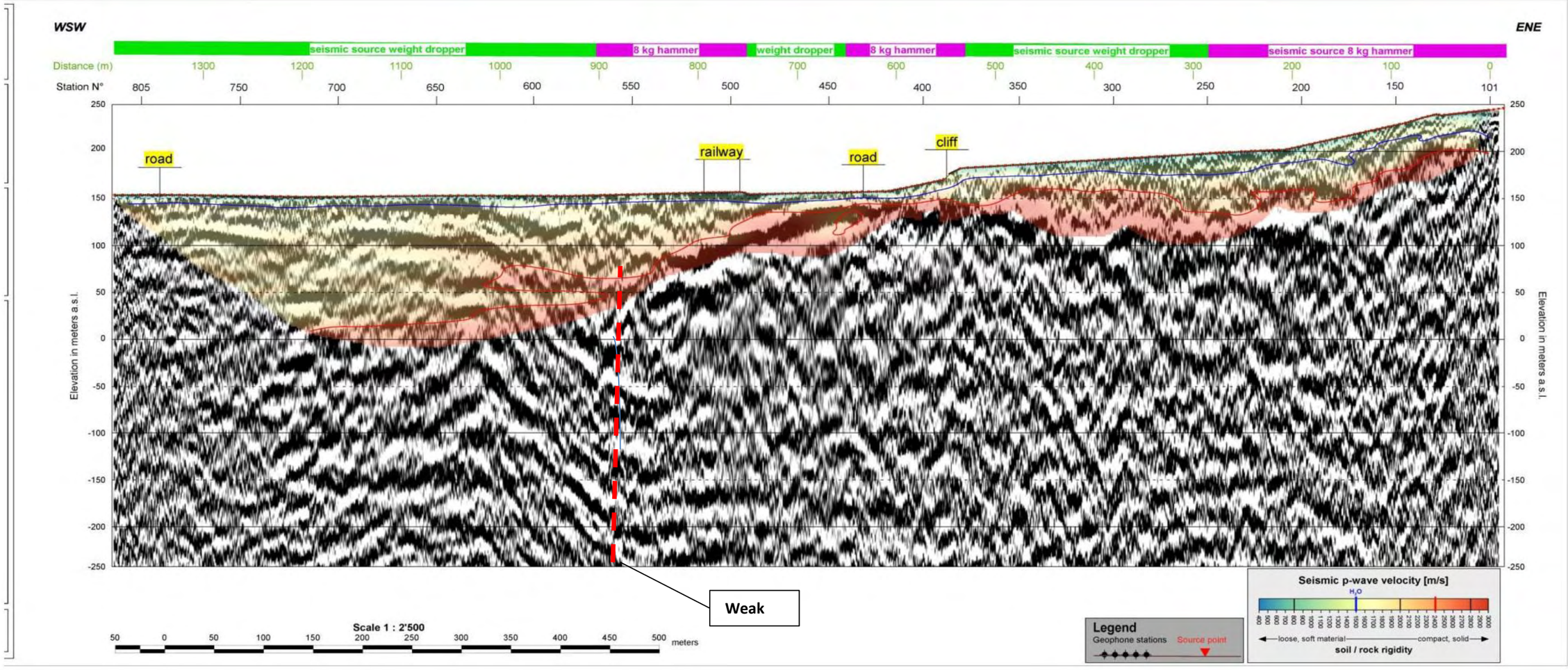

Note: Gray zone represents only the seismic reflection profile . Color represents refraction tomography superimposed on reflection profile.

Inferred Fault

Possible Fault

FIGURE 4
INTERPRETATION OF HRS HYBRID PROFILE 12K-2

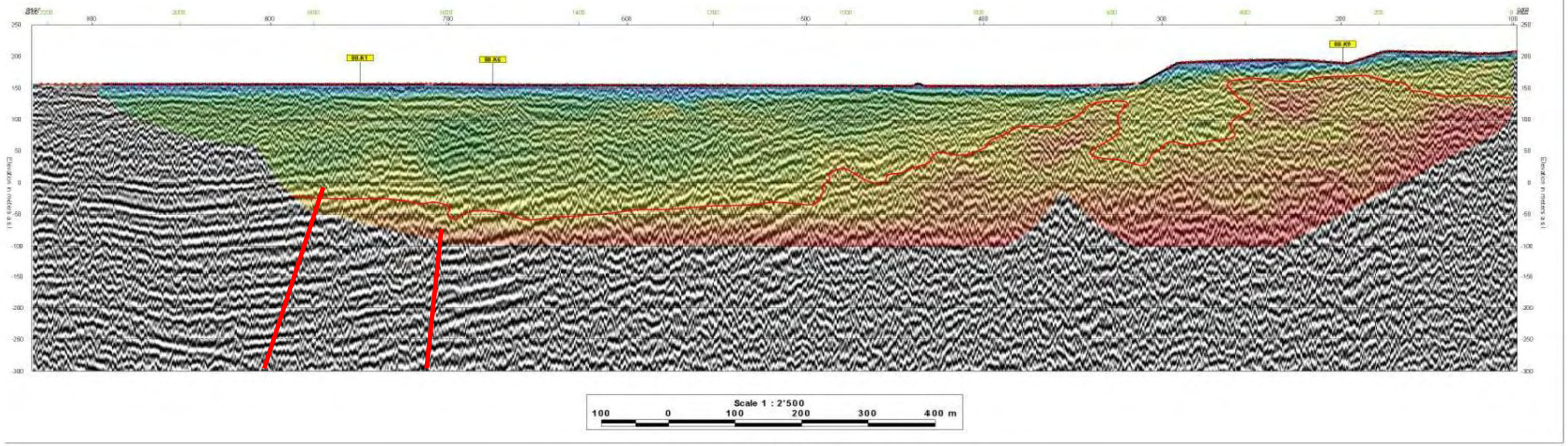

Note: Gray zone represents only the seismic reflection profile . Color represents refraction tomography superimposed on reflection profile.

Inferred Fault

Possible Fault

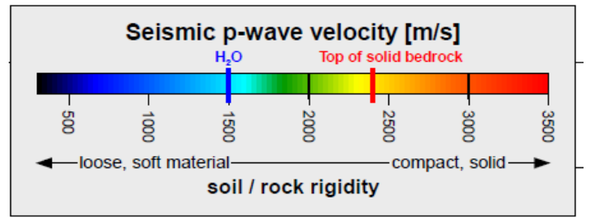

FIGURE 5
INTERPRETATION OF HRS HYBRID PROFILE 08K-5

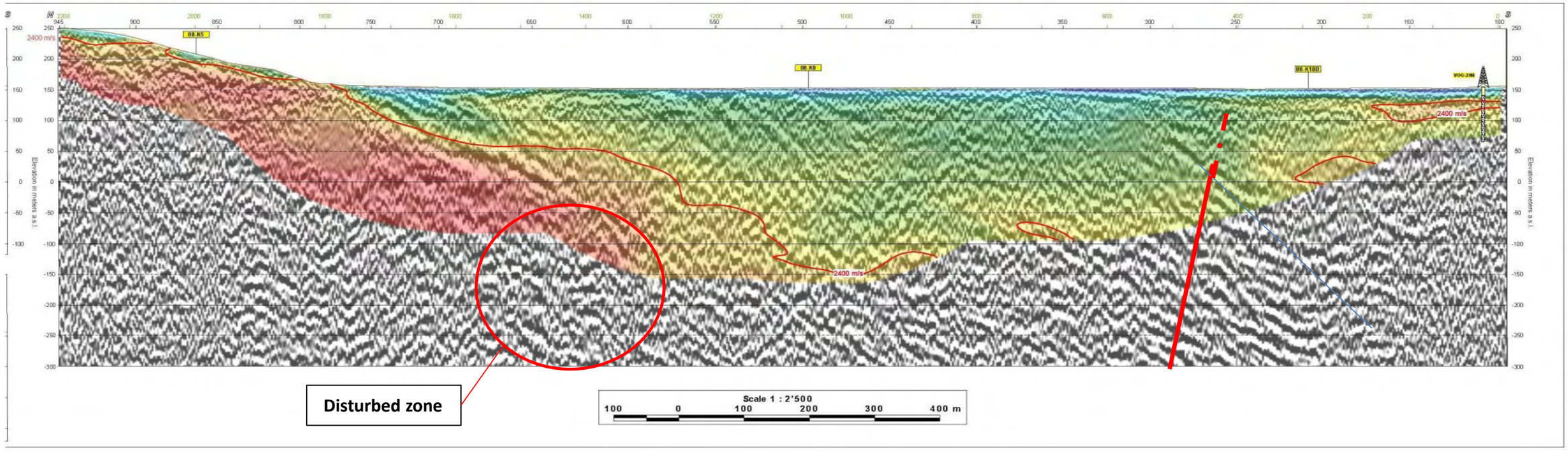

Note: Gray zone represents only the seismic reflection profile . Color represents refraction tomography superimposed on reflection profile.

Inferred Fault

Possible Fault

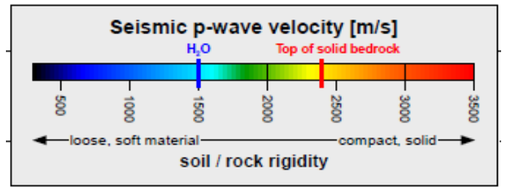

FIGURE 6
INTERPRETATION OF HRS HYBRID PROFILE 08K-9

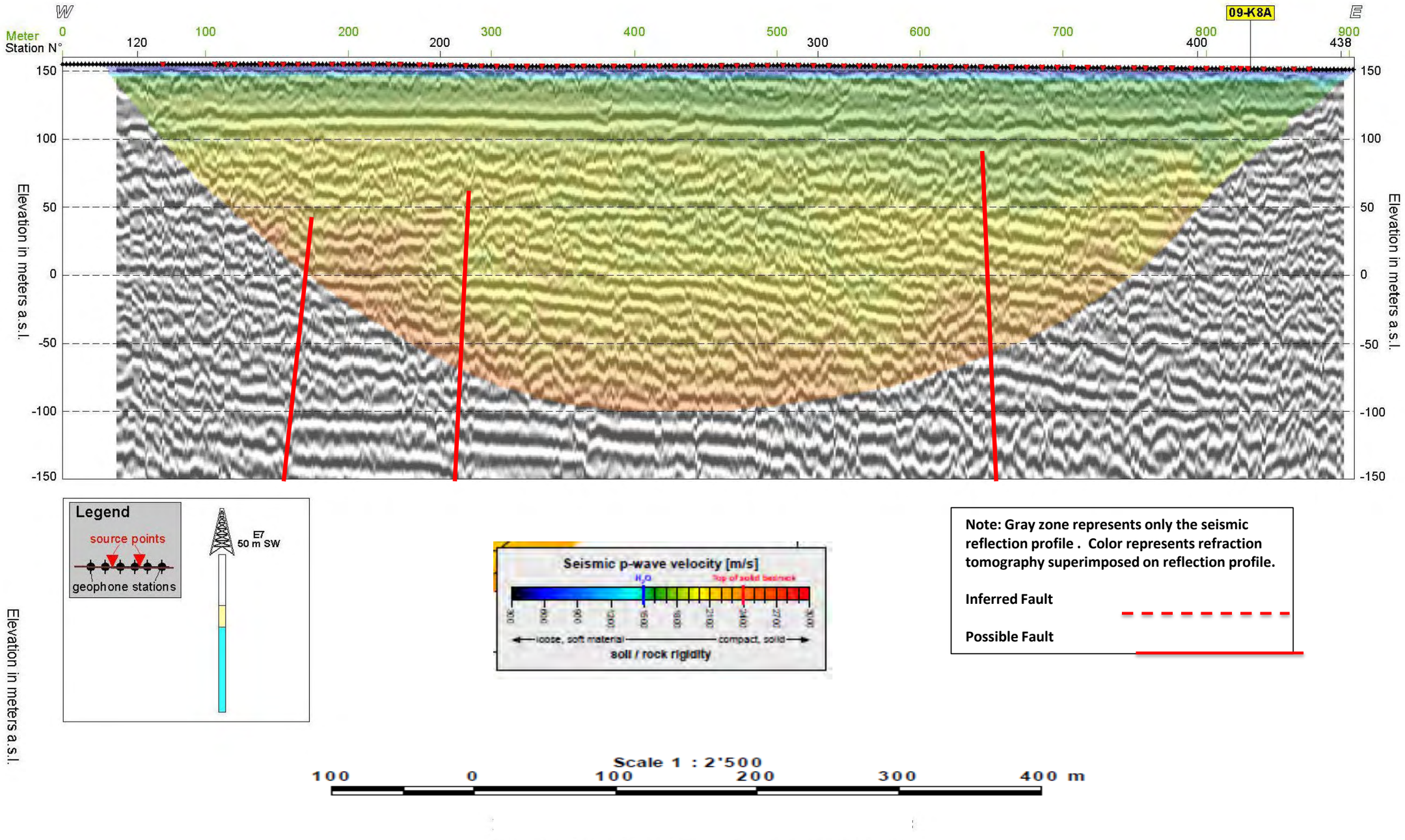

FIGURE 7
INTERPRETATION OF HRS HYBRID PROFILE 08K-8

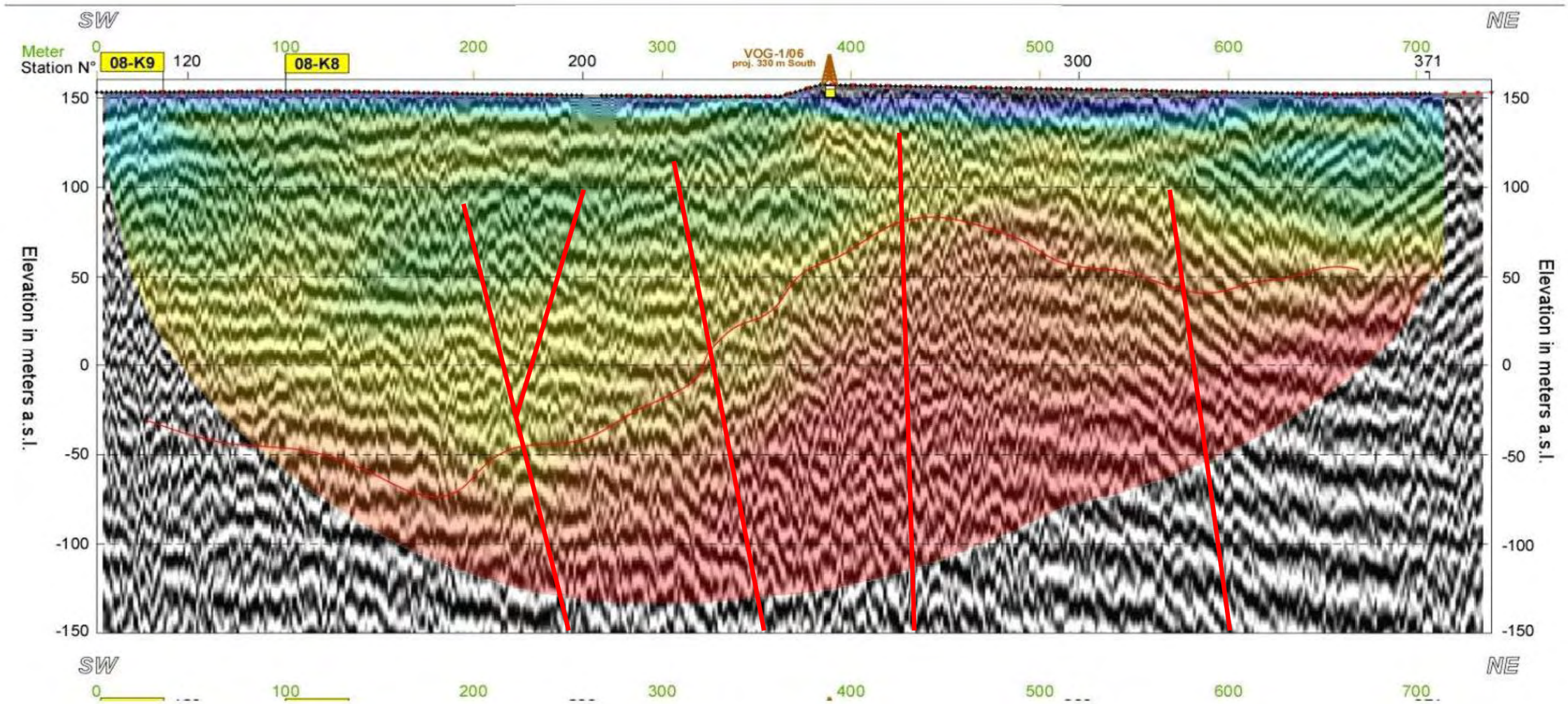

Note: Gray zone represents only the seismic reflection profile . Color represents refraction tomography superimposed on reflection profile.

Inferred Fault

Possible Fault

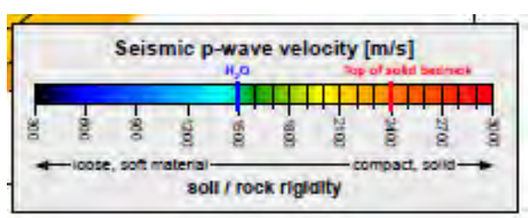

FIGURE 8
INTERPRETATION OF HRS HYBRID PROFILE 08K-8a

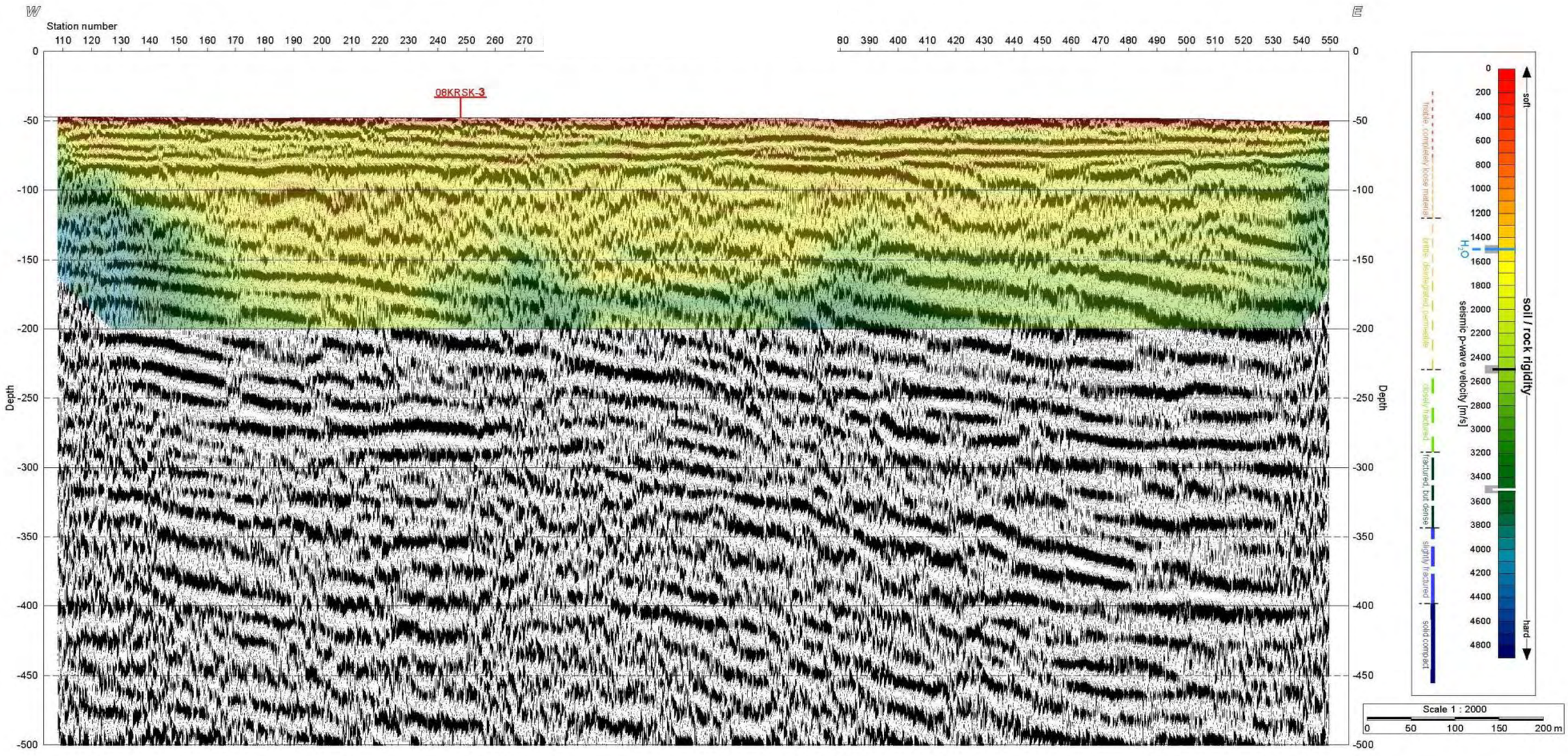

Note: Gray zone represents only the seismic reflection profile . Color represents refraction tomography superimposed on reflection profile.

Inferred Fault

Possible Fault

No Faulting Observed

FIGURE 9
INTERPRETATION OF HRS HYBRID PROFILE 08K-4

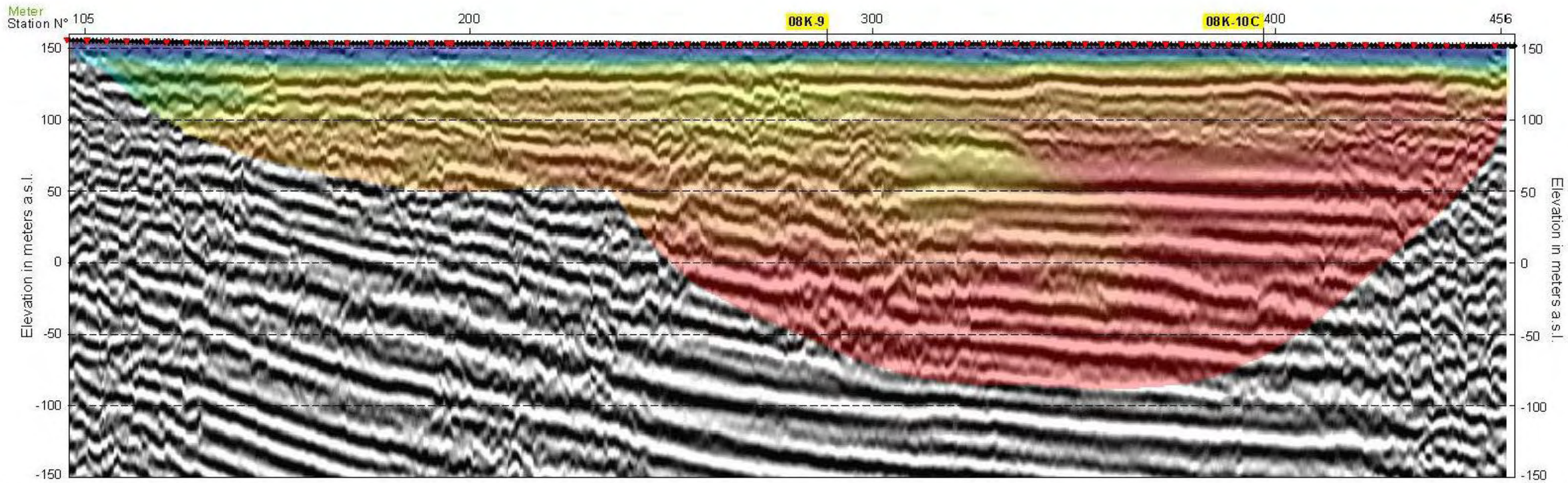

Note: Gray zone represents only the seismic reflection profile . Color represents refraction tomography superimposed on reflection profile.

Inferred Fault

Possible Fault

No Faulting Observed

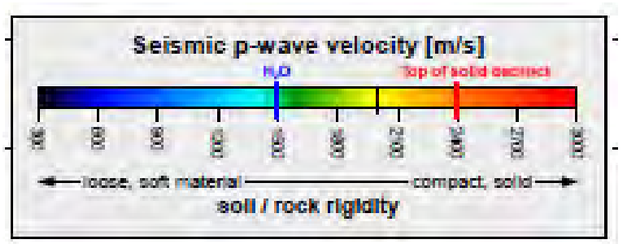

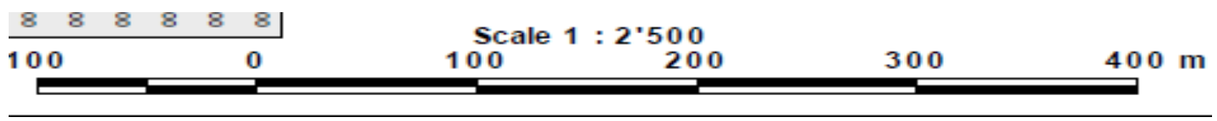

FIGURE 10
INTERPRETATION OF HRS HYBRID PROFILE 08K-10b

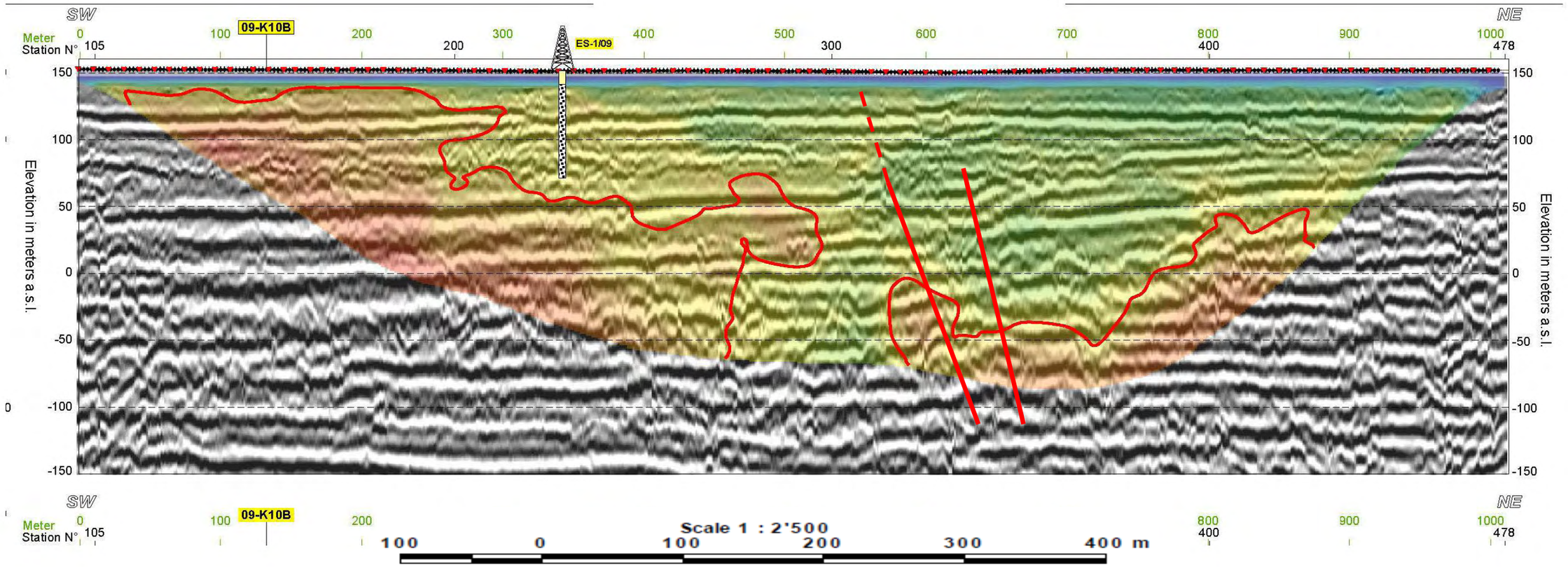

Note: Gray zone represents only the seismic reflection profile . Color represents refraction tomography superimposed on reflection profile.

Inferred Fault - - - - - - - -

Possible Fault ————————

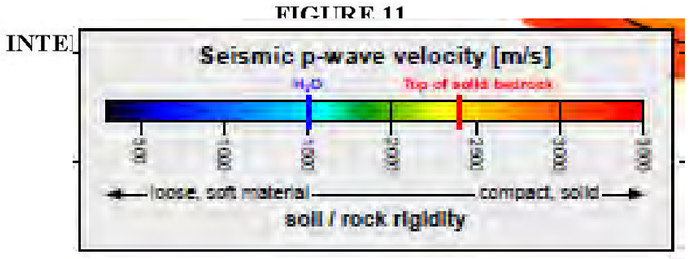

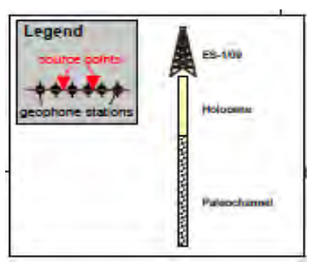

FIGURE 11
INTERPRETATION OF HRS HYBRID PROFILES 08K-10c

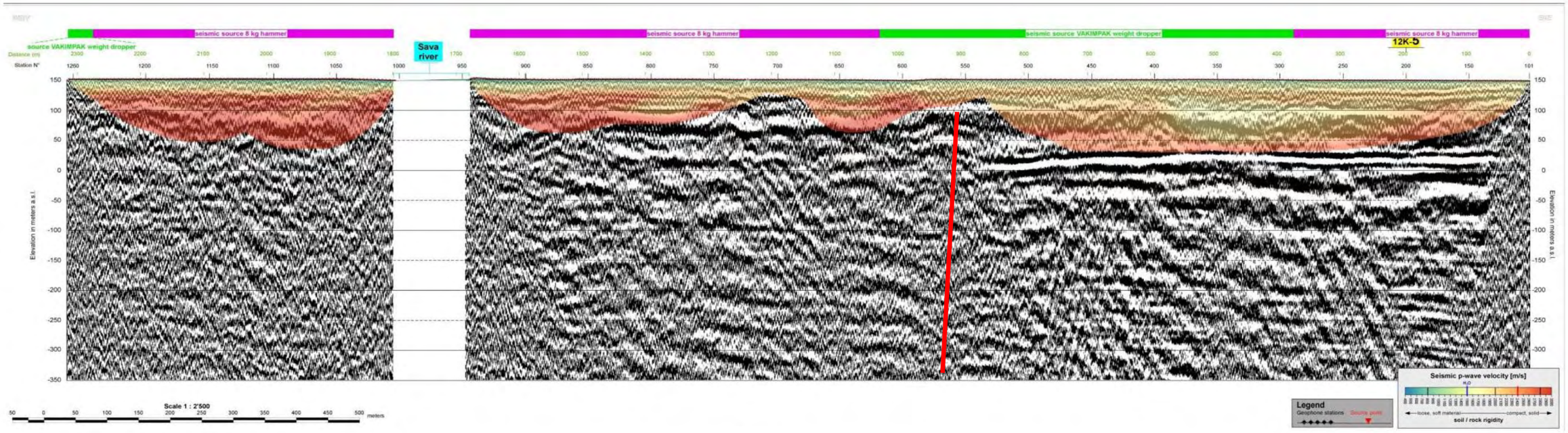

Note: Gray zone represents only the seismic reflection profile . Color represents refraction tomography superimposed on reflection profile.

Inferred Fault

Possible Fault

FIGURE 12
INTERPRETATION OF HRS HYBRID PROFILE 12K-3

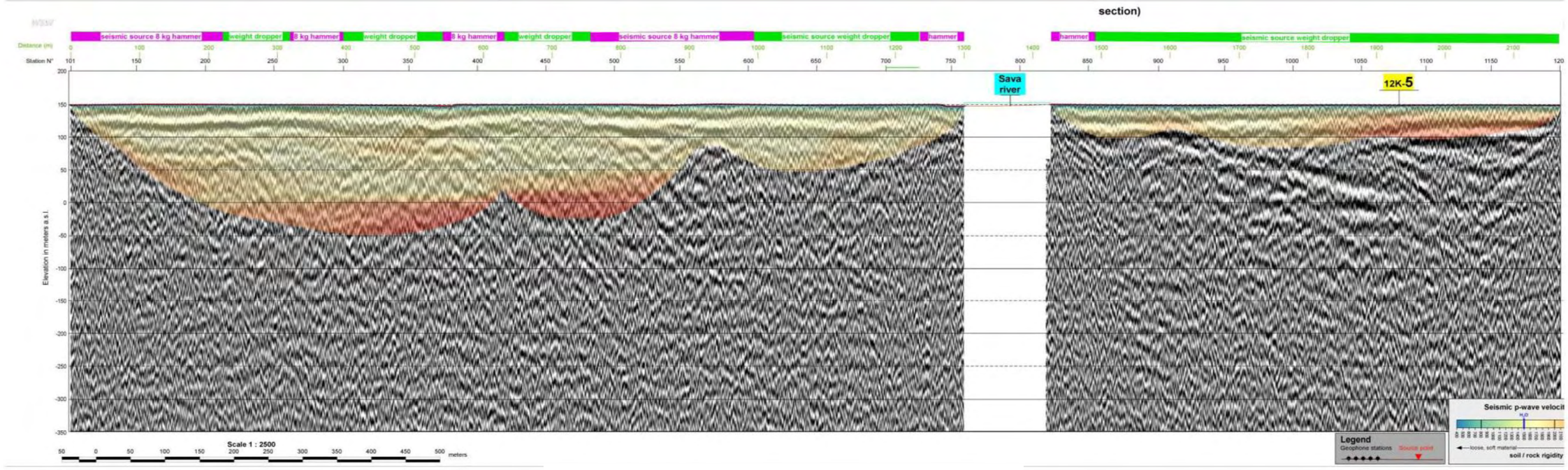

Note: Gray zone represents only the seismic reflection profile . Color represents refraction tomography superimposed on reflection profile.

Inferred Fault

Possible Fault

No Faulting Observed

FIGURE 13
INTERPRETATION OF HRS HYBRID PROFILE 12K-4

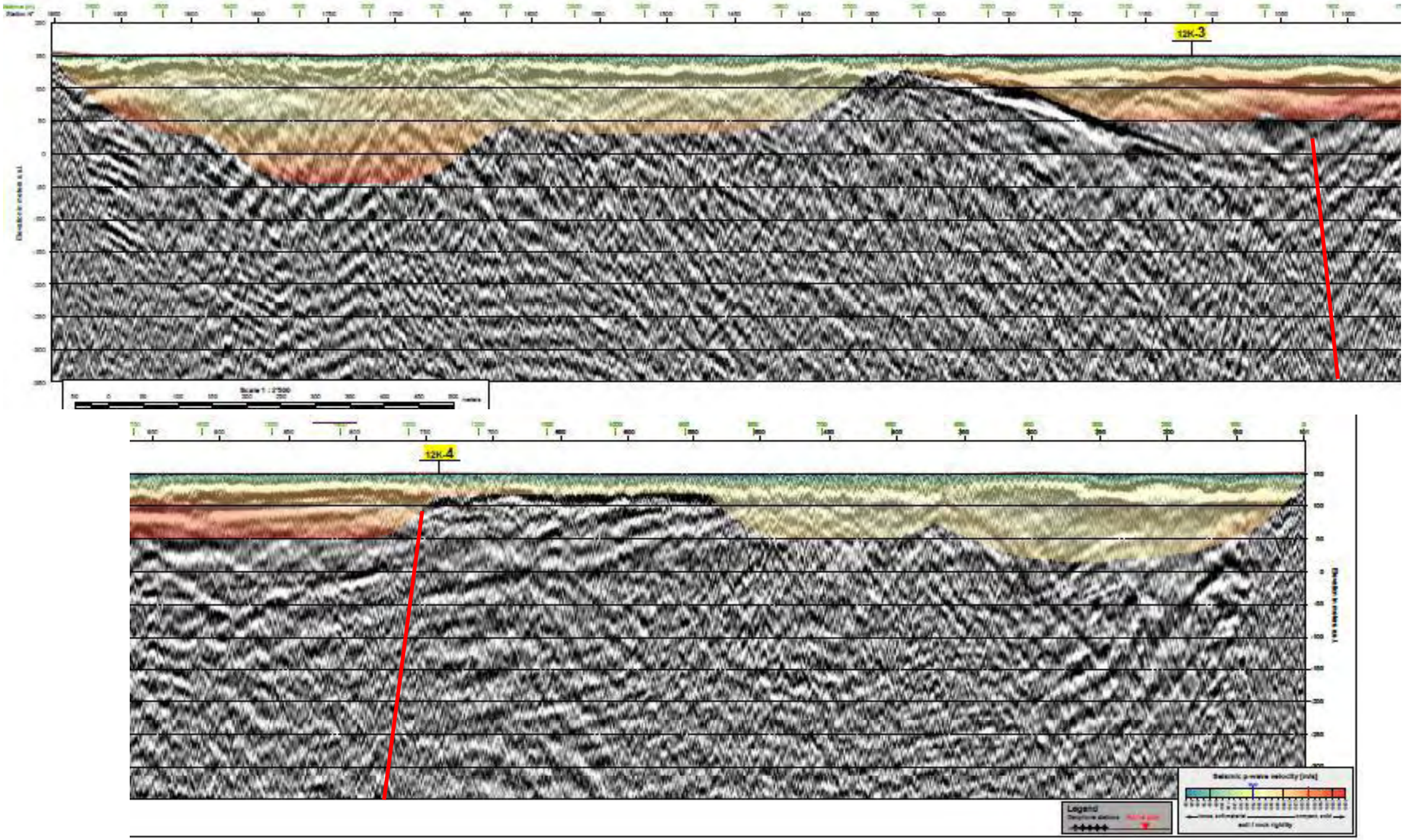

Note: Gray zone represents only the seismic reflection profile . Color represents refraction tomography superimposed on reflection profile.

Inferred Fault

Possible Fault

FIGURE 14
INTERPRETATION OF HRS HYBRID PROFILE 12K-5

APPENDIX 3

PEER REVIEW REPORT: REVIEW OF OSL AGES FROM THE KRŠKO BASIN, SLOVENIA

GEOLOŠKI ZAVOD SLOVENIJE
Dimičeva ulica 14, 1001 Ljubljana

Characterization of the Libna Feature

Macroscopic lithological analyses of gravels as support to age dating and geomorphological/alostratigraphic determination of Quaternary and "Plio-Quaternary" sediments in the Krško Basin

Revision 0

LJUBLJANA, November 2013

p.p.2552 * Tel.: (01) 2809 700* Fax: (01) 2809 753 * davčna št.: 23064145 * št.podračuna 01100-6030346764 Urad Ljubljana

GEOLOŠKI ZAVOD SLOVENIJE
Dimičeva ulica 14, 1001 Ljubljana

Project:		Characterization of the Libna Feature
Contract:		Subconsulting agreement of Oct 19, 2012
Client:		Paul C. Rizzo Associates, Inc
Responsible for task leader. Director:	GeoZS	Marko Komac
Project/task leader:	GeoZS	Miloš Bavec

Report

Authors:	GeoZS	Marijan Poljak Blaž Milanič Igor Rižnar Miloš Bavec

Arch. No. GeoZS:	R-II-30d-5/90-d
Place and date:	Ljubljana, November 8th, 2013

KEY WORDS: NPP Krško II, lithology, Plio-Quaternary, Libna Fault, gravel

Table of contents

Table of figures

Table of appendices

1. Scope of work

The premise of investigations is that the structural deformations in the Krško BasinBasin encompass the pre-Quaternary basement as well as some Quaternary units. In an attempt to better characterize the age of the most recent faulting in Krško Basin, a dating campaign was performed focused primarily, but not only, to the sediments of inferred Plio-Quaternary age; i.e. the sediments of the Globoko Aloformation and its potential equivalents and "lookalikes". Faulting was observed in this aloformation on the Libna fault in the trench #2 on Libna hill.

Structurally, the Globoko Aloformation exhibits structural deformations of both folding and faulting (including the Libna fault) while in younger aloformations only folding is known. The Brežice Aloformation is just slightly tilted from the rims of the Krško Basin towards its central part, while the Drnovo and Vrbina Aloformations show no signs of deformations, at least not at the surface (a short overview of this geological framework is given by Verbič et al., 2000). Knowing that the Globoko Aloformation may not be as uniform as presented in previous works (e.g. Verbič et al., 2000; Swan et al. 2004, Bavec et al., 2010), and given expected methodological limitations in direct dating of known exposures of presumably Globoko Aloformation sediments, we broadened the survey also into younger aloformations, and analyzed the lithological composition of gravels. By that, and supported by geomorphological data, we aimed toward further constraining the Quaternary stratigraphy thus giving grounds for relative age dating beside just direct measurements on every outcrop.

2. Geomorphological and stratigraphic background

This investigation was concentrated primarily on river terraces of the Krško Basin (Figure 1) which origin is associated with paleo-Sava river flow. The terrace system is developed on a system of alluvial aloformations named after Verbič, 2008 the Globoko Aloformation of inferred Plio-Quternary age, Brežice Aloformation or terrace of Mid-Pleistocen (Rissian) age, Drnovo Aloformation of Late Pleistocene (Würmian) age, and Vrbina Aloformation of Holocene age. Their morphostratigraphic position is quite clearly recognizable, where the oldest Globoko Aloformation occupies the highest elevations, and the younger ones are found progressively lower in relief in accordance with their (younger) age.

However, a channel-like feature (called here the paleochannel) laying atop the Miocene basement in the middle part of the Krško Basin, has been recognized in the past (Lapajne, 1975). The paleochannel stretching in general SSW-NNE direction is filed by sediment that by its facies resembles both the Globoko Aloformation as well as Dobrava aloformation. In the western and middle part of the Basin, it is covered by Drnovo and Vrbina Aloformations, and in its eastern part by the Dobrava formation. Verbič (2008) in fact included this sedimentary fill into the Dobrava Aloformation, but due to its paleogeographic position (not being a part of the local alluvial infill as Dobrava Aloformation is), and its lithological characteristics (presence of abundant carbonate component), we propose here, that it should be defined as a separate unit. We propose the name Brezina Aloformation.

Additionally, we compare the results with some samples analyzed upstream Sava in Senovo syncline between Blanca and Sevnica within a GeoZS research project in 2001 - 2003 (Bavec, 2003; Jelen et al., 2004)

3. Lithologic composition of gravel

All Quaternary and Plio-Quaternary aloformations consist of gravel, sand and sparsely of some silt. The (oldest) Globoko Aloformation consists entirely of non-carbonate clasts while all other ones of mixed non-carbonate and carbonate clasts at different ratios. Within this study, we have collected samples from all above listed aloformations and analyzed them for their petrographic composition. In figure 1 and 2, locations of surface and borehole samples are shown. Analyses results are presented on appendices 1-8.

3.1 Methodology of analysis

Samples used in this study were analyzed within this project and in various past projects. In the course of this project, most samples (BOR-1, BRE-1, DOB-1, DOLV-1, LES-1, LIB-1, PES-1, SVAS-1, MRAŠEVO, MRAŠ-1, KAPELE-1, GLOBOKO-1, GLOBOKO-3 are taken from surface exposures, eight samples are taken from the ED-1 borehole, six samples from the VOG-2borehole, six from the ES-1 borehole, four from the Borehole-1, four from the 30 m Borehole and one sample from the CRN Borehole. Samples were analyzed at the Geological Survey of Slovenia by following methodology.

Samples were dried, weighted and soaked in water for 24 hours. All samples were sieved by handheld sieves up to 2 mm grains. Qualitative and quantitative lithological composition of grains larger than 4 mm were determined using handheld magnifier. The lithological content was divided in 21 classes. All fractions were saved. Limestone and dolomite were discriminated by HCl (1:10).

Lithological content of samples Kamnica-616, Kamnica-617, Pg1, Pg2, Pg3, Dr1, Dr2, Am1, Am2, Am3, Am4, Br1, Br2 and Br3 and are taken from Verbič (1995), and lithological content of samples KK5, KK8, KK9, KK9/2, KK13, KK15a, KK21, KK23, Kk24, KK6a are taken from Jelen et al., 2004.

3.2 Interpretation

The Globoko Aloformation has been sampled in the Globoko sand pit (samples: GLOBOKO-1; -2;-3), Kapele hills (KAPELE-1), Mraševo terrace (MRAŠ-1), and from the CRN Borehole (4.0-5.4 m depth). The lithological content of all the samples is almost identical, characterized by clastic sedimentary and volcanic rocks from Paleozic to Mesozoic age of the Southern Alps provenience, and by the absence of carbonate rocks.

The Brezina Aloformation is the first, and supposedly the oldest of several Quaternary aloformations that all differ from the Globoko Aloformation by the abundant content of carbonate rocks. The Brezina Aloformation though occurs only below surface, so the data come from selected boreholes (ED-1, ES-1, VOG-2Borehole #-1 and 30 m Borehole), presented here. As seen from the appendix 8, these samples in general contain carbonate rocks from 0,2 % to up to 83,9 %, vs. non-carbonate ones. On the other hand, the lithologies of non-carbonate rocks are nearly identical to those ones of the Globoko Aloformation (Bole et al., 2013).

The Brežice Aloformation is well exposed at the surface, and it has been sampled at several places in Krško Basin (samples: PES-1, LIB-1, DOB-1, DOLV-1, DOLV-2, BRE-1, BOR-1, LES-1, and SVAS-1). From appendix 8, it can be seen that the lithological content of this unit is almost identical to the previous one. That relates to the ratio of carbonate rocks vs. non-carbonate ones, as well as to the total petrographic content (Bole et al., 2013).

The Drnovo Aloformation was previously sampled by Verbič (2005) from several gravel pits (samples: Dr 1, Dr 2, Pg 1, Pg 2, Pg 3, Kamnica-616, and Kamnica-617). The author analyzed the total content of carbonate rocks (limestone and dolomite) vs. non-carbonate ones. Given a high carbonate content we are comparing this af. with the Brezina and Brežice Aloformations.

The Vrbina Aloformation was also previously sampled by Verbič in year 1995 (samples: Am 1, Am 2, Am 3, Am 4, Br 1, Br 2, and Br 3), and recently it was sampled in the boreholes (Borehole # 1; L-4 and L-1) within this project. Petrographic content (appendix 8) is almost the same among the samples taken by Verbič (1995), and to the samples of the Drnovo Aloformation taken by the same author. However, petrographic content of the borehole samples is slightly different. This can be again due to the different method of sampling and analysis, as in the previous case.

Before above described petrographic analysis, an important question, to which geological mapping could not have given the answer, was the relationship of the Brezina and Brežice Aloformations. To be more specific, weather the Brezina Aloformation is cut into the Brežice terrace (Aloformation) or is it covered by it. An indication on how to possibly answer to this question was obtained by a detailed analysis of collected samples. The leading difference is the amount of dolomite clasts that appears to be higher (up to 12 %) in the Brežice Aloformation than in the Brezina Aloformation (none to max. 2 %). Thus, the first two samples from the 30 m - Borehole taken from intervals 5.0-6.0 m and 6.0-7.0 m depth and contain more dolomite clasts could belong to the Brežice terrace. On the contrary, two other samples taken from 17.0-18.0 and 25.5-26.5 m depth and contain significantly less dolomite could belong to the Brezina Aloformation. From these data we infer that the Brežice aloformation is a younger cover of the Brezina aloformation.

The other important question related to the Globoko Aloformation is whether it is a single stratigraphic unit which is structurally positioned on different terrain levels, or has it been developed during a longer time interval and is in fact stratigraphicaly differentiated. Based solely on results of here described petrographic analyses we may infer that Globoko aloformation is a single unit. The newly acquired age dates however indicate opposite.

3.3 Comparison with samples from the Senovo Syncline

In the Senovo Basin (roughly) corresponding to Senovo Syncline , a number of samples were previously collected by M. Bavec (Jelen et al., 2004, Bavec, 2003) from various (paleo)Sava river terraces (figure 2). The topographically highest of these may correspond to the Globoko Aloformation of the Krško Basin given its topographic position and lithological content (samples: KK 5, KK 8, KK 13, KK 15a, KK 21, KK 23, and KK 24). Several other samples were taken at lower terraces (samples: KK 6a, KK 9, and KK 9/2). Their petrographic content and topographic level can be also correlated with Quaternary alloformations in the Krško Basin. However, these Quaternary aloformations in the Senovo Syncline have not been mapped in detail, so any exact determination of these is not possible at the time being.

4. Age dating

In addition to petrographic analysis, we have also collected samples for age dating of particular lithostratigraphic units. Results were not obtained under the controlled QA procedure and should therefore be taken as informative.

A sample of peat was taken within sandy clay at the interval 3.0-5.0 m of depth in the 30 m Borehole. Thi section belongs to the uppermost alomember of the Dobrava Aloformation. Its ^{14}C age was determined at University of Salento, Italy at 9 804 ± B.P. meaning Early Holocene. Besides this data, we have also obtained additional radiocarbon data from samples analyzed within some other projects. Among these, at least one is relevant here. It is a layer of peat exposed in the Krka river bank app. 2.5 m below the surface in the Drnovo Alloformation. Its ^{14}C age is 17 684 ± 100 y B.P. (Poljak & Milanič, 2011.)

Samples of calcite cement were taken from both levels/terraces of the Brežice alloformation at Krško and Leskovec localities. U/Th radiometric dating of four samples at the Open University, Manchester, UK yielded the age range from 247 to 285 ka (Poljak et al., 2013), what means “Rissian”.

Morphostratigraphic position of aloformations (with exception of the Globoko Aloformation) has been supported herein by their absolute ages. This does not account though for the supposedly oldest Globoko Aloformation where age-dating has not been attempted within this part of the project.

5. References

Bavec, M., 2003: Pliokvartarni sedimenti med Sevnico in Brestanico : preliminarni rezultati raziskav. In: HORVAT, Aleksander (ur.). *16.* - Geološki zbornik, 17, 5-7.

Bavec, M. (ed.) 2010: Geotechnical, geological and seismological (GG&S) evaluations for the new nuclear power plant at the Krško site (NPP Krško II), Geology : phase 1 : revision 1. Ljubljana: Geological Survey of Slovenia, 2010. 178 pp.

Bole, B., Trajanova, M., Kralj, P. & Štrumberger, M., Granulometrijska in litološka sestava vzorcev proda s Krškrga polja. Interno poročilo, 64 str., Geološki zavod Slovenije, Ljubljana.

Poljak, M. & Milanič, B., 2011: Nekaj novih podatkov o starosti nekaterih kvartarnih sedimentov v Krški kotlini. Geološki zbornik, 2, 100-103, Ljubljana.

Jelen, B., Poljak, M., Bavec, M. & Rifelj, H., 2004: Zaključno poročilo o rezultatih raziskovalnega projekta L1-3202-0215-01- Terciarna in kvartarna geodinamika na stičišču Alp, Dinaridov in Panonskega bazena 2001-2004. Poročilo, Geološki zavod Slovenije, Ljubljana.

Poljak, M., Calsteren, P., Marjanac, T., Marjanac, LJ., Bavec, M. & Rižnar, I., 2013: Contribution to the Origin and Age Determination of some Qaternary Sediments in the Krško Basin. Geološki zbornik, 22, 124-127, Ljubljana.

Swan, F. H. et al., 2004: Revised Seismotectonic Model of the Krško Basin, Part 1, PSR-NEK-2.7.1. (Rev 1), 99 pp., Nuklearna elektrarna Krško.

Verbič, T., 1995: Kvartarni sedimenti v vzhodnem delu Krške kotline. Interno poročilo, 248 str., Geološki zavod Slovenije, Ljubljana.

Verbič, T., 2008: Kvartarni sedimenti, stratigrafija in neotektonika vzhodnega dela Krške kotline. Doktorska disertacija, 140 (?) str., Univerza v Ljubljani, Naravoslovnotehniška fakulteta, Ljubljana.

Verbič, T., Rižnar, I., Poljak, M., Demšar, M. & Toman, M., 2000: Qaternary Sediments in the Krško Basin. Second Croatian Geological Congress, Proceedings, 451-457, Zagreb.

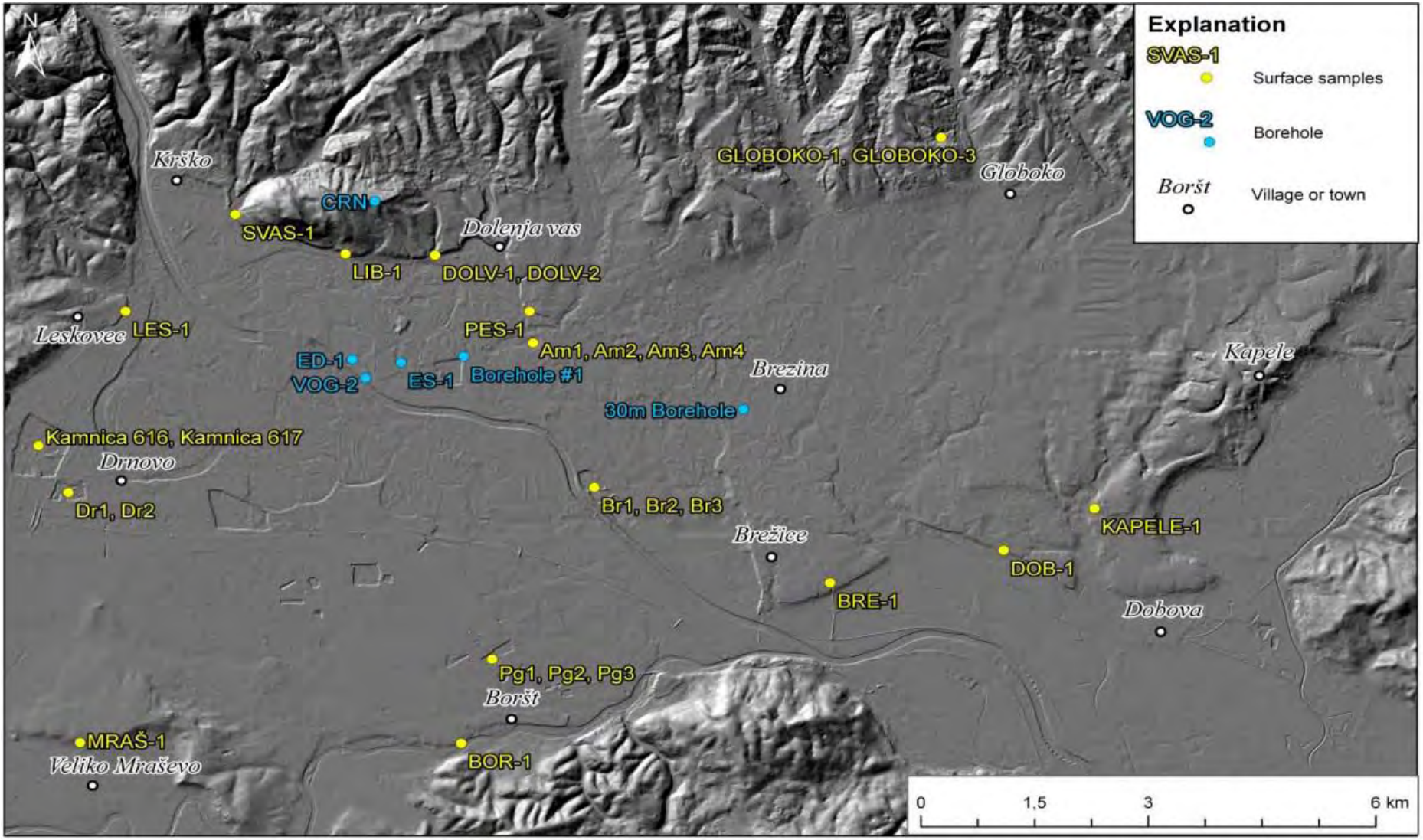

Figure 1: Krško basin surface sample and borehole locations

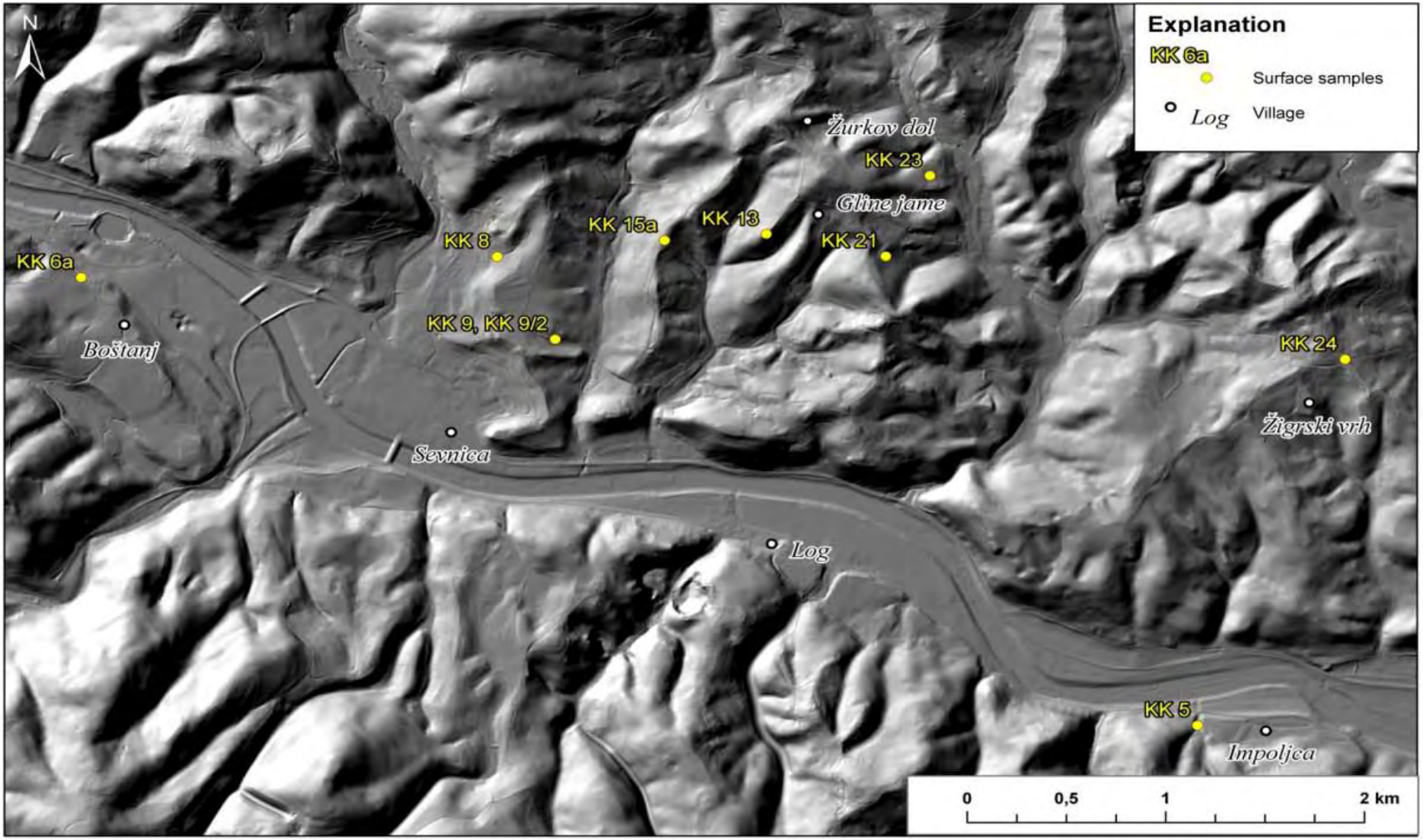

Figure 2: Senovo basin surface sample locations

Appendix 1
Krško basin
Vrbina Aloformation; surface and borehole (Borehole #1) samples analyses

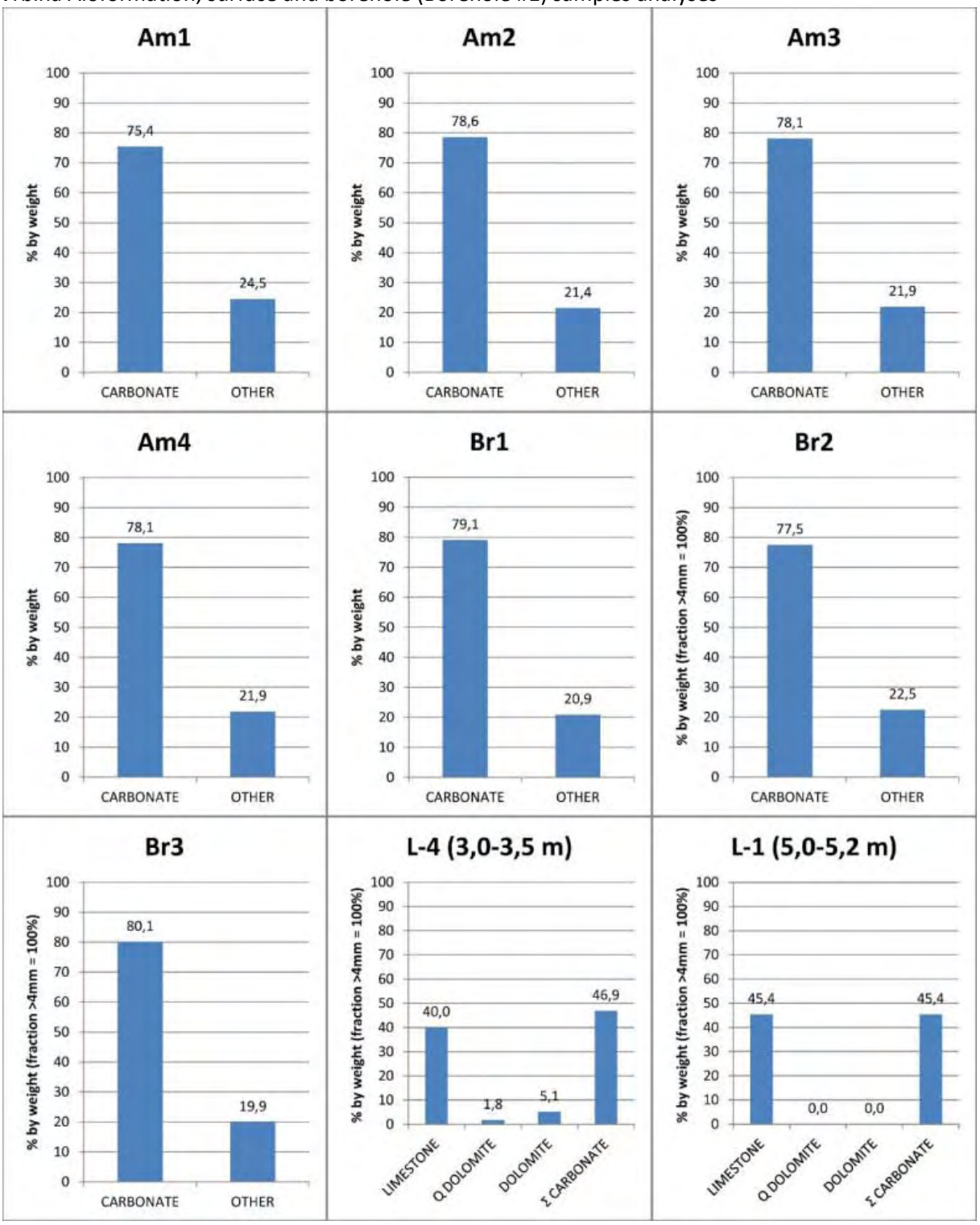

Appendix 2
Krško basin
Drnovo Aloformation; surface samples analyses

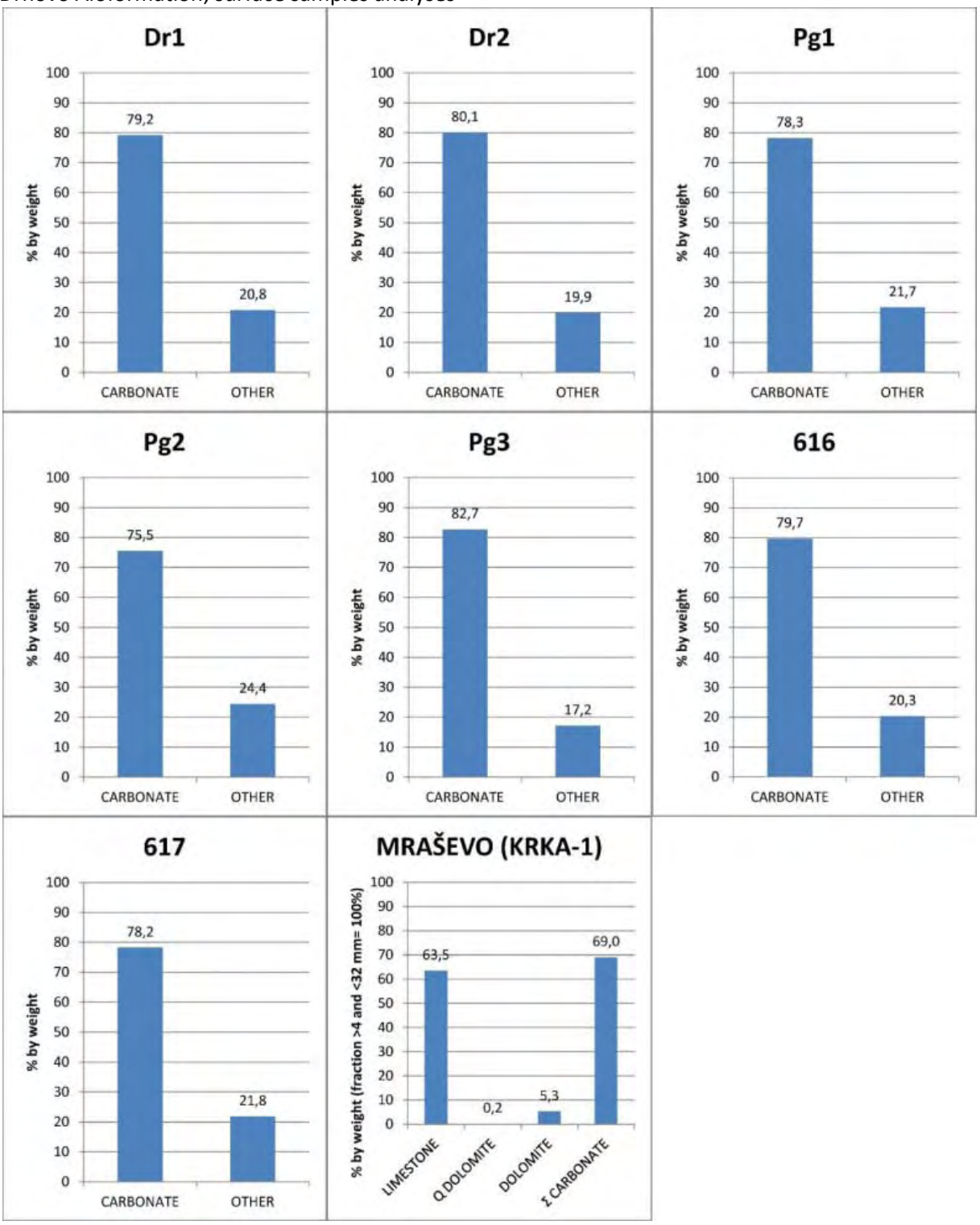

Appendix 3a
Krško basin
Brežice Aloformation; surface samples analyses

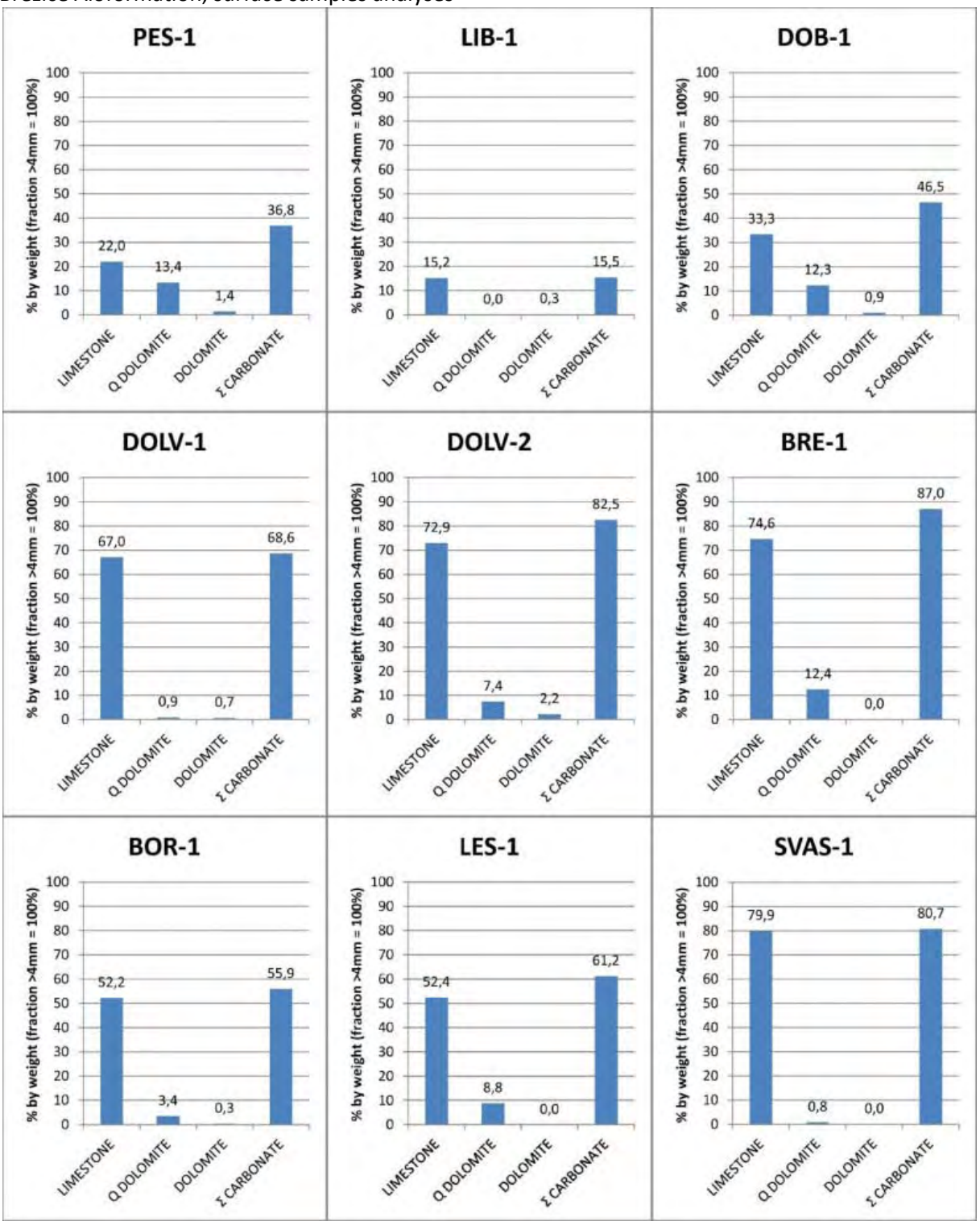

Appendix 3b
Krško basin,
Brežice Aloformation; borehole (30m Borehole) samples analyses

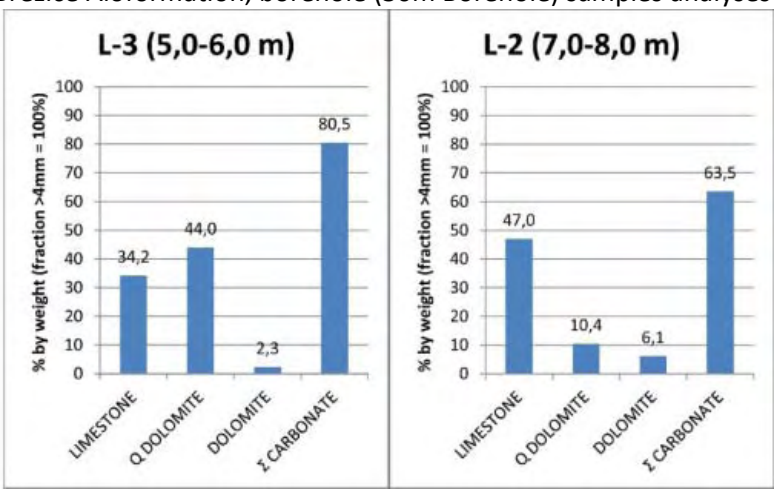

Appendix 4a
Krško basin
Brezina Aloformation borehole (ED-1) samples analyses

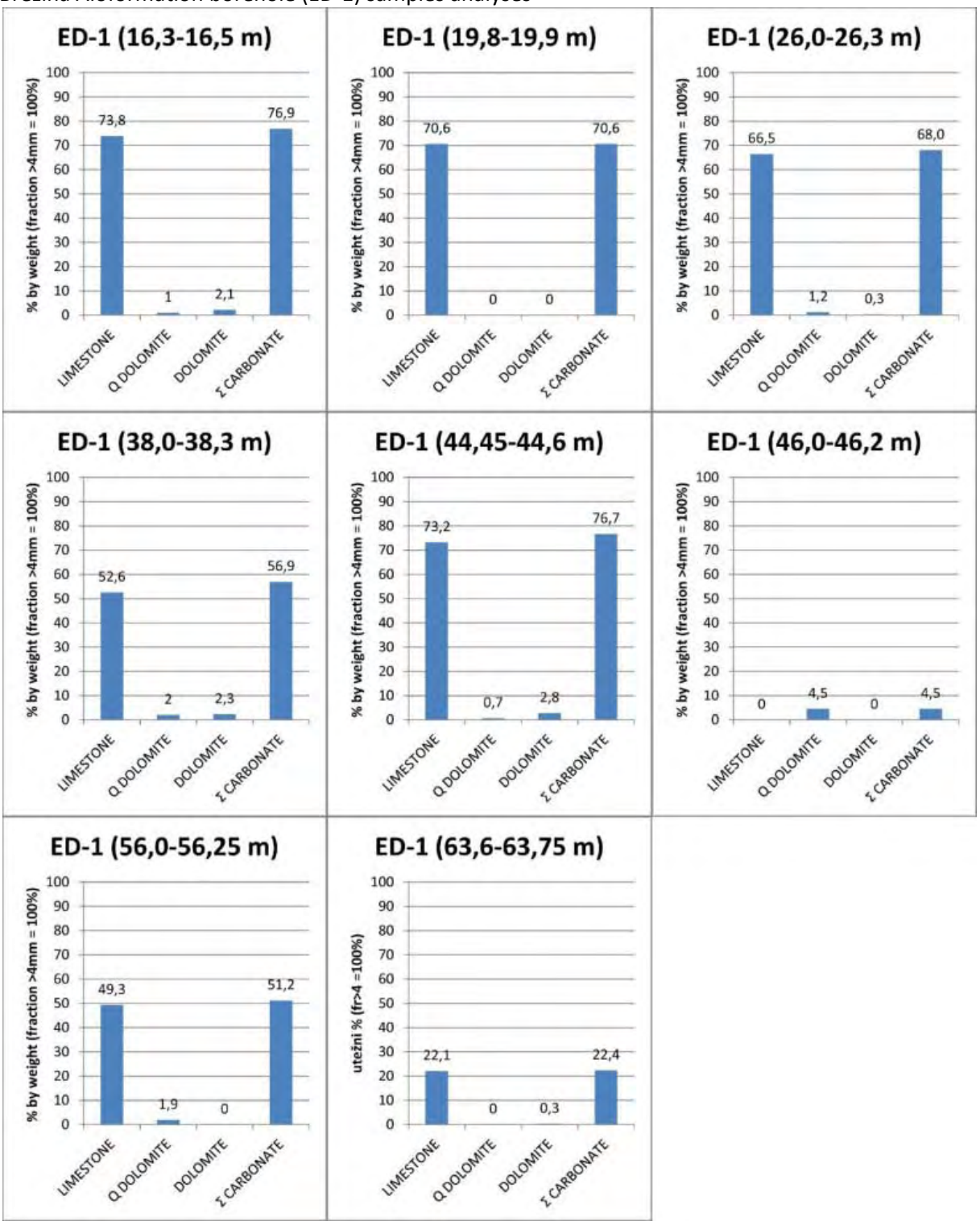

Appendix 4b
Krško basin
Brezina Aloformation; borehole (VOG-2) samples analyses

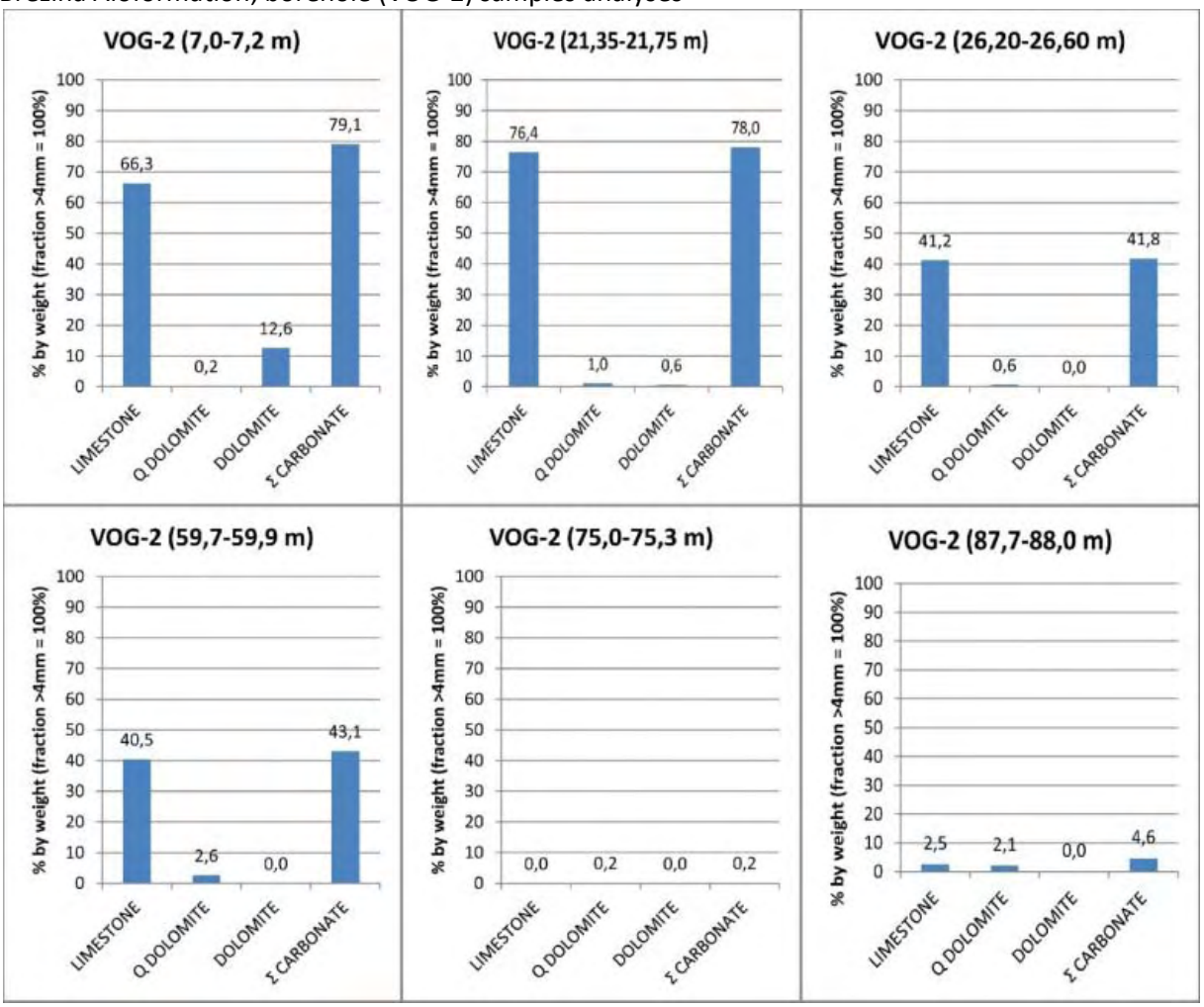

Appendix 4c
Krško basin
Brezina Aloformation; borehole (ES-1) samples analyses

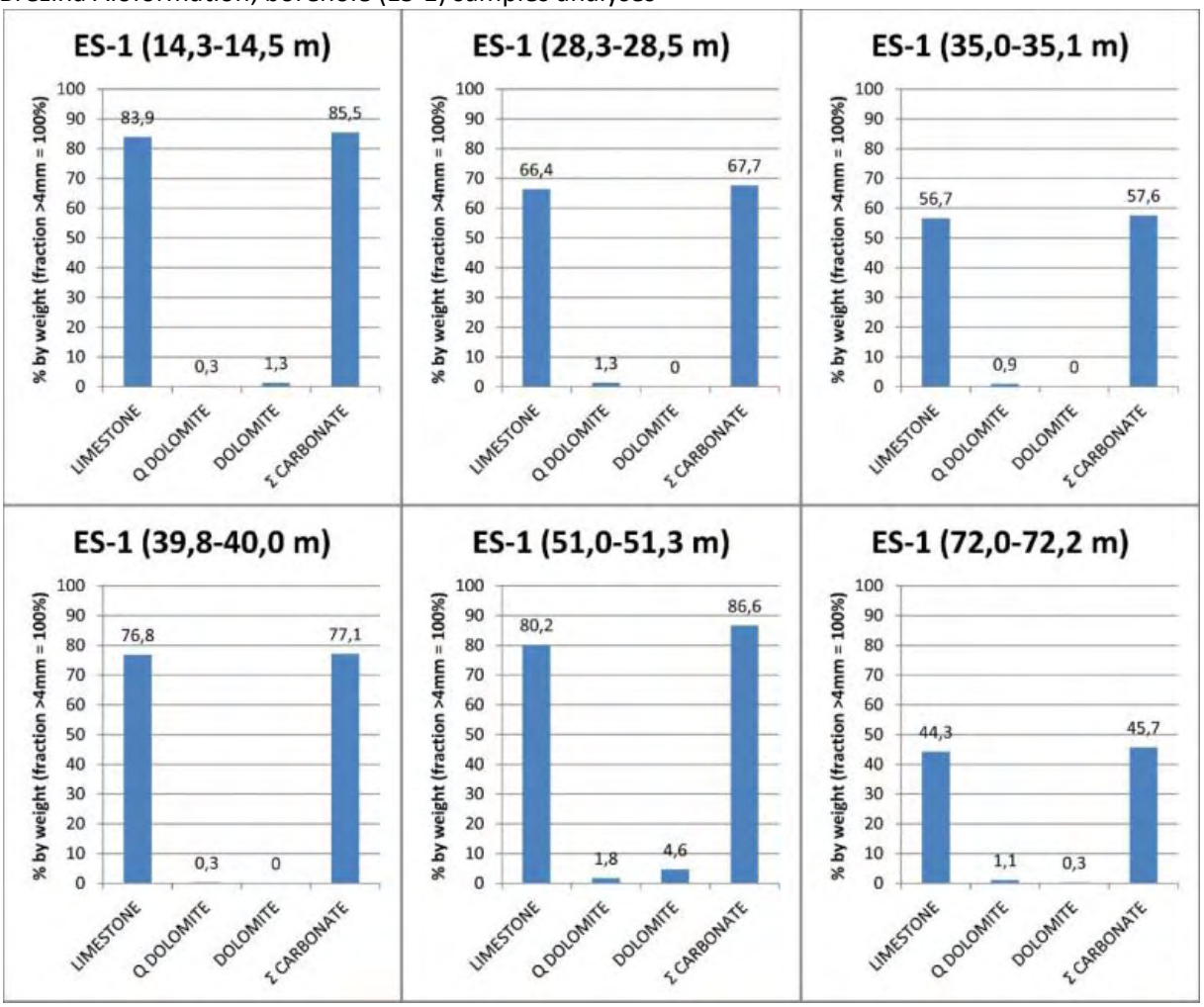

Appendix 4d
Krško basin
Brezina Aloformation; borehole (Borehole #1 and 30m Borehole) samples analyses

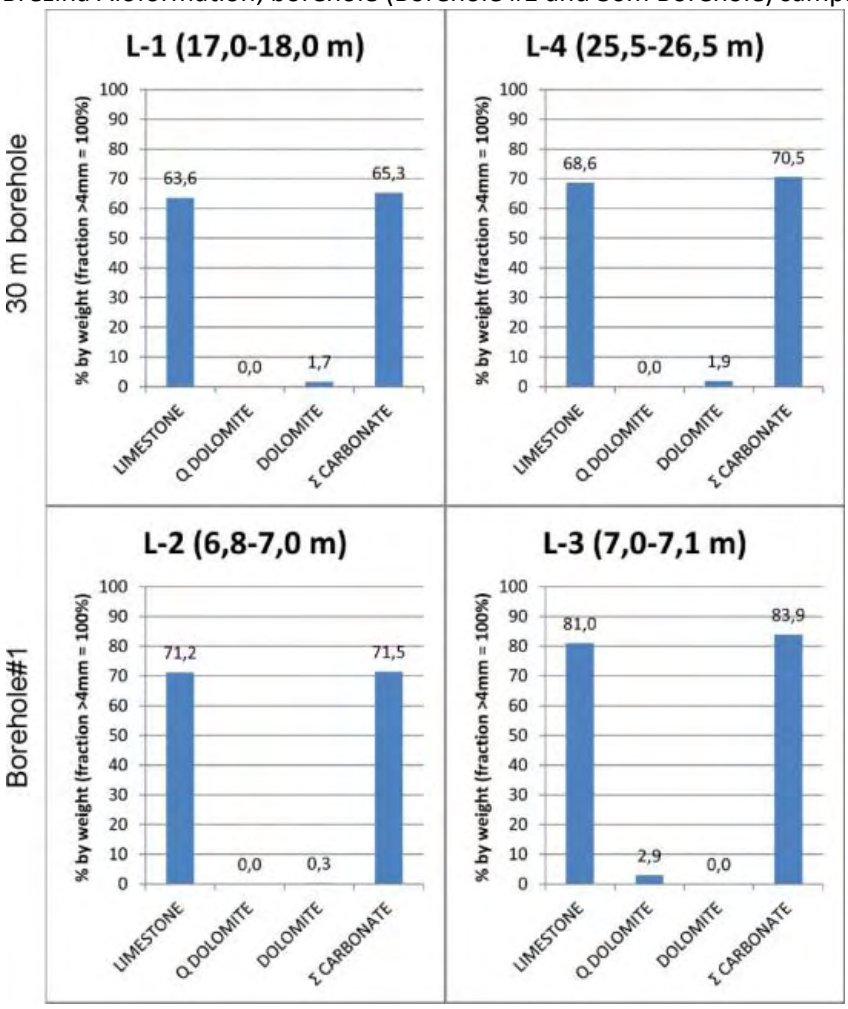

Appendix 5a
Krško basin
Globoko Aloformation; surface and borehole (CRN) samples analyses

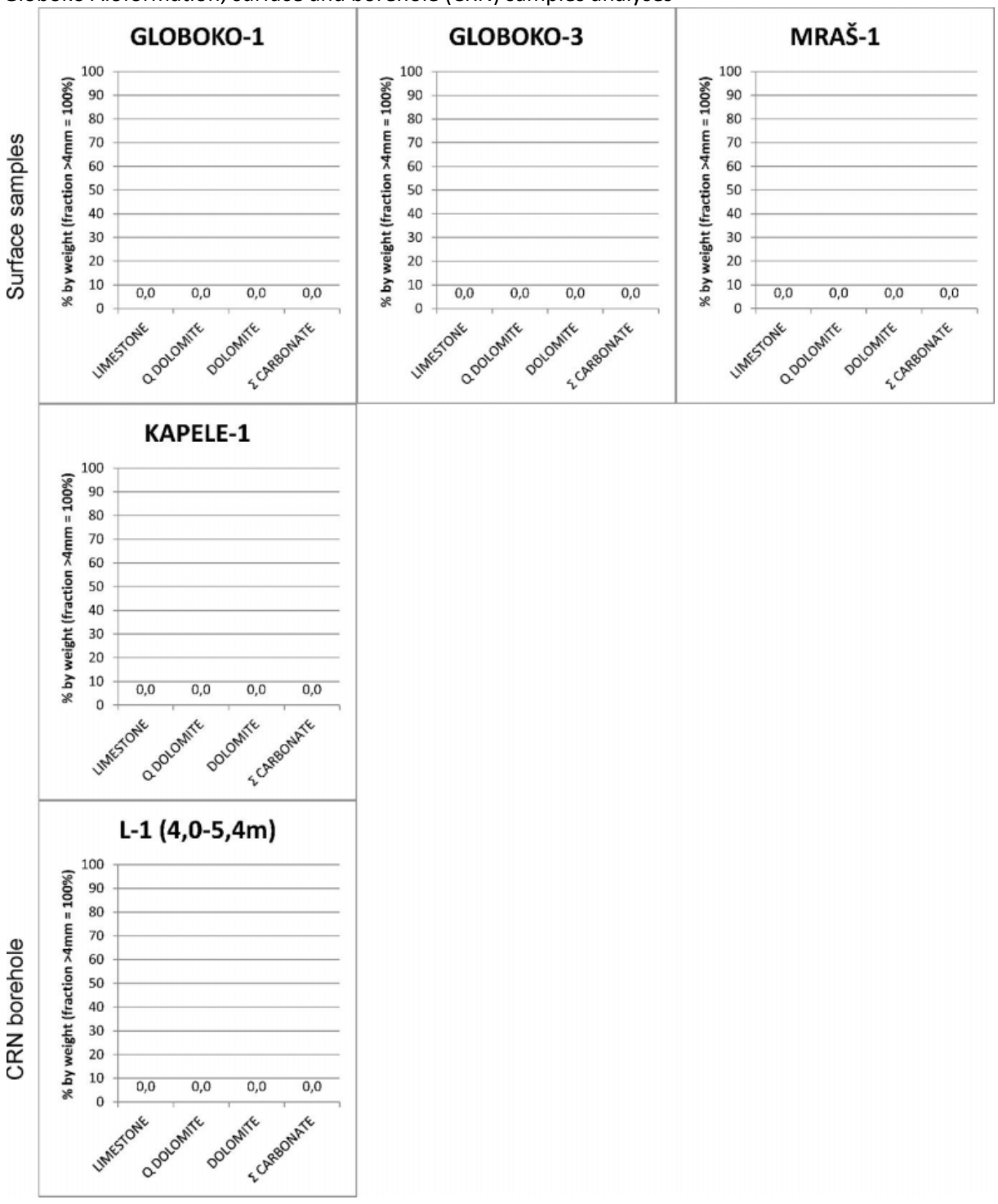

Appendix 5b
Krško basin
Globoko Aloformation; surface and borehole (CRN) samples total content analyses

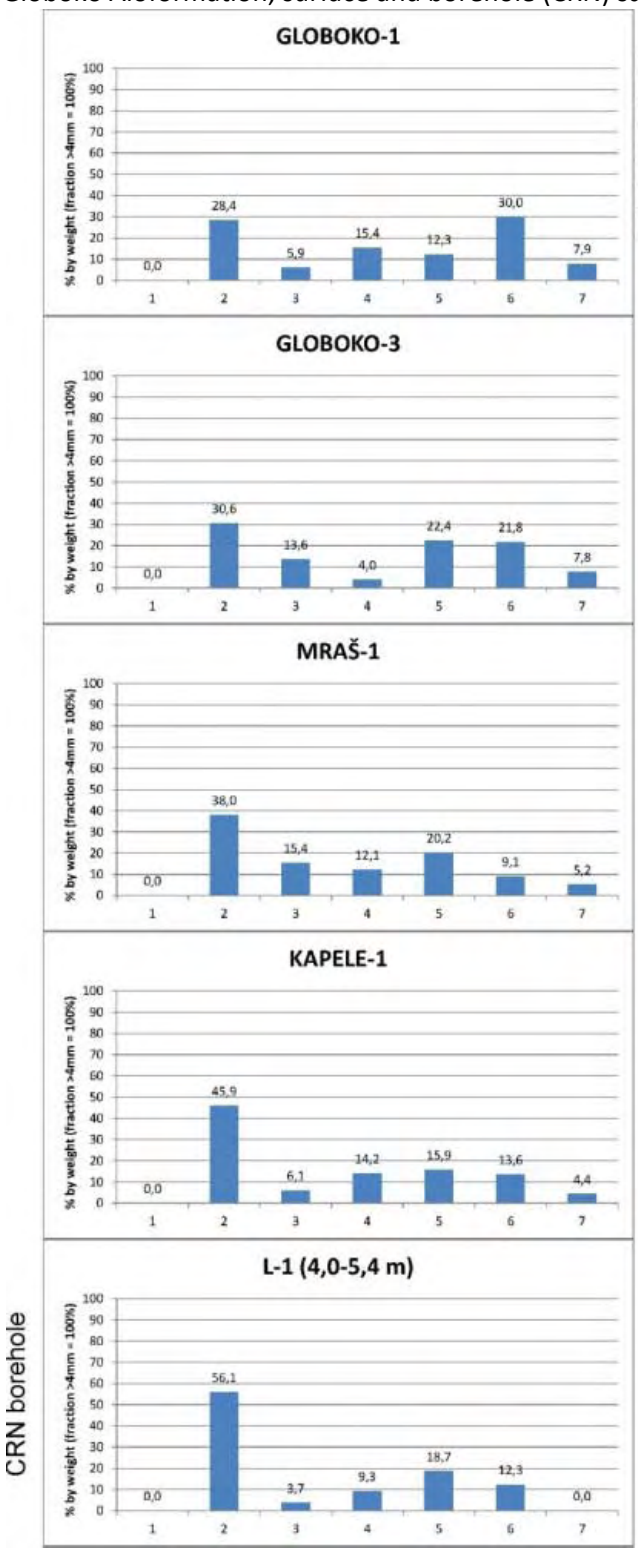

Legend

1	Carbonate rocks (limestone, dolomite, silicious dolomite)
2	Paleozoic clastic rocks
3	Crataceous clastic rocks
4	Chert of various ages
5	Quartz of various ages
6	Triassic and Tertiary vulcanic and vulcanoclastic rocks
7	Sericite-quartz sandstone/siltstone of various ages

Appendix 6
Senovo basin
Globoko Aloformation (?); surface samples analyses

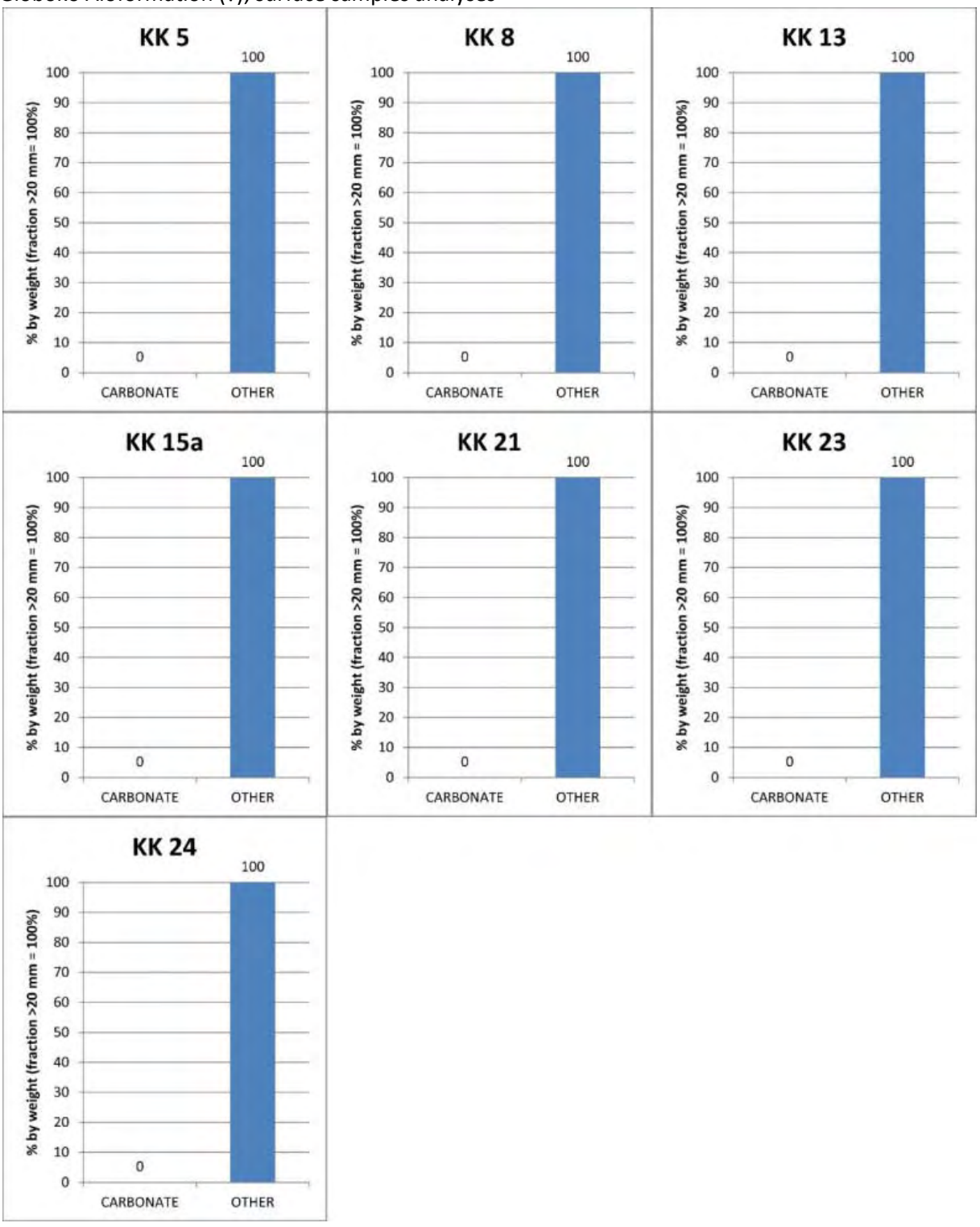

Appendix 7
Senovo basin
Younger and undefined Quaternary aloformations; surface samples analyses

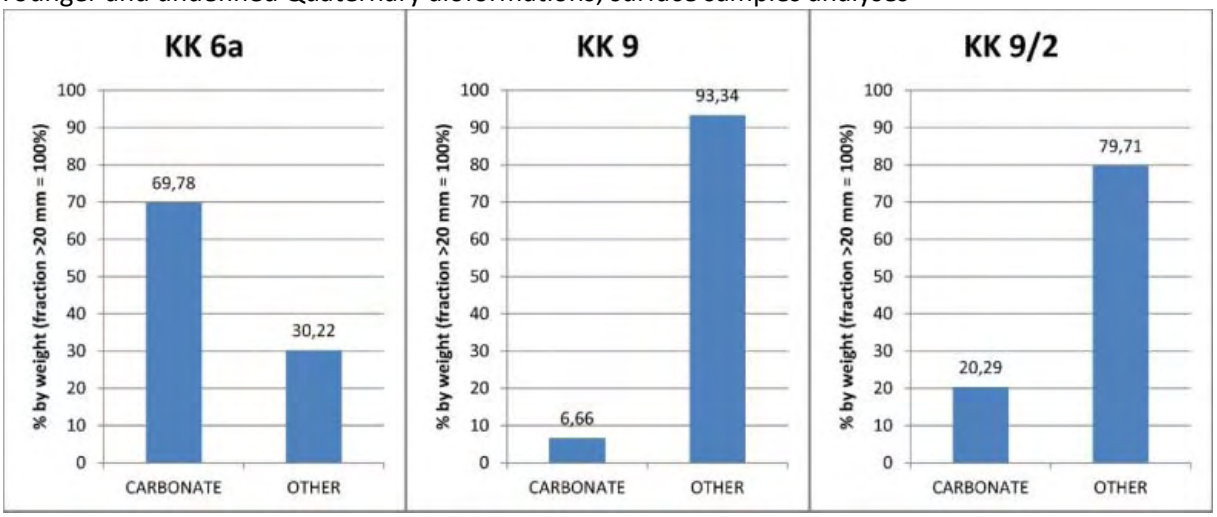

Appendix 8

Lithologic content of Quaternary sediments in the Krško and Senovo basin (surface and borehole data)

Krško basin

Vrbina Aloformation (Holocene)

Surface samples

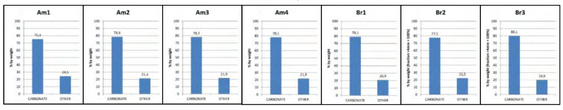

Borehole samples

Borehole #1 (151m a. s. l.)

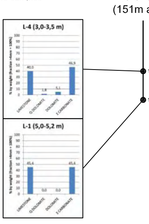

Drnovo Aloformation (Late Pleistocene)

Surface samples

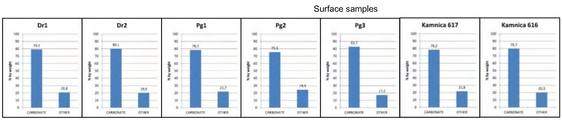

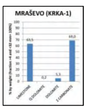

Brežice Aloformation (Middle Pleistocene)

Surface samples

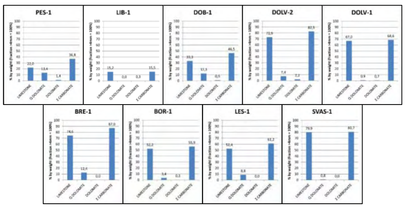

Borehole samples

30m Borehole (151 m a.s.l.)

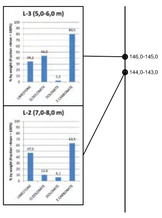

Brezina Aloformation (Middle Pleistocene?)

Borehole samples

Globoko Aloformation

Surface samples

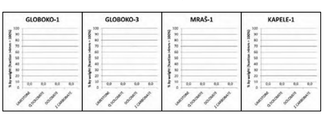

Note: no carbonate rocks

Borehole samples

CRN (322 m a.s.l.)

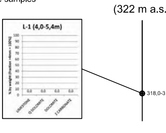

Total content

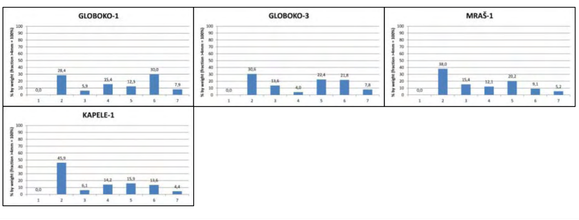

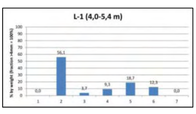

Legend

1	Carbonate rocks (limestone, dolomite, silicious dolomite)
2	Paleozoic clastic rocks
3	Crataceous clastic rocks
4	Chert of various ages
5	Quartz of various ages
6	Triassic and Tertiary vulcanic and vulcanoclastic rocks
7	Sericite-quartz sandstone/siltstone of various ages

Senovo basin

Globoko Aloformation ?

Surface samples

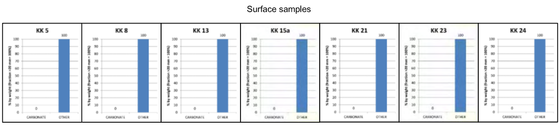

Younger and undefined Quaternary aloformations

Surface samples

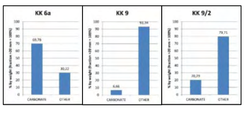

APPENDIX 4

UNIVERISITY OF BERN SWITZERLAND OSL LABORATORY RESULTS

10 October 2013

Review of OSL ages from the Krško basin, Slovenia

This report reviews the analysis procedures and resultant ages from eight samples collected from the Krško basin, Slovenia and analyzed at the Luminescence Lab at the University of Bern, Switzerland. Quartz and feldspar OSL age results ranged from 30 – 240 ka and samples collected from units mapped as the Plio-Quaternary Globoko Formation were much younger than expected. This report describes the validity of the luminescence techniques used to obtain the OSL ages and discusses possible reasons for possible age underestimation. Discussions and interpretations in this report are based solely upon an OSL age report produced by Dr. S. Lowick, supplied data files and discussions with Mike Logan Cline related to the geomorphic and stratigraphic setting of the samples.

Before the possible sources of error and uncertainty in the OSL analyses are discussed, it is important to point out that the analyses followed the most up-to-date protocols and methods. Care was taken to address potential sources of error and test for the correct conditions for analysis. Preheat plateau and dose-recovery tests were conducted to test for the correct pre-heat temperatures to use with these samples. Results from these tests indicate that there was little influence of temperature on the calculated equivalent dose (De) calculated. Moreover, all parameters used to test for the effectiveness of the SAR protocol in quartz De calculation were satisfactory. Further, quartz OSL results from the same unit (Bern-01 and Bern-02, Bern-05 and Bern-06, and USU-01 and GBL2) all produced ages well within error of each other (Fig. 1, Table 1), suggesting that the results are internally consistent. Furthermore, most age results follow a consistent trend of increasing age with elevation, as would be expected with alluvium deposited during a period of long-term incision (Fig. 1).

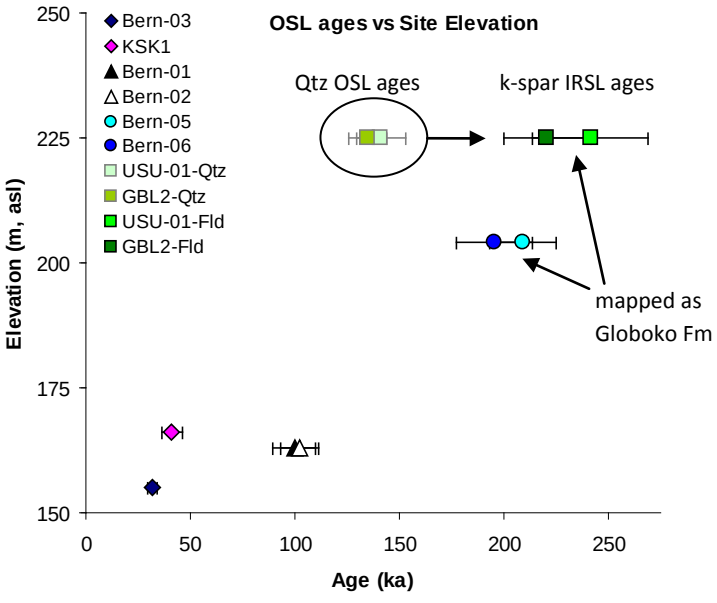

Figure 1. Relationship between OSL age results and fluvial deposit/terrace elevation sampled. Note that samples collected from the same location (as indicated by the same elevation) have resultant ages that are within error of each other. Also note the apparent age reversal when the quartz OSL ages are plotted for samples USU-01 and GBL2 (light green squares). Feldspar IRSL ages from these samples better fit the expected relationship between fluvial deposit elevation and age (darker green and bright green squares). Quartz OSL ages from samples Bern-05 and Bern-06 and feldspar OSL ages from USU-01 and GBL2 are within error of each other and suggest they may be from the same aged deposit. All OSL sample results are much younger than the ~2Ma expected age of the Globoko Fm as derived from deposits >100 m higher in elevation.

Table 1. OSL, ERS and CRN ages from the Krško basin, Slovenia

Method	Sample	elevation	Age (ka)
Qtz OSL[1]	Bern-03	155	31.9 ± 2.4
Qtz OSL[1]	KSK1	166	41.1 ± 4.9
Qtz OSL[1]	Bern-01	163	99.9 ± 10.3
Qtz OSL[1]	Bern-02	163	102.5 ± 9.2
Qtz OSL[1]	Bern-05	204	209.2 ± 16.0[2,3]
Qtz OSL[1]	Bern-06	204	195.3 ± 18.2[2,3]
Qtz OSL[1]	USU-01-Qtz	225	141 ± 11.8[2,3,4]
Qtz OSL[1]	GBL2-Qtz	225	135.1 ± 9.1[2,4]
k-spar IRSL[1]	USU-01-Fld	225	241.4 ± 27.8
k-spar IRSL[1]	GBL2-Fld	225	220.8 ± 20.5
ESR[5]	G 4-2, GBL site	225	190 ± 28
ESR[5]	G 8-2, GBL site	225	211 ± 32
ESR[5]	G 11, GBL site	225	540 ± 81[6]
ESR[5]	ES 1-3 Libna Hill	225	204 ± 31
CRN[7]	Libna Hill	322	1700

[1] OSL results from Lowick Report, Appendix A
[2] Quartz OSL signal at or near saturation
[3] Feldspar contamination, may cause age underestimate
[4] Quartz OSL age underestimate - refer to feldspar IRSL age for same sample
[5] ESR results from Sabet Report on Trenches on Libna Hill, 2011
[6] Result considered unreliable
[7] CRN results from M.L. Cline personal communication

Despite internal consistency, it is possible that some of the older OSL ages (≥ 200 ka) may be producing age underestimates (as originally identified by Lowick in her report). Lines of evidence for age underestimation include: 1) potential mis-mapping of deposits, 2) the expected antiquity of the deposits (~2Ma), 3) feldspar IRSL ages that are ~100ka older than the quartz OSL ages, 4) possible feldspar contamination and 5) potential influence of unstable components of the quartz OSL signal. Each of these are discussed below. There is little evidence that the younger quartz OSL samples are underestimated.

Mis-mapping of deposits

OSL ages were collected from deposits mapped as the Globoko Fm ranged from 100-200 ka (Table 1). IRSL ages from feldspars from the older deposit (USU-01 and GBL2) produced ages closer to 240-220ka (Table 1). These age results are all much younger than the ~2Ma expected age of the Globoko Fm. Possible reasons for this include: 1) uncertainty in regional mapping and the interpretation that all regions mapped as the Globoko Fm are indeed the same deposit and are contemporaneous in age and 2) inaccuracies in the OSL results leading to age underestimates. This report will focus on the second source of uncertainty in the interpretation of the OSL results, but it is important to also address possible uncertainties in mapping.

Figure 2 shows the location of the OSL samples analyzed by S. Lowick at the Bern Luminescence Lab. Much of the area around the flanks of the Krško basin is overlain by gravel deposits mapped as Plio-

Quatenary in age. These gravels have been mapped on Libna Hill and the dissected foothills of the region. CRN age estimates from the Globoko Fm on Libna Hill suggest this unit is 1.7 Ma and probably out of the range of OSL dating (see below). Important to note is that none of the OSL samples discussed here were collected from Libna Hill or other high elevation (>300m) deposits mapped as the Globoko Fm. Instead OSL samples were collected from geomorphically lower surfaces that may represent younger inset alluvium or reworked deposits of the Globoko Fm (Fig. 2). In addition to geomorphic evidence, the consistent relationship between sample age and elevation suggest that the sampled landforms are inset and younger gravel deposits (Fig. 1).

While I have not been in the field to assess if the lower landforms and deposits are younger and are not composed of Plio-Quaternary Globoko Fm, these first-level observations as a geomorphologist lead me to suggest that this is a viable hypothesis. This in turn may suggest that there is no age discrepancy between the OSL results and expected age of the deposits. Additionally, ESR (electron spin resonance) ages from the Globoko pit (GLB on Table 1) range from 211-190 ka and are similar in age to feldspar IRSL ages from the same pit (240-220 ka, Table 1, Fig.2), suggesting that the OSL ages may not be in error, given that both dating methods are able to accurately date these sediments.

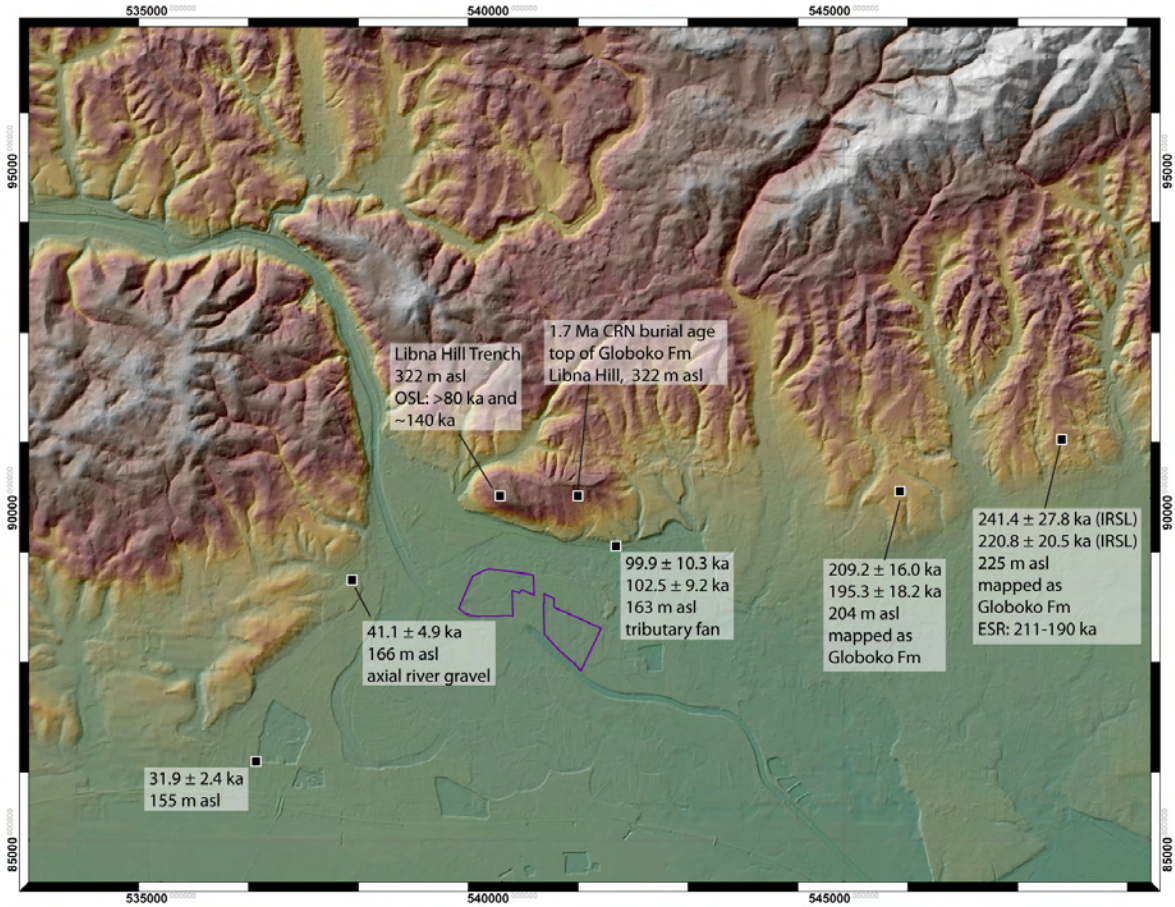

Figure 2. DEM of the Krško basin and location of OSL sample and other sites mentioned in the text.

Affect of the antiquity of the deposits

Quartz OSL samples were collected from fluvial deposits mapped as the Plio-Quaternary Globoko Fm and younger fluvial and alluvial deposits. Previous studies have suggested that the Globoko Fm dates to ~1-2 Ma (Šikid et al., 1979; Verbič, 2004) but could range from 0.3-5 Ma (Swan et al. 2004). Recent CRN (cosmogenic radionuclide) dating results suggest a ~1.7 Ma age for the top of the Globoko Fm on Libna Hill at 322 m asl (M.L. Cline, personal communication). Radiocarbon and OSL (optically stimulated luminescence) ages from a nearby trench suggest the deposits are the age range for these techniques (>43ka and >80ka respectively), although two OSL samples produced finite ages of ~140 ka (Geotechnical, Geological and Seismological Report, 2011).

If the sampled deposits truly are ~2Ma, it is likely that the luminescence signals are saturated (all available luminescence traps have been filled) and that the quartz OSL technique cannot accurately date deposits this old, causing an age underestimate. Resultant age estimates would instead reflect the level of saturation of the samples and rate of decay of any unstable luminescence components. Similar age underestimates for old (>0.5 Ma) samples have been seen elsewhere (e.g. Lai, 2010; Lowick and Preusser, 2011). In her report Lowick discusses the potential sources of error and problems with the Krško basin samples in that four of them are approaching or beyond the $2D_o$ limit for saturation for these samples (Bern-05, Bern-06, USU-01, GLB2). Based on this she recommends that these older quartz OSL ages be considered to 'represent the youngest possible age' of the deposits. In other words, the age results presented should be viewed as minimum age estimates. Causes for the underestimation of high-dose quartz OSL ages is not fully understood but likely relates to unstable signal components and/or laboratory induced linear dose response at higher doses (e.g. Pawley et al 2010; Lowick and Preusser, 2011; Timar-Gabor et al 2012).

Feldspar IRSL ages older than the quartz OSL ages

Evidence for some of the older quartz OSL samples producing age underestimates comes from older feldspar IRSL ages from the same samples. As discussed by Lowick in her report, feldspar IRSL signals saturate at a much higher dose and can be used to date older sediments. While the quartz OSL ages from samples USU-01 and GBL2 are ~130-140ka, the IRSL age results are ~220-240ka (Table 1). These older IRSL ages are more in line with ESR age estimates from the Globoko pit of 211-190 ka (Table 1, Fig. 2). Moreover, these IRSL ages are consistent with the quartz OSL ages from Bern-05 and Bern-06 which were collected from a similar map-unit and geomorphic setting (Table 1, Fig 1 and 2). These observations suggest that the quartz OSL ages from the Globoko pit are underestimated by at least ~100ka. Age underestimation of the ~200ka quartz ages of the Bern 05 and Bern 06 samples is not known at this point because IRSL measurements were not made on these samples. However due to the samples being close to saturation and the use of a saturating exponential plus linear fit to calculate equivalent doses (e.g. Timar-Gabor et al 2012), it is likely that the quartz OSL age results are underestimates and should be interpreted as a minimum age estimate for the deposit. It is important to note that the IRSL ages from the Globoko pit should also be considered as minimum ages as anomalous fading (loss) of the feldspar luminescence signal was not measured or accounted for in these age calculations (e.g. Wintle 1973), which will produce an age underestimate (e.g. Huntley and Lamothe, 2001). Also important to note is that correction for anomalous fading is unlike to increase the luminescence ages by an order of magnitude to fall in line with the expected age of the Globoko Fm.

Possible feldspar contamination of the quartz OSL samples

Laboratory sample processing to isolate coarse-grain quartz and feldspar sand and fine-grained quartz and polymineralic silt for analysis followed standard procedures of sieving, density separation and acid treatments. It is not clear if the purity of the quartz was checked prior to analysis and it doesn't appear to have been monitored during all measurements. While the quartz luminescence signal decay curves appear to be dominated by the fast decaying component targeted for dating, the high luminescence response of the samples (>10-100k counts/second) may suggest feldspar contamination, which can produce inaccurate ages, specifically age underestimates (e.g. Lai and Bruckner, 2008). Where response to IR stimulation was monitored during analysis many samples (n=4) indicated the presence of feldspar within the quartz separate as stated in Lowick's report. To remediate this problem the samples were exposed to IR stimulation prior to measuring the response to blue light to attempt to bleach the signal from the feldspars. While this method has been used in many cases where a pure quartz separate could not be obtained (e.g. Roberts 2007), studies have shown that feldspars can still contribute to the post-IR blue signal and affect resultant ages, commonly by causing an age underestimate (e.g. Roberts, 2007; Lai and Bruckner, 2008), unless anomalous fading of the feldspar signal is taken into account (Vasiliniuc et al., 2013). Anomalous fading in the post-IR OSL signals was not measured nor accounted for, leaving the possibility that samples containing feldspar contamination could be underestimated.

Influence of unstable components of the quartz OSL signal

In addition to the older samples being at or close to saturation and possible evidence for feldspar contamination, quartz OSL results can produce age underestimate due to the contribution of unstable medium and slower decaying OSL components (e.g. Steffen et al. 2009). While this is a possibility, Lowick addresses this and describes the luminescence signal decay as being dominated by the fast decaying component, which has a lifetime of several million years (e.g. Aitken, 1998, Murray and Wintle, 1999), suggesting that this should not be a problem for these samples. However in some settings the fast-decaying quartz luminescence signal has been found to also be unstable and produce age underestimates (e.g. Fan et al. 2011; Murray et al. 2007). The degree to which unstable components may be affecting the quartz age estimates in the Krško basin is unknown at this time, but given their strong fast decaying OSL signals and relative rarity of reported problems with the fast component, it can be assumed that it will be a minor influence if at all.

Summary Statement

After reviewing the OSL data provided and considering conditions that may affect age underestimation of the OSL ages, I have come to the following conclusions:

1. The four samples collected from younger fluvial/alluvial deposits (<100ka) in the Krško basin appear to be producing reliable quartz OSL ages (not near saturation, no evidence of feldspar contamination, and fit geomorphic position).

2. As originally stated by Lowick in her report, the four samples collected from units mapped as the Globoko Fm are producing OSL ages ranging from 195-240ka and should be interpreted as minimum age estimates (near saturation of the quartz luminescence signal, feldspar contamination and no correction of the IRSL ages for anomalous fading). The magnitude to which these samples

underestimate the burial age of the deposits is not known without further testing. However, the feldspar IRSL signals were not near saturation and so can more accurately date these sediments and while not conducted, correction for fading would likely only increase the ages by 20-30%, suggesting corrected IRSL ages of 264-312ka for samples at the Globoko pit (samples USU-01 and GBL2).

3. While it is likely that the reported age estimates for samples from the Globoko Fm slightly underestimate the age of the deposits sampled, it is unlikely that these age estimates are off by an order of magnitude as would be the case if the deposits sampled are ~2 Ma. Instead, given the luminescence properties of the samples and the relationship between the sample age estimate and geomorphic position and elevation (Fig 1 and 2), it is likely that the samples were collected from younger deposits. Moreover, it should be pointed out that luminescence dating techniques only provide an age estimate of the last time sediment was exposed to light. It could be that the sample sites were exposed to a more recent period of transport and deposition that reset the luminescence signal, leading to the younger than expected ages.

The interpretations and discussion presented here is based solely upon the information supplied for review and may be susceptible to error and mis-interpretation. Additional testing and sample analysis would be required to fully address many of the questions related to magnitude of age underestimation of the oldest samples from this study. While available in the form of ESR dating from the Globoko pit, external age control would also be helpful in determining the validity of the OSL ages. Given the information supplied, I do not see any evidence suggesting that the OSL ages are off by more than 20-30% and are likely within error of the last time the sediments were exposed to light prior to deposition.

Tammy Rittenour

Director, USU Luminescence Lab

Assistant Professor, Geology

Utah State University

Logan, UT 84322

References Cited

Fan, A., Li, S-H., Li, B., 2011. Obervation of unstable fast component in the OSL of quartz. Radiation Measurements 46, 21-28.

Huntley, D.J., Lamothe, M., 2001. Ubiquity of anomalous fading in K-feldspars and the measurement and correction for it in optical dating. Can. J. Earth Sci. 38, 1093–1106.

Lai, Z., Bruckner, H., 2008 Effects of feldspar contamination on equivalent dose and the shape of the growth curve for OSL of silt-sized quartz extracted from Chinese Loess. Geochronometria 30, 49-53.

Lai, Z., 2010. Chronology and upper dating limit for loess samples from Louchuan section in the Chinese Loess Plateay using quartz OSL SAR protocol. Journal of Asian Earth Sciences 37, 176-185.

Lowick, S.E. Preusser, F., 2010. Investigating age underestimation in the high dose region of optically stimulated luminescence using fine-grained quartz. Quaternary Geochronology 6,33-41.

Murray, A.S., Wintle, A.G., 1999. Isothermal decay of optically stimulated luminescence in quartz. Radiation Measurements 30, 119-125.

Murray, A.S., Svendsen, J.I., Mangerud, J., Astakhov, V.I., 2007. Testing the accuracy of quartz OSL dating using a known-age Eemian site on the river Sula, northern Russia. Quaternary Geochronology 2, 102-109.

Pawley, S.M., Toms, P., Armitage, S.J., Rose, J., Quartz luminescence dating of Anglian Stage (MIS 12) fluvial sediments: Comparison of SAR age estimates to the terrace chronology of the Middle Thames valley, UK. Quaternary Geochronology 5, 569-582.

Roberts, H.M., 2007. Assessing the effectiveness of the double-SAR protocol in isolating a luminescence signal dominated by quartz. Radiation Measurements 42, 1627-1636.

Šikid, K., Basch, O., Šimunid, A., 1979: Tumač za list Zagreb L 33-78. Osnovna geološka karta SFRJ 1:100.000. Savezni geološki zavod, Beograd.

Steffen, D., Preusser, F., Schlunegger, F., 2009. OSL quartz age underestimation due to unstable signal components. Quaternary Geochronology 4, 353-362.

Swan, H. B., Hanson, K.L., Poljak, M., Živčič, M. & Gosar, A. 2004: Revised Seismotectonic Model of the Krško Basin, Part 1, PRS-NEK 2.7.1 rev. 1. prepared for Nuclear Power Plant Krško, Vrbina 12, Krško, Slovenia; by Geomatrix Consultants, Inc, Oakland, California, USA; in cooperation with University of Ljubljana, Faculty of Civil and Geodetic Engineering Institute of Structural Engineering, Environmental Agency of the Republic of Slovenia, Office of Seismology; and Geological Survey of Slovenia.

Timar-Gabor, A., Vasilinius, S., Vandenberghe, D.A.G., Cosma, C., Wintle, A.G., 2012. Investigations into the reliability of SAR-OSL equivalent doses obtained for quartz samples displaying dose response curves with more than one component. Radiation Measurements 47, 740-745.

Vasiliniuc, S., Vandenberghe, D.A.G., Timar-Gabor, A., Cosma, C., van der Haute, P., 2013, Combined IRSL and post-IR OSL dating of Romanian loess using single aliquots of polymineral fine grains. Quaternary International 293, 13-21.

Verbič, T. 2004: Stratigrafija kvartarja in neotektonika vzhodnega dela Krške kotline. 1. del: stratigrafija. (Quaternary stratigraphy and neotectonics of the Eastern Krško Basin. Part 1: Stratigraphy). – Razprave IV Razreda SAZU XLV-3, 171-225, Ljubljana (Abstract in English).

Wintle, A.G., 1973. Anomalous fading of thermoluminescence in mineral samples. Nature 245, 143–144

APPENDIX 5

PRIME LABORATORY CRN DATA RESULTS

OSL dating of coarse and fine grain samples from the Krško basin, Slovenia

OSL samples were prepared under subdued orange light in the laboratory. Coarse grain samples were prepared following the methods used by Monegato et al. (2010) and fine grain preparation followed that by Lowick and Presser (2011). Samples OSL-Bern-01-Libna, OSL-Bern-02-Libna, OSL-Bern-03-Libna, and KSK1, all had dramatic reactions to hydrochloric acid indicating a high carbonate content, while OSL-Bern-05-Libna, OSL-Bern-06-Libna, OSL-USU-01-Libna and GBL2, showed almost no reaction. All measurements were made on automated Risø TL/OSL DA-20 readers, fitted with an EMI 9235QA photomultiplier tube. Optical stimulation of the quartz (OSL) was performed using blue LEDs, and the OSL signal was detected through a Hoya U-340 transmission filter. Infrared stimulation of feldspar and the polymineral fraction (IRSL) was performed using IR LEDs, and the IRSL signal was detected through a L.O.T.-Oriel D410/30 nm interference filter and a Schott BG-39.

For each sample, material was taken from the surrounding sediment for dose rate calculations, and the specific activities of U, Th, and K were determined using high-resolution gamma spectrometry (cf. Preusser and Kasper, 2001). Each sample was analysed for radioactive disequilibrium in the Uranium decay chain using the approach described by Zander et al. (2007). Samples were weighed before and after oven-drying to determine water content. As all samples were taken from units that at present are far more exposed to the elements than would have been the case for almost all of their burial period, a water content of 25 ± 5 %, was applied to all samples.

OSL characteristics

All estimated dose (D_e) measurements were made using a modified version of the single aliquot regenerative dose (SAR) protocol (Murray and Wintle, 2000), and are described in Table 1. Dose recovery and preheat tests were conducted on both fine (KSK1, Fig.1) and coarse (OSL-Bern-03-Libna, Fig.2; OSL-USU-01-Libna, Fig.4) grain quartz, for temperatures from 220 to 280 °C. As preliminary measurements indicated that OSL-Bern-05-Libna and OSL-Bern-06-Libna contained considerably larger burial doses, a second dose recovery test was run on OSL-Bern-05-Libna using a regenerative dose of ~ 230 Gy. The results are plotted in Figure 3, and confirm that, using a preheat temperature of 260 °C, the SAR protocol was also able to recover larger regenerative doses within 10 % of unity. Preheat temperatures of 240 °C and 260 °C were chosen for all quartz measurements; this was held for 10 s and was also applied to all test doses. The SAR protocol includes a repeat measurement of a regenerative dose, which is used to calculate a recycling ratio. Recycling ratios remained within 10 % of unity, confirming that there was no cumulative effect of repeated treatment during the SAR protocol on sensitivity corrections (Murray and Wintle, 2000). Recuperation of the signal following a zero regenerative dose was monitored, and this did not exceed 5 % of the natural signal for most aliquots. For some aliquots of samples OSL-Bern-05-Libna and OSL-Bern-06-Libna, a high temperature bleach at 280 °C for 40 s after the measurement of each test dose was added as recommended by Murray and Wintle (2003), to test for any recuperation of the signal (Step 7 in the SAR protocol). These aliquots returned D_e values that were within the distribution of D_e values obtained without adding a high-temperature bleach, and confirm that recuperation of the signal in regenerative doses was not a problem.

Step	Treatment	Observed
1	Give dose[a]	
2	Preheat 240/260 °C for 10 s	
3	Stimulate for 60 s at 125°C	L_n or L_x
4	Give test dose	
5	Preheat 240/260 °C for 10 s	
6	Stimulate for 60 s at 125°C	T_n or T_x
7	(Stimulate for 40 s at 280°C)	
8	Return to 1	
	[a] For L_n, this is 0	

Table 1. Modified SAR protocol applied to coarse and fine grain quartz. L_n and L_x are the measurement of the burial dose and subsequent regenerative doses respectively. T_n and T_x are the measurement of test dose applied following the burial dose and subsequent regenerative doses respectively, and used to monitor changes in sensitivity, and correct for them, throughout the SAR protocol.

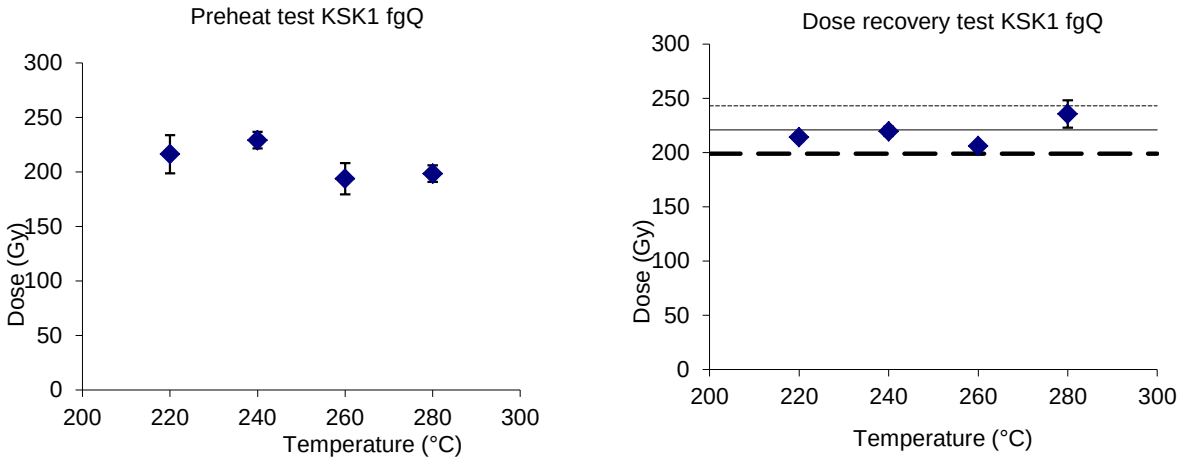

Figure 1. Preheat and dose recovery tests applied to the fine grain fraction of KSK1. For the dose recovery plot on the right, a regenerative dose of 220 Gy was applied. Dashed lines represented 10 % errors.

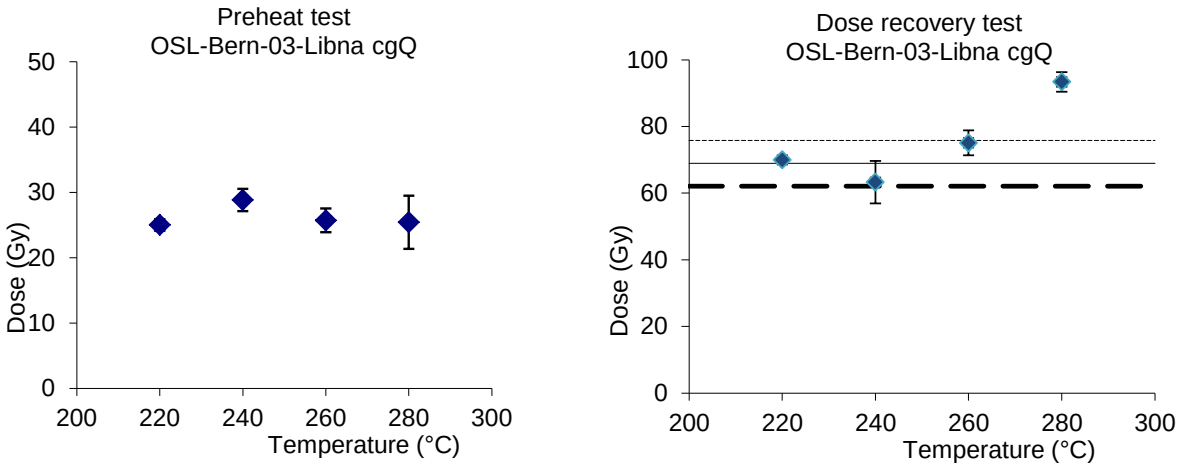

Figure 2. Preheat and dose recovery tests applied to the coarse grain fraction of OSL-Bern-03-Libna. For the dose recovery test a regenerative dose of ~ 70 Gy was applied. A preheat temperature of 260 °C was chosen.

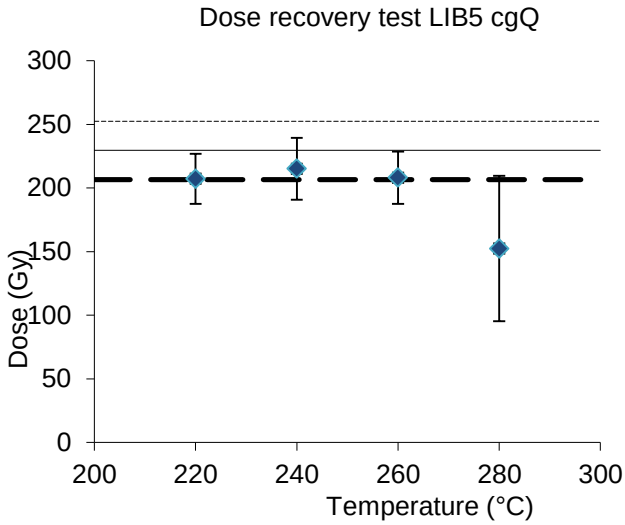

Figure 3. Dose recovery test applied to the coarse grain quartz fraction of OSL-Bern-05-Libna.

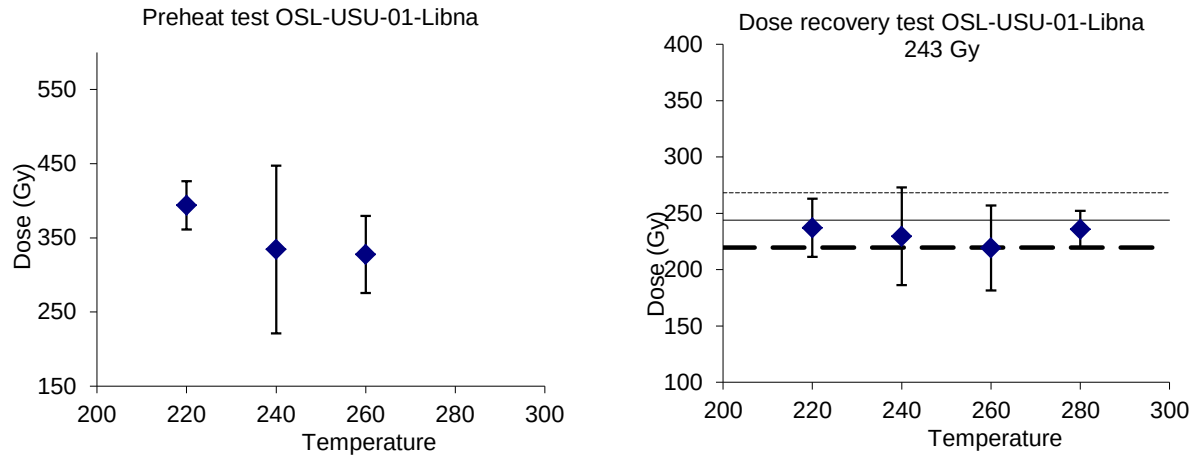

Figure 4. Preheat and dose recovery tests applied to the coarse grain fraction of OSL-USU-01-Libna.

The response of the quartz fraction to IR stimulation was used to detect any feldspar contamination. For some samples it was not always possible to remove an IR response, perhaps due to feldspar inclusions within the quartz grains. In this case, an IR stimulation for 100s at 50 °C was inserted before Steps 3 and 6 of the SAR protocol (Table 1) to remove any contribution from feldspar grains to the subsequent OSL stimulation. An example of the OSL decay curve for samples, KSK1, OSL-Bern-03-Libna and OSL-Bern-05-Libna, and OSL-USU-01-Libna are shown in Figure 5, and confirm that all quartz displayed a rapid decay, indicating that it is dominated by the fast component. Quartz D_e values were determined using the first 0.4 s of the OSL decay curve, and subtraction of a late background calculated using the last 10 s of a 60 s shinedown. The quartz OSL dose response fitted well to a saturating exponential plus linear (SEPL) function, which was used to determine D_e values. All dose rate and burial dose data is reported in Table 2.

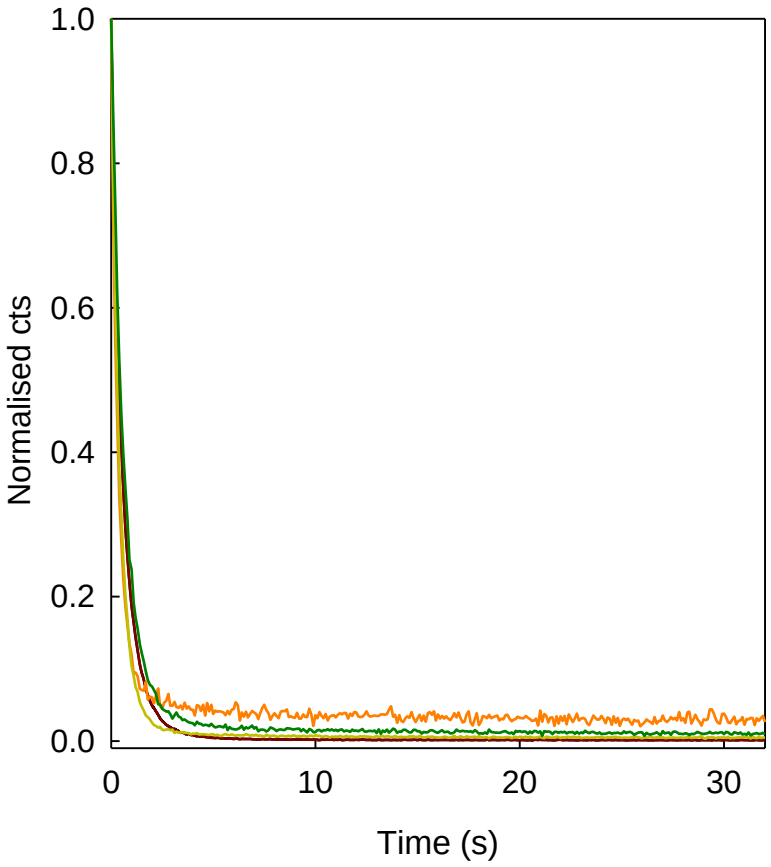

Figure 5. Decay curves for coarse and fine grain quartz from samples KSK1, OSL-Bern-03-Libna and OSL-Bern-05-Libna, and OSL-USU-01-Libna. Raw data has been normalised in order to allow comparison, and shows that all samples display a similar fast decay of the OSL.

OSL Sample	Mineral fraction(µm)	Altitude (masl)	Depth (m)	Aliquots (n)	Over-dispersion (n)	Radionuclide concentration (Bq kg^{-1}) ^{266}Ra			^{232}Th			^{40}K			Dose rate (Gy ka^{-1})			Water[3] (%)	De (Gy)			Age (ka)		
Bem-01-Libna	Q(200-250)	163	2.25	15/18	0.30	15.0	±	0.3	16.7	±	0.9	260.4	±	4.6	1.2	±	0.1	6	122.0	±	9.9	99.9	±	10.3
Bem-02-Libna	Q(100-150)	163	2.40	17/18	0.25	24.2	±	0.4	23.6	±	0.8	283.6	±	3.9	1.5	±	0.1	16	155.5	±	10.2	102.5	±	9.2
Bem-03-Libna	Q(200-250)	155	2.50	14/15	0.15	17.4	±	0.2	10.4	±	0.1	150.6	±	1.9	0.9	±	0.1	2	29.0	±	1.3	31.9	±	2.4
Bem-05-Libna	Q(200-250)	204	3.80	23/27	0.22	16.1	±	0.3	28.5	±	0.7	300.5	±	5.1	1.5	±	0.1	17	306.3	±	15.0	209.2	±	16.0
Bem-06-Libna	Q(200-250)	204	3.80	21/25	0.31	15.4	±	0.5	26.8	±	0.6	302.7	±	4.1	1.4	±	0.1	15	280.5	±	20.2	195.3	±	18.2
KSK1	Q(4-11)	166	2.00	5/5	-	41.8		0.2	46.4		1.4	478.3		5.2	3.0		0.4	11	124.5		2.1	41.1		4.9
	pm(4-11)			5/5	-										3.5	±	0.4		72.8	±	1.8	20.8	±	2.2
USU-01-Libna	Q(200-250)[1]	225	11.00	24/25	0.28	20.5	±	0.5	31.1	±	0.6	415.4	±	6.8	1.8	±	0.3	14	249.1	±	15.8	141.0	±	11.8
	Q(200-250)[2]					30.7	±	2.5							1.9	±	0.3					130.0	±	11.8
	F(160-250)[1]			10/11											2.6	±	0.2		615.8	±	46.8	241.4	±	27.8
GBL2	Q(200-250)[1]	225	8.00	19/26	0.13	21.8	±	0.4	34.1	±	0.8	407.3	±	7.4	1.8	±	0.1	15	247.0	±	8.9	135.1	±	9.1
	Q(200-250)[2]					23.2	±	14.9							1.8	±	0.3					133.6	±	22.5
	F(160-250)[1]			10/11											2.8	±	0.2		597.1	±	43.2	220.8	±	20.5

[1] Calculated using 226Ra

[2] Calculated using 238U

[3] As measured

Table 2. Dosimetry information, water content, D_e values and calculated ages. Concentrations were converted to infinite matrix dose using the standard conversion factors of Adamiec and Aitken (1998). Cosmic radiation contribution was calculated using present day sample burial depth following Prescott and Hutton (1994), and attenuation factors were taken from Mejdahl (1987).

The optically stimulated luminescence (OSL) dose response curve of sedimentary quartz is generally expected to be described by a single saturating exponential function if a single type of trap is assumed to be responsible for the signal (Aitken, 1998). However, quartz ages are increasingly reported that are derived from a high dose linear region of the OSL dose response curve (Roberts and Duller, 2004; Kim et al., 2009; Murray et al., 2008; Pawley et al., 2008; Anselmetti et al., 2010; Lowick et al., 2010a). The success of the SAR protocol relies partly on isolating a signal that displays a single saturating exponential, and this additional linear response is not yet fully understood (Bøtter-Jensen et al., 2003; Wintle, 2008). Subsequently, there is an ongoing debate regarding the reliability of quartz ages derived from this high dose linear region of the dose response curve (Lowick et al., 2010b; Lai, 2010), Nonetheless, ages have been reported that are in agreement with independent dating that were derived from such a high dose linear region (Murray et al., 2008; Pawley et al., 2008). The linear part of the dose response has been shown to most likely be the early expression of a second, and later saturating exponential that requires the measurement of additional higher dose points in order to properly characterize the saturation (Lowick et al., 2010b). This point can be seen in Figure 6, where the dose response curves for aliquot 2 and 40 adequately capture the saturation point of the signal, but aliquot 8 would require the addition of further dose points in order to observe a saturation of the signal. As these Slovenian samples generally fit better to an SEPL, rather than a single saturating exponential, the signals were looked at more closely. Figure 6 shows examples of the variability of the quartz signal and the varying point of saturation for different aliquots. Such variability between aliquots suggests that only very few grains are contributing to the signal measured from each, but also confirms that many of the burial doses measured for the older samples, OSL-Bern-05-Libna and OSL-Bern-06-Libna, and OSL-USU-01-Libna and GBL2, are close to, or at saturation of the signal. From a series of aliquots measured for sample GBL2, the dose response curve for 3 aliquots is illustrated in Figure 6. When fitting a luminescence dose response curve, Wintle and Murray (2006) recommend that only D_e values that fall below 2D0 (a value used to characterize 85 % saturation of the signal) should be considered reliable. When fitted to a single saturating exponential, aliquot 2, 38 and 40 give 2D0 values of 240 Gy, 115 Gy and 160 Gy respectively.

As the D_e values measured were 315 Gy, 211 Gy and 226 Gy respectively, all signals were less than 15 % away from saturation and, as such, can only be considered as representing youngest possible ages. While not done in previous studies, these results suggest that including early saturating aliquots, such as 38 in Figure 6, will reduce even further the youngest possible age, and that in fact, D_e determination might be better limited to later saturating aliquots, such as 12, to identify a youngest possible age. For this particular sample, the youngest possible age would be increased from 135 ka, to 190 ka, although such an approach has not been applied by the OSL community, and would require considerably more measurements to be made, while still being limited to identifying simply a youngest possible age.

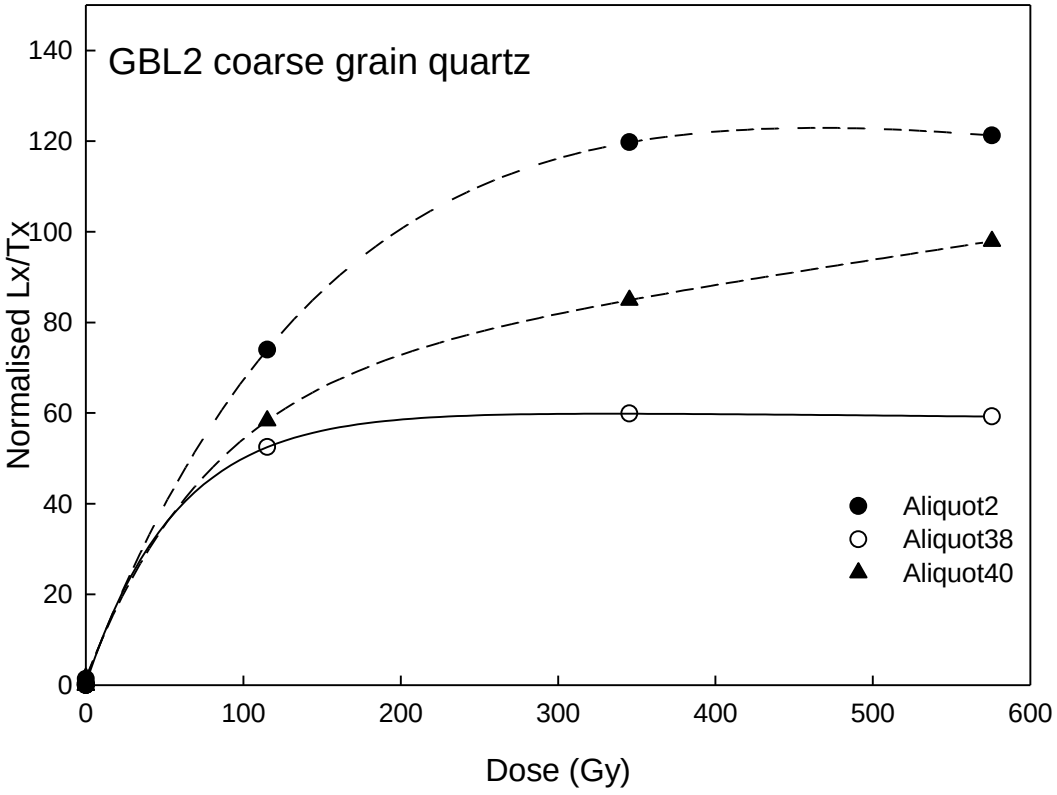

Figure 6 Examples of the dose response measured for different aliquots of the same sample, GBL2. In order to calculate 2D0, as a measure of 85 % saturation of the OSL signal, the dose response curves were fitted to a single saturating exponential and gave 2D0 values of 240 Gy, 115 Gy and 160 Gy for aliquots 2, 38 and 40 respectively. The D_e values calculated for these aliquots were 315 Gy, 211 Gy and 226 Gy, and so all are above 2 D0 and can only be considered youngest ages.

OSL ages

Quartz OSL ages for all samples are listed in Table 2. For samples OSL-Bern-01-Libna, OSL-Bern-02-Libna, OSL-Bern-03-Libna and KSK1, all D_e values remain below 150 Gy and suggest that there should be no problems of saturation of the signal. OSL-Bern-01-Libna and OSL-Bern-02-Libna, both give ages of ~ 110 ± 10 ka, while OSL-Bern-03-Libna, is much younger at 32 ± 2 ka. KSK1 gives a slightly older age of 41 ± 5 ka. The age of OSL-Bern-05-Libna and OSL-Bern-06-Libna, taken within 2 m of each other in the same unit, give similar ages within errors, and suggest an age of ~ 200 ± 20 ka. Despite GBL2 laying 3 m above OSL-USU-01-Libna, these two samples give similar ages of ~ 140 ± 10 ka. However, for all four of these considerably older samples, D_e values are generally all > 250 Gy, and are therefore close to saturation, and can only be considered as youngest possible ages.

To gain more information on the age of the samples, a coarse grain feldspar fraction was measured for OSL-USU-01-Libna and GBL2, and these results are also given in Table 2. D_e values for the feldspar fraction were determined using the first 10 s of the IRSL decay curve, with background subtraction calculated using the last 200 s. The feldspar IRSL dose response curve fitted well to a saturating exponential plus linear function, which was used to determine D_e values, and is illustrated in Figure 7. This fraction also gave similar ages for both OSL-USU-01-Libna and GBL2, within errors, with ages of 230 - 240 ka, and so considerably older than the quartz OSL ages by almost 60 %. 2D0 was also determined using a single saturating exponential and indicated that the signal was below 85 % of saturation at ~ 450 Gy, and so below the mean value of the burial dose. An example of the dose response from both OSL and IRSL is illustrated in Figure 7, and confirm the much earlier saturation of the OSL signal.

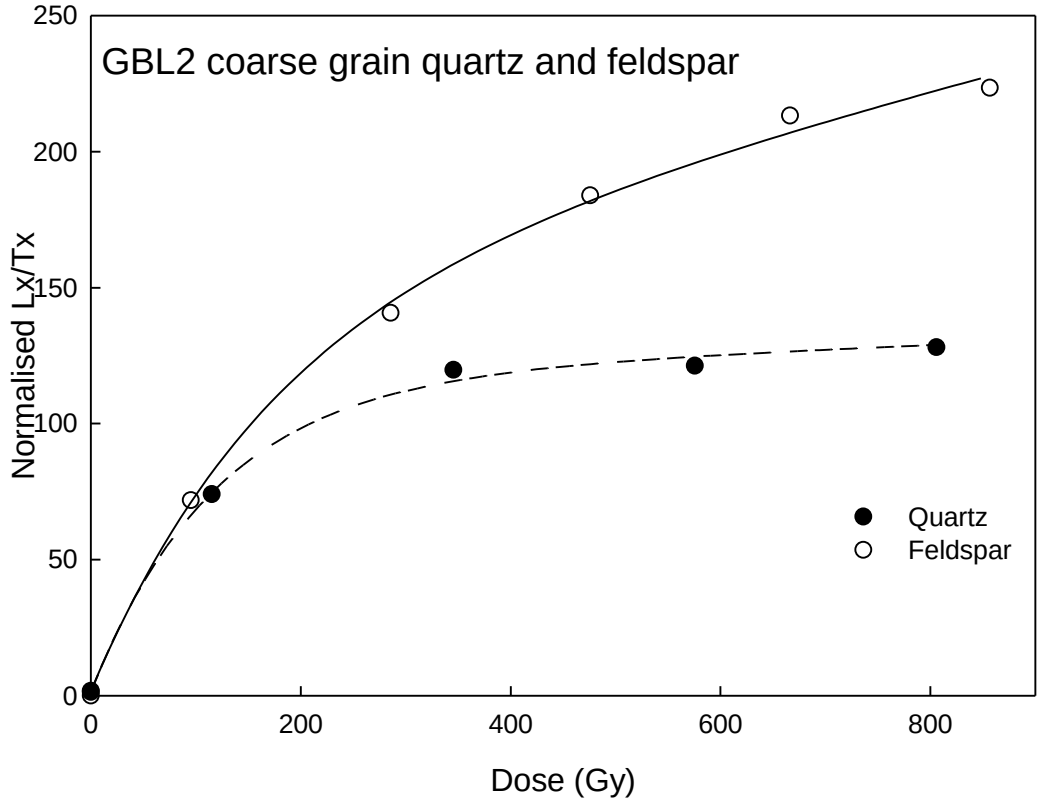

Figure 7 Examples of dose response curves for coarse grain quartz (OSL) and feldspar (IRSL) for sample GBL2. When fitted to a single saturating exponential, 2D0 for each mineral fraction is 230 Gy and 540 Gy for quartz and feldspar respectively.

The polymineral fine grain fraction of KSK1, was also measured. Surprisingly, unlike samples OSL-USU-01-Libna and GBL2GLB2, the IRSL ages were significantly younger, at ~ 20 ka, and it is not clear why the relation between IRSL and OSL ages is not the same as for the older samples. A fading test was conducted on the polymineral fraction of KSK1 and a g-value of ~ 2 % was calculated. As this would only increase the age by ~ 20 % it cannot explain the discrepancy between the OSL and IRSL and requires further investigation. It would be useful to measure the feldspar fraction of OSL-Bern-01-Libna, OSL-Bern-02-Libna, OSL-Bern-03-Libna to see if this discrepancy can be explained.

With regard to the calculation of dose rates, there was some indication of a loss of Uranium over time for samples OSL-USU-01-Libna and GBL2. In order to calculate the influence of this on burial ages, both maximum and minimum ages were calculated using both the 226^{Ra} and 238^{U} values respectively. The effects on final age calculations remained below 7%, and well within the uncertainties derived from estimating water content (cf. Preusser and Degering, 2007).

With regard to water content, a 10 % reduction in water content, for example for sample OSL-USU-01-Libna, from 25 % to 15 %, would result in a reduction in age of ~ 10 %. Conversely, an increase of 10 % in water content would result in an increase in age of ~ 10 %. However, for the older samples, the fact that they are close to saturation, and therefore minimum ages, precludes any recalculation of water content. For the younger samples, the estimation of water content could be reconsidered, but it will still only have a 10 % effect on ages, as for the example given for OSL-USU-01-Libna.

References

Adamiec, G., Aitken M., 1998. Dose-rate conversion factors: update. Ancient TL 16, 37-50.

Aitken, M. J., 1985. Thermoluminescence dating. Academic Press, New York.

Anselmetti, F. S., Drescher-Schneider, R., Furrer, H., Graf, H. R., Lowick, S., Preusser, F., Riedi, M. A., 2010. A ~180,000 years sedimentation history of a perialpine overdeepened glacial trough (Wehntal, N-Switzerland). Swiss Journal of Geosciences, 103, 345-361.Bøtter-Jensen, L., McKeever, S.W.S., Wintle, A.G., 2003. Optically Stimulated Luminescence Dosimetry. Elsevier, Amsterdam.

Kim, J.C., Duller, G.A.T., Roberts, H.M., Wintle, A.G., Lee, Y.I., Yi, S.B., 2009. Dose dependence of thermally transferred optically stimulated luminescence signals in quartz. Radiation Measurements 44, 132-143.

Lai, Z., 2010. Chronology and the upper dating limit for loess samples from Luochuan section in the Chinese Loess Plateau using quartz OSL SAR protocol. Journal of Asian Earth Sciences 37, 176-185.

Lowick, S.E., Preusser, F., 2011. Investigating age underestimation in the high dose region of optically stimulated luminescence using fine grain quartz. Quaternary Geochronology 6 (1), 33-41.

Lowick, S. E., Preusser, F., Pini, R., Ravazzi, C., 2010a. Underestimation of fine grain quartz OSL dating towards the Eemian: Comparison with palynostratigraphy from Azzano Decimo, northeastern Italy. Quaternary Geochronology, 5, 583-590.

Lowick, S.E., Preusser, F., Wintle, A.G., 2010b. Investigating quartz optically stimulated luminescence dose-response curves at high doses. Radiation Measurements 45 (9), 975-984.

Mejdahl V., 1987. Internal radioactivity in quartz and feldspar grains. Ancient TL 5, 10–17.

Monegato, G., Lowick, S.E., Ravazzi, C., Banino, R., Donegana, M., Preusser, F., 2010. Middle to Late Pleistocene palaeoenvironmental evolution of the southeastern Alpine Valeriano Creek succession (northeastern Italy). Journal of Quaternary Science 25, 617-632.

Murray, A., Buylaert, J.-P., Henriksen, M., Svendsen, J.-I., Mangerud, J., 2008. Testing the reliability of quartz OSL ages beyond the Eemian. Radiation Measurements 43, 776-780.

Murray, A. S., Wintle, A. G., 2000. Luminescence dating of quartz using an improved single-aliquot regenerative-dose protocol. Radiation Measurements 32, 57-73.

Murray, A.S., Wintle, A.G., 2003. The single aliquot regenerative dose protocol: potential for improvements in reliability. Radiation Measurements 37, 377-381.

Pawley, S.M., Bailey, R.M., Rose, J., Moorlock, B.S.P., Hamblin, R.J.O., Booth, S.J., Lee, J.R., 2008. Age limits on Middle Pleistocene glacial sediments from OSL dating, north Norfolk, UK. Quaternary Science Reviews 27, 1363-1377.

Prescott, J.R., Hutton, J.T., 1994. Cosmic ray contributions to dose rates for luminescence and ESR dating: Large depths and long-term time variations. Radiation Measurements 23, 497-500.

Preusser, F., Degering, D., 2007. Luminescence dating of the Niederweningen mammoth site, Switzerland. Quaternary International, 164-165, 106-112.

Preusser, F., Kasper, H. U., 2001. Comparison of dose rate determination using high-resolution gamma spectrometry and inductively coupled plasma-mass spectrometry. Ancient TL 19, 17-21.

Roberts, H.M., Duller, G.A.T., 2004. Standardised growth curves for optical dating of sediment using multiple-grain aliquots. Radiation Measurements 38, 241-252.

Wintle, A.G., 2008. Luminescence dating: where it has been and where it is going. Boreas 37, 471-482.

Wintle, A. G., Murray, A. S., 2006. A review of quartz optically stimulated luminescence characteristics and their relevance in single-aliquot regeneration dating protocols. Radiation Measurements 41, 369-391.

Sequence						
slo0	**Position**	**Sample**	**Mineral**	**cg/fg**	**Measurement**	
543j	2-8	USU-01-Libna	F	cg	Preheat test	
547j	1-12	USU-01-Libna	Q	cg	Dose recovery test	
549j	8-12	USU-01-Libna	Q	cg	De	
560j	2-12	USU-01-Libna	F	cg	De	
560j	14-24	GBL2	F	cg	De	
562j		USU-01-Libna	Q	cg	Preheat te	post IR OS
566j	21-28	KSK1	Q	fg	Dose recovery test	
566j	29-40	KSK1	Q	fg	Preheat test	
569j	1-5	KSK1	Q	fg	De	
569jb	3+5	KSK1	Q	fg	Extended dose respc	
577e	12-20	KSK1	F pm	fg	De	
580e	34-38	USU-01-Libna	F	cg	De	
580e	40-44	USU-01-Libna	F	cg	De	
600 RL	2-12	USU-01-Libna	Q	cg	De	
601 RL	2-12	USU-01-Libna	Q	cg	De	
602j	1-5	KSK1	Q	fg	De	
603RL	2-24	Bern-03-Libna	Q	cg	De	
604RL	2-6	Bern-01-Libna	Q	cg	De	
604RL	14-18	Bern-05-Libna	Q	cg	Dose recovery test	
604RL	8-12	Bern-02-Libna	Q	cg	De	
604RL	20-24	Bern-06-Libna	Q	cg	De	
605RL	14-24	Bern-02-Libna	Q	cg	De	
605RL	26-48	Bern-05-Libna	Q	cg	De	
605RL	2-12	Bern-01-Libna	Q	cg	De	
606e	2-12	Bern-01-Libna	Q	cg	De	
606e	14-24	Bern-02-Libna	Q	cg	De	
606e	26-48	Bern-03-Libna	Q	cg	Preheat test	
607RL	2-6	Bern-01-Libna	Q	cg	De	
607RL	8-12	Bern-02-Libna	Q	cg	De	
607RL	14-48	Bern-06-Libna	Q	cg	De	
611j		GBL2	Q	cg	De	
612j		GBL2	Q	cg	De	
619j	2-24	Bern-03-Libna	Q	cg	Dose recovery test	
619j	26-48	Bern-05-Libna	Q	cg	Dose recovery test	
625RL	21+23	KSK1	F pm	fg	Fading test	

Measurement sequences

APPENDIX 6

GEOZS REPORT ON GEOLOGIC BORINGS IN THE KRŠKO BASIN

RESULTS

10Be

BillingID: ***2013114*** **Submitter:** ***Cline, M. Logan***

Sample Identification			Aliquot	Native	Target	Carrier	10Be/Be (E-15) +/- Error (E-15)	Error %	current (nA)
PLID	UserID		g	mg	mg	mg			
201301564	Cblk-3167-1				0.6	0.277	5.9 +/- 1.1	18.5	4153
201301563	RIZZO-CRN-JAN2013-1.0		7		0.6	0.284	92 +/- 5	4.9	4418
201301561	RIZZO-CRN-JAN2013-6.0		5		0.6	0.282	25 +/- 4	14.5	3975
201301560	RIZZO-CRN-JAN2013-8.0		3		0.6	0.279	15.3 +/- 1.8	11.7	3982
201301559	RIZZO-CRN-JAN2013-10.5		19		0.6	0.277	60 +/- 4	6.3	3939
201301558	RIZZO-CRN-JAN2013-15.0		3		0.6	0.290	13.5 +/- 1.6	11.5	3662

PRIME Lab, Purdue University, 1396 Physics Building. West Lafayette, IN 47907 - 1396